



MINISTÉRIO DA EDUCAÇÃO
SECRETARIA DE EDUCAÇÃO PROFISSIONAL E TECNOLÓGICA
INSTITUTO FEDERAL DE EDUCAÇÃO, CIÊNCIA E TECNOLOGIA DE MINAS GERAIS
CAMPUS OURO PRETO
Rua Pandiá Calógeras, 898 – Bairro Bauxita – Ouro Preto – Minas Gerais – CEP 35.400-000
(31) 3559-2150

RELATÓRIO INDIVIDUAL DE TRABALHO (RIT)

REFERENTE AO SEMESTRE LETIVO/ANO 01/2018		
IDENTIFICAÇÃO DO SERVIDOR		
NOME RAPHAEL HERMANO SANTOS DINIZ		
CAMPUS OURO PRETO		
ÁREA OU CURSO CODACIB		
MATRÍCULA SIAPE 2411649	FONE 31-993124366	E-MAIL raphael.diniz@ifmg.edu.br
TIPO DE VÍNCULO <input checked="" type="checkbox"/> Efetivo <input type="checkbox"/> Substituto <input type="checkbox"/> Temporário ou Colaboração Técnica		
REGIME DE TRABALHO <input checked="" type="checkbox"/> 40h D.E. <input type="checkbox"/> 40h <input type="checkbox"/> 20h		
ATIVIDADES DOCENTES DESENVOLVIDAS NO SEMESTRE LETIVO		
ATIVIDADES DE ENSINO Listar disciplinas ministradas, orientações discentes (concluídas no decorrer do semestre ou em andamento), horários disponibilizados para o atendimento ao discente e demais atividades de ensino descritas no Plano Individual de Trabalho Docente (PIT). Aulas (em horas de 60 min) → CH – 20 <ul style="list-style-type: none">• Biologia I – 4 aulas semanais de 50 minutos• Biologia II – 4 aulas semanais de 50 minutos• Biologia III – 4 aulas semanais de 50 minutos Estudos orientados para alunos em progressão parcial (por disciplina) → CH – 01 <ul style="list-style-type: none">• Biologia I – 1 turma Orientação de estágio, tutoria ou monitoria (por orientação) → CH – 02 <ul style="list-style-type: none">• Orientação de monitoria → estudante Laura Lima de Oliveira• Orientação de estágio → Talita Cristina		
ATIVIDADES DE PESQUISA Relatar o andamento dos projetos e demais atividades de extensão listadas no Plano Individual de Trabalho Docente (PIT). No caso de projetos, indicar o cronograma de execução (prazos atuais) e as atividades desenvolvidas no decorrer do semestre. Colaboração em projeto de pesquisa sem fomento – CH – 10 <ul style="list-style-type: none">• “Elaboração de uma sequência didática e de um jogo didático para o ensino de Biologia Celular no Ensino Médio”• “Utilização de programação computacional como ferramenta didática no ensino de genética” Coordenação de grupo de pesquisa – CH – 02 <ul style="list-style-type: none">• Grupo de Pesquisa Básica, Aplicada e Educacional em Ciências Biológicas Participação como membro de conselho científico, em editoras de revistas científicas indexadas – CH – 01 <ul style="list-style-type: none">• Revista IGCiência, alocada no endereço: http://revistas.faculdadeguanambi.edu.br/index.php/fgciencia/index Co-orientação de alunos em projetos científicos – CH – 02 <ul style="list-style-type: none">• Fernanda Camilo Gonçalves• Rafaela de Freitas Favares• Carlos Oliveira Pereira• Célio Junio Mendonça das Dores		
ATIVIDADES DE EXTENSÃO Relatar o andamento dos projetos e demais atividades de extensão listadas no Plano Individual de Trabalho Docente (PIT). No caso de projetos ou programas, indicar o cronograma de execução (prazos atuais) e as atividades desenvolvidas no decorrer do semestre.		
ATIVIDADES DE GESTÃO E REPRESENTAÇÃO Descrever as principais atividades desenvolvidas na gestão institucional do IFMG de acordo com a função; ou atividades em comissões/fiscalizações realizadas no decorrer do semestre de acordo com o Plano Individual de Trabalho Docente (PIT). Coordenação de curso – CH – 10 <ul style="list-style-type: none">• Coordenador da Área de Biologia – CODACIB – 22/11/2017 a 20/05/2018		

ATIVIDADES DE CAPACITAÇÃO	
Descrever o andamento das atividades de capacitação realizadas e seu cronograma atual	
PRODUTOS DE ENSINO, PESQUISA E/OU EXTENSÃO	
Descrever a produção listada no Plano Individual de Trabalho Docente (PIT).	
Publicação em revistas Qualis A1 e A2 – CH – 24 <ul style="list-style-type: none"> Cachaça yeast strains: alternative starters to produce beer and bioethanol – Revista: Antonie van Leeuwenhoek – doi: 10.1007/s10482-018-1063-3 1px1p links glucose-induced calcium signaling and plasma membrane H⁺-ATPase activation in <i>Saccharomyces cerevisiae</i> cells – Revista: FEMS Yeast Research - doi: 10.1093/femsyr/fox088 	
Publicação em revistas Qualis B1 e B2 – CH – 10 <ul style="list-style-type: none"> Screening of Yeasts Isolated from Brazilian Environments for the 2-Phenylethanol (2-PE) Production – Revista: Biotechnology and Bioprocess Engineering – doi: 10.1007/s12257-018-0119-6 	
PONTUAÇÃO	
Confrontar a pontuação obtida no Plano Individual de Trabalho (PIT) com a produção obtida neste Relatório Individual de Trabalho (RIT).	
Pontuação total do Plano Individual de Trabalho Docente (entregue no início do semestre letivo)	57
Pontuação total deste Relatório Individual de Trabalho Docente	82
Caso haja diferença na pontuação, JUSTIFIQUE:	
Ocorreu no período a publicação de artigos científicos em revistas Qualis A1 e A2	

PARECER DA COORDENAÇÃO

Aprovado em 08/11/18

JFMatos

OBSERVAÇÃO:

O Relatório Individual de Trabalho deve ser acompanhado da relação dos documentos comprobatórios das atividades efetivamente desenvolvidas no período.

Professora: Raphael Hermano Santos Diniz

Raphael Hermano Santos Diniz

Coordenador de Área/Curso: Januária Fonseca Matos

JFMatos

Diretor de Ensino: Venilson Luciano Benigno Fonseca

Ouro Preto 01 de novembro de 2018.

Professor: RAPHAEL HERMANO SANTOS DINIZ (CODACIB)

Hora	Segunda	Terça	Quarta	Quinta	Sexta
07:00	0	0	0	OPIEDIF.2016.1-3D2	OPIADMI.2018.1-1D2
07:00	0	0	0	0	0
08:00	0	0	0	OPIEDIF.2016.1-3D2	OPIADMI.2018.1-1D2
08:00	0	0	0	0	0
09:00	0	0	0	OPIADMI.2017.1-2D2	OPIADMI.2018.1-1D1
09:00	0	0	0	0	0
10:00	0	0	0	OPIADMI.2017.1-2D2	OPIADMI.2018.1-1D1
10:00	0	0	0	0	0
11:00	0	0	0	0	0
11:00	0	0	0	0	0
12:00	0	0	0	0	0
13:00	0	0	0	OPIADMI.2017.1-2D1	OPIEDIF.2016.1-3D1
13:00	0	0	0	0	0
14:00	0	0	0	OPIADMI.2017.1-2D1	OPIEDIF.2016.1-3D1
14:00	0	0	0	0	0
15:00	0	0	0	0	0
15:00	0	0	0	0	0
16:00	0	0	0	0	0
16:00	0	0	0	0	0
17:00	0	0	0	0	0
17:00	0	0	0	0	0
18:00					
18:45					
19:00					
19:00					
19:45					
19:45					
19:50					
20:40					
20:40					
21:00					
21:30					
21:30					
21:50					
22:15					
23:00					

OBS: Por residir em Viçosa.

LOCAIS DAS AULAS PRESENCIAIS - ESTUDOS ORIENTADOS (INTEGRADO)

DISCIPLINA	CURSO	PROFESSOR	PAVILHÃO	SALA
BIOLOGIA I	ADMINISTRAÇÃO	KEILA	EDIFICAÇÕES	106
BIOLOGIA I	AUTOM/EDIFIC	RAPHAEL	EDIFICAÇÕES	102
BIOLOGIA I	METALURGIA	THALITA	EDIFICAÇÕES	106
BIOLOGIA I	MINERAÇÃO	MÍRIAM	EDIFICAÇÕES	107
BIOLOGIA II	TODOS OS CURSOS	MARGALY	MINERAÇÃO	108
DESENHO TÉCNICO	METALURGIA	LUCIANA DO VALE	DESENHO	103
DESENHO TÉCNICO	MINERAÇÃO	ADRIANO PINTO	DESENHO	103
EDUCAÇÃO FÍSICA I	EDIFICAÇÕES		EDUCAÇÃO FISICA	101
ELETRÔNICA DIGITAL I	AUTOMAÇÃO	RONALDO TRINDADE	AUTOMAÇÃO	109
ELETROELETRÔNICA	AUTOMAÇÃO	MAYCON	AUTOMAÇÃO	101
ESTABILIDADE DAS CONSTRUÇÕES	EDIFICAÇÕES	FLÁVIO TEIXEIRA	EDIFICAÇÕES	111
FILOSOFIA I	MINERAÇÃO	PAULA RENATA	MINERAÇÃO	107
FILOSOFIA II	AUTOMAÇÃO	PAULA RENATA	MINERAÇÃO	107
FÍSICA I	TODOS OS CURSOS	MÁRIO EUSTÁQUIO	EDIFICAÇÕES	101
FÍSICA III	TODOS OS CURSOS	MÁRIO EUSTÁQUIO	EDIFICAÇÕES	103
GEOGRAFIA I	EDIFIC/MINER.	ALEX DE CARVALHO	MINERAÇÃO	101
GEOGRAFIA II	AUTOM/MINER.	HENRIQUE AMORIM	MINERAÇÃO	102
GEOLOGIA GERAL	MINERAÇÃO	ARIANA / REGINATO	MINERAÇÃO	101
GEOLOGIA APLICADA	MINERAÇÃO	REGINATO	MINERAÇÃO	101
HISTÓRIA I	TODOS OS CURSOS	PAULO MONTE ALTO	EDIFICAÇÕES	109
LÍNGUA ESTRANGEIRA INGLÊS III	METALURGIA	FERNANDO GONÇALVES	LÍNGUAS	104
LÍNGUA PORTUGUESA I	TODOS OS CURSOS	PRISCILA	EDIFICAÇÕES	107
LÍNGUA PORTUGUESA II	TODOS OS CURSOS	ELKE PENA	EDIFICAÇÕES	109
LINGUAGEM DE PROGRAMAÇÃO	AUTOMAÇÃO	FRANCISCO CÉSAR	AUTOMAÇÃO	106
MATEMÁTICA I	ADMINISTRAÇÃO	CLÁUDIO VITA	EDIFICAÇÕES	101
MATEMÁTICA I	MINERAÇÃO	MÁRCIO ANDRÉ / CÁSSIO VIDIGAL	EDIFICAÇÕES	104
MATEMÁTICA I	METALURGIA	SÁVIO / JOÃO NEPOMUCENO	EDIFICAÇÕES	103
MATEMÁTICA I	EDIFICAÇÕES	ROBERTO BRÁULIO / AFONSO	EDIFICAÇÕES	111
MATEMÁTICA I	AUTOMAÇÃO	JÚLIO PAULO / GENTIL	EDIFICAÇÕES	102

MATEMÁTICA II	ADMIN/METAL/MINER	GISLENE	EDIFICAÇÕES	104
MATEMÁTICA II	AUTOM/EDIFIC	RODRIGO TOFFOLO	EDIFICAÇÕES	104
MATEMÁTICA III	TODOS OS CURSOS	MARCOS DIAS	EDIFICAÇÕES	109
MECÂNICA DOS SOLOS	EDIFICAÇÕES	GILBERTO RAMALHO	EDIFICAÇÕES	109
MINERALOGIA	MINERAÇÃO	ARIANA	JOALHERIA	103
PESQUISA MINERAL	MINERAÇÃO	CARLA LACERDA	MINERAÇÃO	109
PETROGRAFIA	MINERAÇÃO	FERNANDO ANTÔNIO	MINERAÇÃO	110
PROJETO DE PESQUISA INTEGRADO	METALURGIA		METALURGIA	101
QUÍMICA I	TODOS OS CURSOS	SORAYA	EDIFICAÇÕES	110
QUÍMICA II	TODOS OS CURSOS	DOMINGOS	EDIFICAÇÕES	102
QUÍMICA III	TODOS OS CURSOS	LYDIA	EDIFICAÇÕES	101
REDES INDUSTRIAIS	AUTOMAÇÃO	HUGO RAFAEL	AUTOMAÇÃO	106
TECNOLOGIA DAS CONSTRUÇÕES I	EDIFICAÇÕES	MARCELO NASCIMENTO	EDIFICAÇÕES	110
SERVIÇOS E EQUIPAMENTOS	MINERAÇÃO	AMILTON	MINERAÇÃO	109
SOCIOLOGIA I	MINERAÇÃO	LUCIANO JOSÉ	MINERAÇÃO	107



INSTITUTO FEDERAL
MINAS GERAIS

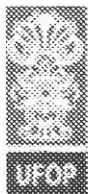
Diretoria de Ensino
Coordenação Pedagógica

Declaração

Declaro para os devidos fins que **Raphael Hermano Santos Diniz**, siape 2411649, professor no Instituto Federal Minas Gerais – *campus* Ouro Preto acompanhou a atividade de monitoria, da disciplina de Biologia da aluna: Laura Lima de Oliveira, durante o ano de 2018.

Fabíula Tatiane Pires
Fabíula Tatiane Pires
Coordenadora Pedagógica

Fabíula Tatiane Pires
Pedagoga
IFMG *Campus* Ouro Preto
SIAPE: 2157027



Ouro Preto, 12 de março de 2018

Declaro para os devidos fins que o professor Raphael Hermano dos Santos Diniz desempenhou a função de supervisor de estágio acompanhou e orientou Talita Cristina Oliveira, aluna do curso de ciências biológicas da Universidade Federal de Ouro Preto. Esse estágio foi realizado no Instituto Federal de Minas Gerais, Campus Ouro Preto no segundo semestre do ano de 2017 e no primeiro semestre de 2018 e que este se constituiu em atividade de campo de 40h da disciplina "Estágio Supervisionado de Ensino de Ciências II".

Fábio Augusto Rodrigues e Silva
Professor Adjunto da Universidade Federal de Ouro Preto - UFOP
Coordenador da disciplina Estágio Supervisionado em Ciências

Ministério da Educação
Secretaria de Educação Profissional e Tecnológica

Certificado

O INSTITUTO FEDERAL DE MINAS GERAIS - CAMPUS OURO PRETO certifica que **RAPHAEL HERMANO SANTOS DINIZ**, CPF nº **060.521.386-02**, participou como **Co-Orientador** do projeto de **PESQUISA** intitulado "**Utilização de programação computacional como ferramenta didática no ensino de genética.**" no III Seminário de Inovação, Pesquisa, Pós Graduação e Extensão (III SIPEX), realizado entre os dias 15 e 17 de outubro de 2018.

Ouro Preto - MG, 05 de novembro de 2018

CHAVE: 181105w5Qp1vcw

www.certificadolivre.com.br

Ministério da Educação
Secretaria de Educação Profissional e Tecnológica

Certificado

O INSTITUTO FEDERAL DE MINAS GERAIS - CAMPUS OURO PRETO certifica que **RAPHAEL HERMANO SANTOS DINIZ**, CPF nº **060.521.386-02**, participou como **Co-Orientador** do projeto de **PESQUISA** intitulado "**Elaboração de uma sequência didática e de um jogo didático para o ensino de Biologia Celular no Ensino Médio**" no III Seminário de Inovação, Pesquisa, Pós Graduação e Extensão (III SIPEX), realizado entre os dias 15 e 17 de outubro de 2018.

Ouro Preto - MG, 05 de novembro de 2018

CHAVE: 181105BN81rgXj

www.certificadolivre.com.br

Grupo de pesquisa

Grupo de Pesquisa Básica, Aplicada e Educacional em Ciências Biológicas

Endereço para acessar este espelho: dgp.cnpq.br/dgp/espelhogrupo/7734451508324836

Identificação

Situação do grupo: Certificado

Ano de formação: 2018

Data da Situação: 15/05/2018 15:31

Data do último envio: 20/04/2018 21:11

Líder(es) do grupo: Raphael Hermano Santos Diniz

Área predominante: Ciências Biológicas; Biologia Geral

Instituição do grupo: Instituto Federal Minas Gerais - IFMG

Unidade: Instituto Federal Minas Gerais - Campus Ouro Preto



Endereço / Contato

Endereço

Logradouro: Rua Pandiá Calógeras

Número: 898

Complemento: Pavilhão de Segurança do Trabalho, sala 112, CODACIB

Bairro: Bauxita

UF: MG

Localidade: Ouro Preto

CEP: 35400000

Caixa Postal:

Localização geográfica

Latitude: -20.395094743263716

Longitude: -43.502151775649224

Contato do grupo

Telefone: (31) 3559-2203

Fax: ()

Contato do grupo: raphael.diniz@ifmg.edu.br

Website:

Repercussões

Repercussões dos trabalhos do grupo

O grupo conta com pesquisadores cuja formação básica são: Ciências Biológicas, Nutrição, Farmácia e Educação Física. Estes pesquisadores atuam auxiliando outras instituições de pesquisa em seus respectivos projetos, além de realizarem pesquisas na própria Instituição. Destacam-se projetos e artigos publicados na área da: saúde, microbiologia e educação.

Participação em redes de pesquisa

Rede de pesquisa	Website/Blog
Nenhum registro adicionado	

Linhas de pesquisa

Nome da linha de pesquisa	Quantidade de Estudantes	Quantidade de Pesquisadores
Educação e Ensino-Aprendizagem de Ciência.	0	7
Microbiologia Aplicada à Saúde e Biotecnologia	0	3
Saúde e Educação	0	7

Recursos humanos

Pesquisadores	Titulação máxima	Data inclusão
Elizângela Fernandes Ferreira	Mestrado	20/03/2018
Januaria Fonseca Matos	Doutorado	20/03/2018
Keila Lopes Mendes	Doutorado	20/03/2018
Margaly Aparecida de Aguiar Vita	Graduação	20/03/2018
Miriam Conceicao de Souza Testasicca	Doutorado	20/03/2018
Raphael Hermano Santos Diniz	Doutorado	20/03/2018
Thalita Macedo Araújo	Mestrado	20/03/2018

Estudantes	Nível de Treinamento	Data inclusão
Nenhum registro adicionado		

Técnicos	Formação acadêmica	Data inclusão
Nenhum registro adicionado		

Colaboradores estrangeiros	País	Data inclusão
Nenhum registro adicionado		

Egressos

Pesquisadores	Período de participação no grupo
Nenhum registro adicionado	

Estudantes	Período de participação no grupo
Nenhum registro adicionado	

Instituições parceiras relatadas pelo grupo

Nome da Instituição Parceira	Sigla	UF	Ações
Universidade Federal de Ouro Preto	UFOP	MG	<input type="checkbox"/>
Universidade Federal de Viçosa	UFV	MG	<input type="checkbox"/>

Indicadores de recursos humanos do grupo

Formação acadêmica	Pesquisadores	Estudantes	Técnicos	Colaboradores estrangeiros	Total
Doutorado	4	0	0	0	4
Mestrado	2	0	0	0	2
Graduação	1	0	0	0	1

DECLARAÇÃO DE PARECERISTA
REVISTA FG CIÊNCIA - ISSN: 2236-9449

Declaro que Raphael Hermano Santos Diniz tornou-se colaborador voluntário na qualidade parecerista *ad hoc* de artigos científicos submetidos à revista FG Ciência, alocada no endereço <http://revistas.faculdadeguanambi.edu.br/index.php/fgciencia/index>, na internet, a partir de maio de 2018.

Guanambi, 09 de maio de 2018,



Juliana M. dos Santos Lopes
EDITORACHefe DA REVISTA UNIFG CIÊNCIAS


Juliana Mendonça dos Santos Lopes

Editora chefe – FG Ciência



MINISTÉRIO DA EDUCAÇÃO
SECRETARIA DE EDUCAÇÃO PROFISSIONAL E TECNOLÓGICA
INSTITUTO FEDERAL DE EDUCAÇÃO, CIÊNCIA E TECNOLOGIA DE MINAS GERAIS
CAMPUS OURO PRETO
DIRETORIA DE INOVAÇÃO, PESQUISA E EXTENSÃO
Rua Pandiá Calógeras, 898 – Bairro Bauxita – Ouro Preto – Minas Gerais – CEP 35.400-000
(31) 3559 2148 – dipe.ouropreto@ifmg.edu.br

DECLARAÇÃO

Declaramos para os devidos fins que **Míriam Conceição de Souza Testasicca** atuou como orientadora no projeto “**Elaboração de uma sequência didática e de um jogo didático para o ensino de Biologia Celular no Ensino Médio**”, com co-orientação de Margaly Aparecida De Aguiar Vita, Thalita Macedo Araújo, Keila Lopes Mendes e Raphael Hermano Santos Diniz, através do Programa Institucional de Bolsas do Instituto Federal de Minas Gerais - Campus Ouro Preto. Neste projeto, vigente de março de 2018 a dezembro de 2018, a referida professora orientou as alunas: Fernanda Camilo Gonçalves e Rafaela de Freitas Tavares - bolsas de iniciação científica, modalidade PIBIC Jr.

Ouro Preto, 30 de outubro de 2018.

Assinatura manuscrita em tinta azul, aparentemente de Dayse Layne Rodrigues de Souza.

Dayse Layne Rodrigues de Souza
Auxiliar em Administração
Diretoria de Inovação, Pesquisa, Pós Graduação e Extensão
IFMG - *Campus* Ouro Preto



MINISTÉRIO DA EDUCAÇÃO
SECRETARIA DE EDUCAÇÃO PROFISSIONAL E TECNOLÓGICA
INSTITUTO FEDERAL DE EDUCAÇÃO, CIÊNCIA E TECNOLOGIA DE MINAS GERAIS
CAMPUS OURO PRETO
DIRETORIA DE INOVAÇÃO, PESQUISA E EXTENSÃO
Rua Pandiá Calógeras, 898 – Bairro Bauxita – Ouro Preto – Minas Gerais – CEP 35.400-000
(31) 3559 2148 – dipe.ouropreto@ifmg.edu.br

DECLARAÇÃO

Declaramos para os devidos fins que **Thalita Macedo Araújo** atuou como orientadora no projeto “**Utilização de programação computacional como ferramenta didática no ensino de genética.**”, com co-orientação de Osvaldo Novais Junior, Míriam Conceição De Souza Testasicca, Margaly Aparecida De Aguiar Vita, Keila Lopes Mendes e Raphael Hermano Santos Diniz, através do Programa Institucional de Bolsas do Instituto Federal de Minas Gerais - Campus Ouro Preto. Neste projeto, vigente de março de 2018 a dezembro de 2018, a referida professora orientou os alunos: Carlos Oliveira Pereira e Célio Júnio Mendonça das Dores- bolsas de iniciação científica, modalidade PIBIC Jr.

Ouro Preto, 30 de outubro de 2018.

Assinatura manuscrita em tinta azul, aparentemente de Dayse Layne Rodrigues de Souza.

Dayse Layne Rodrigues de Souza
Auxiliar em Administração
Diretoria de Inovação, Pesquisa, Pós Graduação e Extensão
IFMG - Campus Ouro Preto



MINISTÉRIO DA EDUCAÇÃO
SECRETARIA DE EDUCAÇÃO PROFISSIONAL E TECNOLÓGICA
INSTITUTO FEDERAL DE EDUCAÇÃO, CIÊNCIA E TECNOLOGIA DE MINAS GERAIS
CAMPUS OURO PRETO
GABINETE DA DIREÇÃO-GERAL

Rua Pandiá Calógeras, nº 898, Bairro Bauxita, Ouro Preto, CEP 35400-000, Estado de Minas Gerais

PORTARIA Nº 002 DE 04 DE JANEIRO DE 2018.

Dispõe sobre designação de SUBSTITUTO de ocupante de Função Gratificada do IFMG - Campus Ouro Preto.

O DIRETOR-GERAL SUBSTITUTO DO INSTITUTO FEDERAL DE EDUCAÇÃO, CIÊNCIA E TECNOLOGIA DE MINAS GERAIS - *CAMPUS OURO PRETO*, nomeado pela Portaria nº 059 de 27 de outubro de 2015, publicada no DOU de 10/11/2015, Seção 2, pág. 21, e no uso das atribuições que lhe são conferidas pela Portaria IFMG nº 475 de 06 de abril de 2016, publicada no DOU de 15 de abril de 2016, seção 2, pág.17, retificada pela Portaria IFMG nº 805, de 04 de julho de 2016, publicada no DOU de 06 de julho de 2016, Seção 2, pág. 22, e pela Portaria IFMG nº 1078, de 27 de setembro de 2016, publicada no DOU de 04 de outubro de 2016, Seção 2, pág. 20,

RESOLVE:

Art. 1º. DESIGNAR o servidor **RAPHAEL HERMANO SANTOS DINIZ**, ocupante do cargo efetivo de Professor do Ensino Básico, Técnico e Tecnológico, Matrícula SIAPE nº 2411649, para a função de **Coordenador SUBSTITUTO da Área de Biologia - CODACIB do IFMG - Campus Ouro Preto**, Função Gratificada - código FG-04, nos afastamentos, impedimentos legais ou regulamentares do titular, no período de 22/11/2017 a 20/05/2018.

Art. 2º. Determinar que a presente Portaria seja devidamente publicada no Boletim de Serviços do IFMG - *Campus Ouro Preto*.

Art. 3º. Determinar que a Gestão de Pessoas adote as providências cabíveis à aplicação da presente Portaria.

Art. 4º. Esta Portaria entra em vigor na data de sua publicação.

Ouro Preto, Estado de Minas Gerais, 04 de janeiro de 2018.

Professor **RONALDO SILVA TRINDADE**
Diretor-Geral SUBSTITUTO do Instituto Federal de Educação, Ciência e Tecnologia de Minas Gerais - *Campus Ouro Preto*

Cachaça yeast strains: alternative starters to produce beer and bioethanol

Thalita Macedo Araújo · Magalhães Teixeira Souza · Raphael Hermano Santos Diniz ·
Celina Kiyomi Yamakawa · Lauren Bergmann Soares · Jaciane Lutz Lenczak ·
Juliana Velasco de Castro Oliveira · Gustavo Henrique Goldman ·
Edilene Alves Barbosa · Anna Clara Silva Campos · Ieso Miranda Castro ·
Rogelio Lopes Brandão

Received: 10 November 2017 / Accepted: 7 March 2018
© Springer International Publishing AG, part of Springer Nature 2018

Abstract This work was performed to verify the potential of yeast strains isolated from *cachaça* distilleries for two specific biotechnological applications: beer and bioethanol production. In the beer production, the strains were tested for characteristics required in brewery practices, such as: capacity to ferment maltose and maltotriose, ability to grow at lowest temperatures, low H₂S production, and flocculation profile. Among the strains tested, two of them showed appropriate characteristics to produce two different beer styles: lager and ale. Moreover, both strains were tested for *cachaça* production and the results confirmed the capacity of these strains to

improve the quality of *cachaça*. In the bioethanol production, the fermentation process was performed similarly to that used by bioethanol industries: recycling of yeast biomass in the fermentative process with sulfuric acid washings (pH 2.0). The production of ethanol, glycerol, organic acids, dry cell weight, carbohydrate consumption, and cellular viability were analyzed. One strain presented fermentative parameters similar to PE2, industrial/commercial strain, with equivalent ethanol yields and cellular viability during all fermentative cycles. This work demonstrates that *cachaça* distilleries seem to be an interesting environment to select new yeast strains to be used in biotechnology applications as beer and bioethanol production.

Electronic supplementary material The online version of this article (<https://doi.org/10.1007/s10482-018-1063-3>) contains supplementary material, which is available to authorized users.

Keywords Beer · Bioethanol · *Cachaça* · Flavoring compounds

T. M. Araújo · M. T. Souza · R. H. S. Diniz ·
E. A. Barbosa · A. C. S. Campos · I. M. Castro ·
R. L. Brandão (✉)
Laboratório de Biologia Celular e Molecular, Núcleo de
Pesquisas em Ciências Biológicas (NUPEB),
Universidade Federal de Ouro Preto (UFOP), Ouro Preto,
Minas Gerais CEP: 35400-000, Brazil
e-mail: rlbrand@nupeb.ufop.br

Introduction

Cachaça is defined as a typical and unique spirit obtained by the distillation of fermented sugarcane with an alcohol content of 38–48% (v v⁻¹), at 20 °C (Brazil 2005). It is the third most consumed distilled beverage in the world, behind only vodka and soju (Russian and Korean distilled beverages, respectively) with an estimated annual production around 1.5 billion liters (Faria-Oliveira et al. 2015). In turn, the Brazilian

C. K. Yamakawa · L. B. Soares · J. L. Lenczak ·
J. V. de Castro Oliveira · G. H. Goldman
Laboratório Nacional de Ciência e Tecnologia do
Bioetanol (CTBE), Centro Nacional de Pesquisa em
Energia e Materiais (CNPEM), Campinas, São Paulo,
Brazil

bioethanol industry also uses sugarcane as a raw material and annually produces an estimated 27.3 billion liters of fuel ethanol (IBGE 2016).

Cachaça producers start the preparation of the inoculum for fermentation from a small amount of sugarcane juice (containing wild yeast and bacteria strains) supplemented with corn meal, rice bran, biscuits, lemon juice, etc. This suspension is mixed in sufficient quantity to form a slurry and left for spontaneous fermentation at rest for 12–24 h. Then, when the release of CO₂ indicating fermentative activity is observed, diluted sugarcane juice (1:1) is added again, with further fermentation for over 24 h. This step is repeated until the cell concentration achieves adequate levels, approximately 20% of the volume of the fermentation vat (10⁹ cell mL⁻¹ of yeast cells). Fermentation occurs in vats made of stainless and/or carbon steel for 24 h; then, the fermented must is distilled in copper alembics or steel columns. Afterward, a new fermentative cycle begins using the residual yeast in the fermentation vats. This procedure is repeated until the completion of the annual *cachaça* production, which lasts 4–6 months (Martini et al. 2010; Pataro et al. 2000; Schwan et al. 2001; Vicente et al. 2006). Therefore, *cachaça* production is characterized by spontaneous fermentation by microbiota present in the fermentative must in the equipment and facilities used for *cachaça* production (Faria-Oliveira et al. 2015). Therefore, it can be considered as a unique environment with high competition between different species of microorganisms; with continuous replacement of strains, *Saccharomyces cerevisiae* predominates, but different species are also found (Oliveira et al. 2008; Pataro et al. 2000; Schwan et al. 2001). These species belong to the genera *Kluyveromyces*, *Candida*, *Pichia*, *Debaromyces*, *Rhodotorula*, and other less frequent and different species from the *Saccharomyces* genus (*S. exiguus*, *S. paradoxus*, *S. servazzii*, and *S. unisporus*, the last species reclassified as *Kazachstania unispora*, Kurtzman, 2003).

On the other hand, it is known that the fermentative process related to *cachaça* production is characterized by high selective pressure due to different factors: competition among microorganisms, daily exposure to high ethanol concentration and osmotic pressure, absence of temperature control, and continuous reuse of the inoculum without treatment between the fermentative cycles (Faria-Oliveira et al. 2015). This singular environment favors the selection of yeast

strains with potential adaptive advantages for their utilization in other biotechnological processes, as demonstrated in previous works (Alvarez et al. 2014; Conceição et al. 2015).

Most probably due to this particular and selective environment, *cachaça* yeast strains present potential characteristics to be used in different biotechnological applications (Conceição et al. 2015). Indeed, *cachaça* yeast strains exhibit resistance against different factors, particularly relevant for bioethanol production: (i) presence of metals, (ii) low pH (< 3.0), (iii) high ethanol concentration (8–10%), and (iv) high osmolarity (> 18% carbohydrate concentration).

Another important characteristic of the *cachaça* industry is its idleness, since the production occurs during the sugarcane harvest, between May and November or October and March (depending on the Brazilian region). Thus, as a beverage industry, *cachaça* distilleries could better explore the infrastructure (fermentation room, vats, bottling machine, etc.) by improving the productive capacity with the production of other beverages. In this sense, beer production could be an excellent alternative, and there are many reasons to support such an idea. As it is already known, beer production is performed with strict temperature control and more restrict microbiological surveillance; therefore, the production of *cachaça* with such concepts could lead to an improvement of its final quality.

Beer is the most consumed alcoholic beverage in the world and when compared to non-alcoholic beverages, occupies the third position, only behind water and tea. More than 80% of all beer consumed in the world is lager style and up to almost 12% are special ale beers. Particularly, Brazil figures in the third position among the largest world producers of beer with 135.500 hL surpassed only by China (506.500 hL) and the USA (224.093 hL; Group 2013). In spite of the fact that the world market is dominated by commercial mega-breweries who are able to sell large volumes of several brands, there has been a strengthening of production on a smaller scale of the so-called special beers. In this regard, and since the second half of the 1980s, many microbreweries were created in Brazil that have been responsible for the production of diversified styles with high standard quality.

However, to use *cachaça* yeast strains in beer production, we also need to consider the beer styles

that would be eventually produced. In general, beer styles can be classified into three groups: ale, lager, and lambic (predominance of spontaneous fermentation). An ale yeast ferments between 16 and 25 °C, whereas a lager yeast ferments at lower temperatures, between 6 and 15 °C (Vidgren et al. 2010). Furthermore, it is known that the presence of acetate and ethyl esters is characteristic of ale beers, although the concentration of different aromatic compounds can be affected by many conditions during the production process (Brányik et al. 2008; Kobayashi et al. 2008; Saerens et al. 2008, 2010; Yu et al. 2012). Ale yeasts are predominantly classified as *S. cerevisiae*, although some strains are hybrids between *S. cerevisiae* and *Saccharomyces kudriavzevii* (González et al. 2010). In turn, lager yeasts are the result of a hybridization process between *S. cerevisiae* and *Saccharomyces eubayanus* that led to the appearance of *Saccharomyces pastorianus* that was further domesticated in the brewery environment (Libkind et al. 2011). Taking into account all this information, we studied the characteristics of *cachaça* yeast strains in the context of beer production.

Interestingly, some *cachaça* yeast strains have shown ethanol yields in 24 h similar to yeast strains generally used in the bioethanol industry. Besides, they also showed other important characteristics to be used in the fuel ethanol industry, such as low foam production and high resistance against stressing conditions like sulfuric acid washings and aluminum toxicity (Conceição et al. 2015). Indeed, in spite of the robustness and flexibility demonstrated by *cachaça* yeast strains, the Brazilian bioethanol industry uses only a small number of commercial yeast strains, without exploitation of the microbial richness accessible in other areas to support industrial innovation (Amorim et al. 2011). Although distilleries for fuel production in Brazil are quite more complex, also because they are generally used for sugar production, the fact that both industries (*cachaça* and bioethanol) use the same raw material (sugarcane) would allow the production of fuel ethanol in *cachaça* distilleries. To do so, the producers need only introduce a special column distiller (already available in the Brazilian market), allowing the *cachaça* producers to incorporate fuel ethanol in their product portfolio.

Therefore, considering the potential biotechnological properties of the *cachaça* yeast strains, we show in this work a strategy to select yeast strains, originally

isolated from vats of *cachaça* fermentation, that could be used to improve the quality of *cachaça* but also to produce beer and bioethanol, improving the productive capacity of the facilities found in *cachaça* distilleries.

Materials and methods

Strains and culture conditions

In this work, 118 yeast strains were previously isolated from *cachaça* distilleries in different cities of four Brazilian states: Bahia, Minas Gerais, Rio de Janeiro, and Espírito Santo. These strains were biochemically selected according to the methodology already described (Vicente et al. 2006). Briefly, samples of fermented must were collected from *cachaça* distilleries and triplicates of decimal dilutions in sterilized water were inoculated on yeast extract/peptone (YP) medium [2% peptone, 1% yeast extract, and 2% agar (each w v⁻¹)] supplemented with 2% (w v⁻¹) sucrose and 0.1% (w v⁻¹) chloramphenicol at 30 °C. Pools of colonies (480) from each distillery were screened in liquid YP media containing a different carbon source (glucose, galactose, or maltose) and according to stress resistance at 30 °C: (i) high osmolarity (20% glucose or 20% sucrose), (ii) high ethanol content (15% v v⁻¹), and (iii) drug resistance [5,5',5''-trifluoro-DL-leucine (TFL) and cerulenin, 1 mmol L⁻¹ and 25 µmol L⁻¹, respectively] to test for the potential production of isoamyl acetate and ethyl caproate, respectively (Bussey and Umbarger 1970; Ichikawa et al. 1991; Satyanarayana et al. 1968). Only the test on resistance at high temperature was performed at 37 °C.

Flocculation ability and invertase activity, considered beneficial for *cachaça* production, were also analyzed. Flocculation ability was evaluated using the modified Helm's assay (D'Hautcourt and Smart 1999). Yeast cultures were grown on yeast extract/peptone/dextrose (YPD) medium, for 72 h, washed twice with 500 mmol EDTA (pH 7.0), sonicated and submitted to flocculation test (Powell et al. 2003). A sample of ~ 10⁸ cells mL⁻¹ was washed with 0.51 g L⁻¹ of CaSO₄ and resuspended in a solution containing: 0.51 g L⁻¹ of CaSO₄, 6.8 g L⁻¹ of sodium acetate, 4.05 g L⁻¹ of acetic acid, and 4% (v v⁻¹) ethanol (pH 4.5). Yeast cells in control tubes were resuspended in

500 mM EDTA (pH 7.0). After a 15 min sedimentation period, samples (100 μ L) were taken from just below the meniscus, dispersed in H₂O (900 μ L), and the absorbance at 600 nm ($A_{600\text{nm}}$) was measured. The % of flocculation was estimated from six replicas using the formula: $(A_{\text{control}} - A_{\text{sample}}) / 100 \times A_{\text{control}}$. On the other hand, the invertase activity was performed in derepressive conditions, using YP supplemented with 2% raffinose. The higher invertase activity indicates that the yeast can efficiently hydrolyze sucrose, resulting in fructose and glucose (Ekunsanmi and Odunfa 1990).

The selected yeast strains were stored in YP medium supplemented with 2% (w v⁻¹) glucose and 30% glycerol (w v⁻¹) at -80 °C. All strains are available in the culture collection of the Research Center of Biological Sciences from Federal University of Ouro Preto – Campus do Morro do Cruzeiro – 35.400-000 Ouro Preto, MG, Brazil (propp@ufop.br).

Screening of yeast strains for beer production

To test the potential of *cachaça* yeast strains for beer production, the collection of 118 yeast strains was also grown on YP medium supplemented with 2% glucose or 2% maltose at 30 °C with agitation (200 rpm). Additionally, maltotriose fermentation by specific yeast strains was assayed by growing them in YP with 2% maltotriose in the absence or presence of antimycin A (2 mg L⁻¹, Sigma-Aldrich, MO, USA) at 30 °C for 72 h (Zastrow et al. 2001). Next, samples were taken every 2 h for 72 h, and the growth was monitored following $A_{600\text{nm}}$ in a spectrophotometer BioMate3 (Thermo Fisher Scientific, Waltham, MA, USA). The specific growth rate (μ) for each culture at the exponential growth phase was determined by linear regression of the plot $\ln A_{600\text{nm}}$ versus time (h). Strains able to grow on maltose/maltotriose were further grown in 96-well plates with 300 μ L of YP with glucose 2%, at 15, 20, and 30 °C without agitation for 72 h. Samples were taken every 6 h for 72 h and the growth profiles were also evaluated by the plot $\ln A_{600\text{nm}}$ versus time (h).

The production of hydrogen sulphide (H₂S) was determined using the bismuth sulphite agar, Wilson-Blair medium (Merck, Darmstadt, Germany; Jiranek et al. 1995). A 10- μ L culture sample was deposited on the plate and incubated at 30 °C for 72 h. Colonies were evaluated for the intensity of brown/black color,

which is directly correlated with H₂S production, using a four-level qualitative scale: negative (-), low (+), high (++) and very high (+++) H₂S production. *Candida albicans* ATCC18804 was used as positive control (very high H₂S production) and the commercial *S. cerevisiae* US-05 and WB-06 were used as negative controls (no H₂S production).

The production of the phenolic compound 4-vinylguaiacol (4VG) was analyzed from yeast strains grown in yeast nitrogen base broth (Sigma-Aldrich, MO, USA) supplemented with 2% (wt/vol) glucose and 1 mM ferulic acid at 25 °C for 3 days. Cultures were centrifuged at 1000 $\times g$ for 5 min at 4 °C, and 10-mL samples were taken to perform the extraction of 4VG from the supernatant by addition of 0.5 g of NaCl and 5 μ L of 1% (vol/vol) *n*-decanol. Then, three successive extractions using 4, 2, and 2 mL of dichloromethane during 5 min were performed; the extracts were concentrated by N₂. All samples were resuspended in 500 μ L of dichloromethane and 10 μ L were derivatized using 25 μ L of pyridine and 75 μ L of N,O-bis(trimethylsilyl)trifluoroacetamide (BSTFA) at 80 °C for 30 min. Then, 20 μ L of triplicate samples were injected in a Shimadzu GSMS-QP2010 Plus chromatographer, equipped with a mass quadrupole detector for detection and quantification of 4VG. Chromatographic conditions were as follows: Phenomenex[®] column [ZB-SHT Inferno, 30 m \times 0.25 mm \times 0.1 μ m; splitless rate 2 min; flow of carrier gas (helium 99.999%) 1.52 mL min⁻¹; split rate 1:20]. The temperature of the column during the chromatographic analysis was initially programmed at 60 °C for 2 min and then was raised to 300 °C at a ramp of 10 °C min⁻¹, and finally 300 °C for 2 min. Triplicate samples of 20 μ L of distillate were injected in the column.

Molecular identification of the yeast strains

All yeast strains from our collection were previously submitted to taxonomic identification by molecular techniques on the basis of 5.8 S-internal transcribed spacer (ITS) rRNA region amplification and restriction analysis using standard procedures (White et al. 1990; Lõoke et al. 2011). The ITS regions (ITS1/5.8 S/ITS2) of the strains used in this work were amplified, and the amplicon was sequenced using the Applied Biosystems' (ABI) 3130 platform Life Technologies (Myleus Biotechnology, Belo Horizonte, Minas

Gerais, Brazil). Then, to confirm the molecular identification of the yeast cells, these sequences were analyzed using the basic local alignment search tool (BLASTn) service from the National Center for Biotechnology Information (NCBI 2004). The 5.8 S-ITS sequence from *S. cerevisiae* S288c was used as reference. Bit scores obtained indicate how good the alignment was; on the other hand, the corresponding E-values indicate the statistical significance of a given pairwise alignment. The closer the E-value is to zero, the higher the biological significance of the data.

Considering that mitochondrion genomes in hybrid yeasts are inherited in a uniparental way (Querol and Bond 2009), and that several works have demonstrated that the mtDNA genome in lager brewing yeast originates from the parental *S. bayanus* strain, the sequence of the mitochondrial *COXII* gene was also analyzed to define the origin of a specific cachaça yeast strain (Nakao et al. 2009). The sequence was compared with other *Saccharomyces* strains using the BLAST (<http://blast.ncbi.nlm.nih.gov/Blast.cgi>).

Determination of ploidy by flow cytometry

The yeast ploidy was estimated by flow cytometry by SYTOX green dye method (Haase and Reed 2002). Cells were grown in YP medium containing 2% of glucose ($w v^{-1}$) for 8–12 h. Approximately 5×10^6 cells were centrifuged and washed with deionized water. Cells were resuspended in 1 mL of 70% ethanol and maintained for 1 h at room temperature. Yeast cells were centrifuged, resuspended in sodium citrate (50 mM, pH 7.2) with RNase solution (0.25 mg mL^{-1}) and incubated at 37 °C for 2 h. Then, 50 μL of proteinase K (20 mg mL^{-1}) was added, and the cells were incubated at 50 °C for 2 h. The samples were homogenized by sonication, centrifuged, and resuspended in 0.1 mL of sodium citrate containing 30 nM of SYTOX green dye (Thermo Fisher Scientific, Waltham, MA, USA). The samples were maintained for at least 20 min at room temperature in the dark. The analyses were performed on a FACSCalibur system (Becton Dickinson Immunocytometry Systems, San Jose, CA, USA). Ploidy was estimated on the basis of the fluorescence intensity compared with reference *S. cerevisiae* strains: the haploid (S288c α) and the diploid (S288c a/α).

Beer production

Brewing was performed in 50-L cylindrical/conical tanks (pilot scale). Two formulations were used for wort production: (a) lager beer (pilsner style): malt wort (pilsner malt 22.5% $w v^{-1}$) with a gravity of 13 °Plato; (b) Weissbier: mixture of pilsner malt 8 kg, wheat malt 4 kg, and roasted malt 0.15 kg, with a gravity of 13 °Plato. The worts were prepared in 31 L of water at 42 °C. The mashing program comprised the following stages: 42 °C for 30 min; 52 °C for 15 min; 62 °C for 15 min; and 69 °C for 30 min. The breweries' spent grain, the filtration layer, and the sweet wort were filtered and boiled with hop (pellets, 30 g, 12% $w v^{-1}$ of α -acids) for 60 min. Then, the cooled wort was inoculated using selected yeast strains. Control experiments were performed using commercial strains: WB-06 (*S. cerevisiae*, ale) and W-34/70 (*S. pastorianus*, lager; Fermentis, Germany). Yeast strains were grown on YP medium supplemented with 2% glucose at 30 °C for 24 h under agitation (200 rpm) in an orbital shaker, and then pitched to a cell density of 5×10^6 cells mL^{-1} . The fermenters were maintained at 20 °C for 8 days (ale wort) and at 11 °C for 5 days (lager wort). The concentration of soluble solids in the fermenters was measured daily throughout by using a densimeter (Anton Paar, DMA, 35A). The percentage of apparent attenuation was calculated from the formula:

$$\text{Apparent attenuation (\%)} = \frac{[(\text{original gravity} - \text{final gravity})]}{100 \times (\text{original gravity})}$$

Beer maturations were performed at 4 °C for 14 days.

Cachaça production

Cachaça production was performed as previously described (Barbosa et al. 2016). Selected yeast strains were grown in 4 mL of YPD medium at room temperature for 48 h. This culture was used to inoculate 1000 mL of YPD incubated in an orbital shaker (200 rpm) at 30 °C for 48 h. After this period, the inoculum was transferred to a 20-L plastic recipient containing 2 L of sugarcane juice, previously sterilized and supplemented with 1% peptone and 2% yeast extract. After 24 h of incubation, the supernatant was withdrawn, and a new culture medium was added and the multiplication phase was restarted. This

procedure was done until 2 L of cell mass (10^9 cells mL^{-1}) were obtained. Then, the inoculum was transferred to stainless-steel tanks with 5 L of sterile sugarcane juice diluted to 5 °Brix. The sugarcane juice was extracted from the cane variety RB 765418, cultivated under organic management conditions in Salinas City, MG, Brazil. The mixture was allowed to ferment without agitation at room temperature with progressive addition of sugarcane juice until a final volume of 40 L was achieved. After 24 h, 30 L of fermented must was withdrawn and distilled in copper alembics discarding the “head” and “tail” fractions (around 10% of initial and final distillate, respectively). Samples of “heart” fractions were kept in 750-mL glass bottles. The fermentation process was followed by measuring ethanol production ($\% \text{ v v}^{-1}$) and consumption of soluble solids (°Brix) using a digital densimeter.

Ethanol production

To test the bioethanol production, the strain LBCM1047 was used because it was able to produce, on a laboratory scale, higher ethanol concentrations in the presence of 20% sucrose or 33% glucose [very-high-gravity (VHG) fermentations] in both cases comparable to PE2, a commercial bioethanol strain (Fermentec, Brazil). It also presents the capacity to actively survive at very low pH (around 2.4) and in the presence of toxic concentrations of aluminum (Conceição et al. 2015). Therefore, we decided to test it in conditions similar to those found in an industrial environment.

Fermentative must was formulated and standardized for all alcoholic fermentations with molasses and sugarcane juice, with a final concentration of 185 g L^{-1} of total reducing sugars (TRS). Approximately 162 g of wet yeast mass were diluted with 384 mL of sterile water and transferred to the 2-L bioreactor (BioFlo® 115, New Brunswick, NJ, USA). Each fermentative cycle was preceded by an acid treatment of the yeast cells recovered by centrifugation at 800 rpm. The treatment was performed at pH 2.0 with H_2SO_4 (2.0 mol L^{-1}) for 30 min at 33 °C. The fermentative cycle was started with addition of must fed once through peristaltic pump and maintained at 33 °C and 200 rpm. After 8 h, fermented medium was withdrawn and centrifuged ($13,000 \times g$, 15 min, 4 °C). The supernatant was discarded and 162 g of yeast pellet

was resuspended in 384 mL of sterile water and transferred back to the bioreactor for the subsequent cycle on the next day. During this period, yeast suspension was maintained at 10 °C under agitation at 100 rpm and 0.3 vvm of aeration. A new fermentative cycle was started with acid treatment followed by fermentation and centrifugation. This methodology was repeated for six cycles; all fermentations were performed in duplicate.

To determine the biomass dry weight, samples were centrifuged ($3000 \times g$, 5 min, 4 °C), and the pellet was washed twice with demineralized water and dried at 85 °C. To analyze the cellular viability and budding, samples were stained with methylene blue and counted using a Neubauer chamber and optical microscopy (Lee et al. 1981).

Analytical procedures

In the bioethanol production, samples were analyzed hourly in an ALPHA Fourier transform infrared (FT-IR) spectrometer (Brucker, MA, USA) to quantify TRS and ethanol concentration. Samples of fermentation must, and initial and final fermentation were analyzed using a high-performance liquid chromatography (HPLC) system (Shimadzu C-R7A, Kyoto, Japan) to determine the fermentation parameters. For that purpose, sucrose, glucose, fructose, organic acids, glycerol, and ethanol were separated with Aminex HPX-87H or HPX-87P columns (BIO-RAD, Hercules, CA, USA) at 45 °C using $5 \text{ mmol L}^{-1} \text{H}_2\text{SO}_4$ as mobile phase at a flow rate of 0.6 mL min^{-1} and detected with an refractive index (RI) detector (Shimadzu RID-6A).

The following fermentative parameters were determined:

$$\text{Ethanol yield } (Y_{P/S}) = (\Delta E)/(\Delta S) \quad (\text{g g}^{-1})$$

$$\text{Ratio glycerol per ethanol } (K_G) = (\Delta G)/(\Delta E) \quad (\text{g g}^{-1})$$

$$\text{Ratio lactic acid per ethanol } (K_{AC}) = (\Delta LA)/(\Delta E) \quad (\text{g g}^{-1})$$

$$\text{Volumetric productivity} = (\Delta E)/[\text{FM} \times t] \quad (\text{g L}^{-1}\text{h}^{-1})$$

$$\text{Cellular growth rate} = (X_f - X_i) / [FM \times t] \quad (\text{g L}^{-1}\text{h}^{-1})$$

$$Y_i = (X_i \times (CB + M) / \rho FV) \quad (\text{g L}^{-1})$$

$$Y_f = [X_f \times (W / \rho w)] \quad (\text{g L}^{-1})$$

$$\text{Specific ethanol production rate} = (\Delta E) / [(Y_f - Y_i) \times t] \quad (\text{g g}^{-1}\text{h}^{-1})$$

$$\text{Ratio ethanol per g of cell } (K_L) = (X_f - X_i) / (\Delta E) \quad (\text{g g}^{-1})$$

where ΔE is the difference between final and initial ethanol concentration; ΔS is the difference between initial and final TRS concentration; ΔG is the difference between final and initial glycerol concentration; ΔLA is the difference between final and initial lactic acid concentration; FM is the final volume of fermented must (L); t is the time (8 h); X_i is the initial cell concentration; X_f is the final cell concentration; Y_i is the initial biomass present in the bioreactor; CB is the cellular biomass inoculated in the bioreactor; M is the mass of fermentative must (L); ρFV is the density of cellular biomass inoculated; Y_f is the total biomass in the final of fermentation; and ρw is the density of the fermented must.

Beer and *cachaça* samples were analyzed for volatile compounds (higher alcohols, esters, acetaldehyde, and diacetyl) and ethanol by gas chromatography coupled with flame ionization detection (GC-FID; Varian, Palo Alto, CA, USA). For analysis, 5.48 mL of sample (in triplicate) was dispensed into a 15-mL vial containing 20 μL of *n*-pentanol (internal standard). Samples were heated to 60 °C for 25 min, and 5 mL of headspace was injected to the analytical column DB-WAX (polietilenglycol, 60 m \times 0.25 mm \times 0.25 μm , J&W, Albany, NY, USA), in splitless mode (2 min) at a split ratio of 1:30. The temperatures of the injection block and FID were 225 and 280 °C, respectively. Hydrogen gas was used as sample carrier. The oven temperature was held at 40 °C for 3 min, then increased to 50 °C at a rate of 20 °C per min, held at 50 °C for 2 min, then increased to 100 °C at a rate of 5 °C per min, held at 100 °C for 2 min, then increased to 250 °C at a rate of 30 °C per min, and finally held at 250 °C for 2 min.

Statistical analysis

Statistical analyses were performed applying the Tukey test, Scott–Knott test, and analysis of variance at 5% probability level ($p < 0.05$).

Results

Selection and molecular characterization of yeast strains from different distilleries

Considering that previous results at our laboratory demonstrated the biotechnological potential of yeast strains for other applications (Alvarez et al. 2014; Conceição et al. 2015), we decided to select and/or test yeast strains with potential use for beer and bioethanol production as a broader strategy to optimize the utilization of the infrastructure already existent in *cachaça* distilleries.

As an example, Table 1 shows the screening procedure that led us to select strains named LBCM 1045 (producer 1), LBCM 1047 (producer 2), and LBCM 1078 (producer 3). In the first step, 480 isolated colony yeasts were obtained from three different *cachaça* distilleries, in a total of 1440 isolated colonies. Next, 1102 isolates (76.5%) were selected for further assays based on their ability to grow in different carbon sources, which, based on yeast taxonomy, increases the probability of selecting *S. cerevisiae* species. Then, 759 isolates ($\pm 52.7\%$) presented higher resistance against different types of stress being able to grow in a media with high osmolarity (20% sucrose), high alcohol content (15%), and/or at high temperature (37 °C). These stress-tolerant strains were grown in the presence of TFL and cerulenin. In this way, 48 isolates (3.3% of the original set) were able to grow in the presence of both drugs, being therefore potential candidates for the production of higher-quality *cachaça*. During the next selective step, 33 yeast strains presenting flocculation ability were subsequently tested for invertase activity determined in derepressive conditions (YP supplemented with 2% raffinose). The higher invertase activity has been used to identify yeast strains able to efficiently hydrolyze sucrose resulting in fructose and glucose. It should be noted that among the three select strains used in this work to produce beer and *cachaça* (LBCM45 and LBCM78) and fuel ethanol (LBCM47),

Table 1 Screening of potential *cachaça* yeast producers isolated from *cachaça* fermentation vats

<i>Cachaça</i> producer	Initial selected colonies ^a	Selected yeast by carbon source test ^{a,b}	Stress-resistant yeasts ^{a,c}	Drug-resistant yeasts ^{a,d}	Flocculant yeasts ^a	Yeast with high invertase activity ^{a,e}
1	480	439	287	14	6	1
2	480	472	359	19	19	1
3	480	191	113	15	8	1
Total	1440	1102	759	48	33	3

^aThe data is shown as absolute numbers

^bCellular growth in different carbon sources (2% glucose, galactose, or maltose)

^cStress resistance against high osmolarity (glucose 20%, sucrose 20%); high alcohol content (15%); high temperature (37 °C)

^dDrug resistance against 5,5',5''-trifluoro-DL-leucine (TFL) and cerulenin

^eYeast with invertase activity superior to 10,000 U of enzymatic activity

the last one presented a flocculation behavior (below 50%) that does not impair its use in bioethanol industry.

Table 2 shows the percentage of identity, number of gaps, bit scores, and E-values corresponding to the ITS region (ITS1-5.8 S-ITS4) of different *cachaça* yeast strains using the strain *S. cerevisiae* S288c as reference. The obtained sequences presented up to 96–98% identity when compared with the reference strain; besides, the observed bit scores and E-values suggest that all *cachaça* yeast strains analyzed are *S. cerevisiae*. Moreover, the *COXII* gene sequence of LBCM1045 seems to be closer to *S. cerevisiae* S288c with 99% identity than the *S. pastorianus* W34/70 with 94% identity (data not shown).

Additionally, the analysis of the ploidy of strains LBCM 1045, LBCM 1078, and LBCM 1047 indicates

that all are diploids, similar to *S. cerevisiae* S288c (*a/α*) used here as a standard diploid strain (Fig. 1).

Selection and characterization of *cachaça* yeast strains for beer production

Sugars present in the brewing wort for beer production are mostly maltose (50–60%), maltotriose (15–20%), and glucose (10–15%; Alves et al. 2008). Therefore, the fermentation efficiency of beer process is related to the ability of yeast strains to ferment these sugars. Among the 118 yeast strains isolated, as demonstrated in Table 1, 62 were able to grow on maltose at specific growth rates $\geq 50\%$ from that observed on glucose (Supplementary Material). However, the strains LBCM1000, LBCM1010, LBCM1013, LBCM1020, LBCM1045, LBCM1067, and LBCM1078 showed the highest growth rates on maltose, maltotriose, and

Table 2 Alignment of the internal transcribed spacer region (ITS1-5.8s-ITS4) of different yeast *cachaça* strains using the strain of *Saccharomyces cerevisiae* S288c as reference

<i>Cachaça</i> yeast strain	Identity	% Identity	Gaps	Bit score	E-value
LBCM03	840/841	99	1/841	1546	0.0
LBCM17	840/841	99	1/841	1546	0.0
LBCM29	840/841	99	–	1548	0.0
LBCM37	840/850	99	10/850	1506	0.0
LBCM45	840/848	99	8/848	1515	0.0
LBCM47	840/841	99	1/841	1546	0.0
LBCM50	840/841	99	1/841	1546	0.0
LBCM66	841/841	100	0/841	1554	0.0
LBCM73	840/841	99	1/841	1546	0.0
LBCM76	840/841	99	1/841	1546	0.0
LBCM106	839/842	99	2/842	1537	0.0

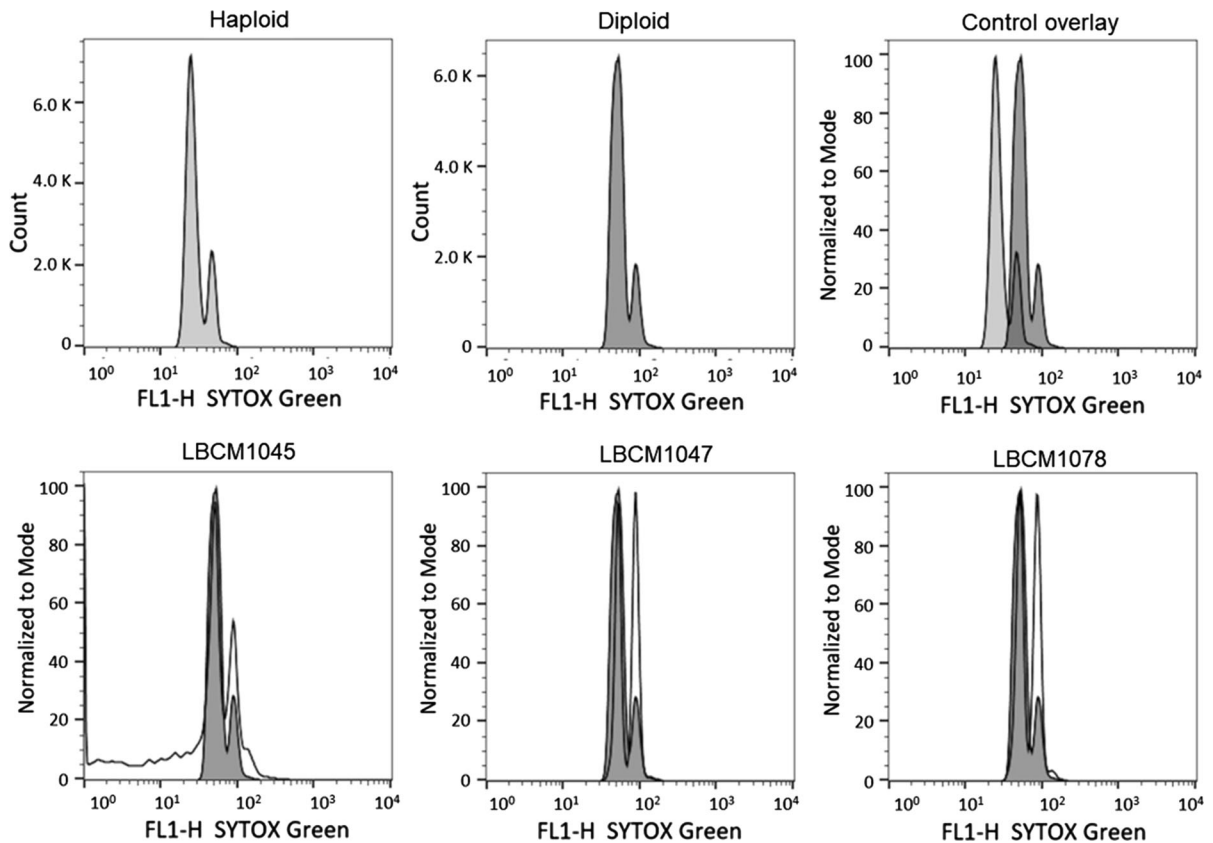


Fig. 1 Determination of ploidy by fluorescence flow cytometry. Cells were processed through the staining protocol with SYTOX[®] green (see “Materials and methods”). SYTOX[®]

green fluorescence was analyzed using FlowJo[®] software. Fluorescence histograms present cell peaks at the G0/G1 and G2/M border

glucose when compared with the commercial brewing strains (Table 3).

During biosynthesis of the amino acid methionine, yeasts produce low levels of hydrogen sulfide (H₂S). Although this is an important step in cellular metabolism, even small amounts of H₂S are harmful, affecting the organoleptic characteristics of beverages (Saerens et al. 2010). Results indicated that strains LBCM1000, LBCM1013, LBCM1020, LBCM1045, and LBCM1078 produce low levels of H₂S, similar to commercial strains (Table 3).

Brewing practices generally occur between 6 and 25 °C (Vidgren et al. 2010), so the ability to grow at low temperatures was also used as selective criteria. Among the 5 remaining strains analyzed (LBCM1000, LBCM1013, LBCM1020, LBCM1045, and LBCM1078), only strain LBCM1000 was not able to grow at 15 and at 20 °C, reducing the number of strains with potential for beer production to 4 (Table 3).

Another selective criterion was the ability to flocculate at the end of the fermentation, since natural flocculation provides a cost-efficient way to separate yeast cells from the fermented product (Verstrepen et al. 2003). In this regard, strain LBCM1045 exhibited a flocculation rate above 70% (Table 3) with appreciable production of macroscopic flocks (not shown), whereas the other 3 strains (LBCM1013, LBCM1020, and LBCM1078) presented a flocculation rate below 50% (Table 3).

The last criterion was the production of flavoring compounds in a standard condition. Therefore, all four remaining *cachaça* strains (LBCM1013, LBCM1020, LBCM1045, and LBCM1078), one commercial lager (W34/70), and one ale strain (WB-06) were compared (Fig. 2) regarding the production of higher alcohols (panel A), acetate (panel B), and medium-chain fatty acid (MCFA) esters (panel C).

Table 3 Suitable characteristics of yeast strains (growth on maltose and maltotriose, growth at low temperatures, as well as H₂S production and flocculation ability) as potential beer producers

Yeast strain	Criteria 1		Criteria 2	Criteria 3		Criteria 4
	Specific growth rates (h ⁻¹) on 2% (w/v)			H ₂ S production	Growth at	
	Glucose	Maltose	15 °C		20 °C	
LBCM1000	0.44	0.38	+	-	-	41 ± 9
LBCM1010	0.35	0.33	++	+	+	62 ± 9
LBCM1013	0.47	0.35	+	+	+	33 ± 7
LBCM1020	0.49	0.39	+	+	+	43 ± 2
LBCM1045	0.38	0.29	-	-	+	78 ± 7
LBCM1067	0.43	0.32	+++	+	+	39 ± 6
LBCM1078	0.45	0.33	+	+	+	42 ± 3
W34/70 ^a	0.32	0.35	+	+	+	35 ± 6
S04 ^a	0.46	0.43	+	+	+	49 ± 10
US05 ^a	0.89	0.80	-	+	+	54 ± 9
WB06 ^a	0.43	0.41	-	+	+	44 ± 5

^aCommercial brewing strain

Altogether, our results lead us to select strains LBCM1045 and LBCM1078 that showed similar characteristics when compared with commercial lager and ale strains, respectively. Moreover, considering that the capacity to ferment maltotriose is also a very important characteristic for beer production, the strains LBCM1045, LBCM1078, and the commercial lager W34/70 were tested for their capacity to ferment maltotriose. Although that the commercial strain presented the highest capacity to ferment maltotriose, both selected *cachaça* yeast strains also showed the capacity to ferment maltotriose here, as demonstrated by the cellular growth rate (μ) in the presence of antimycin A (inhibitor of cell respiration; Table 4). Additionally, although strain LBCM45 presents some similarities as compared with the lager commercial strain W34/70, it still shows a typical ale behavior, as demonstrated by the higher production of 4VG as compared with strain W34/70 (Table 4).

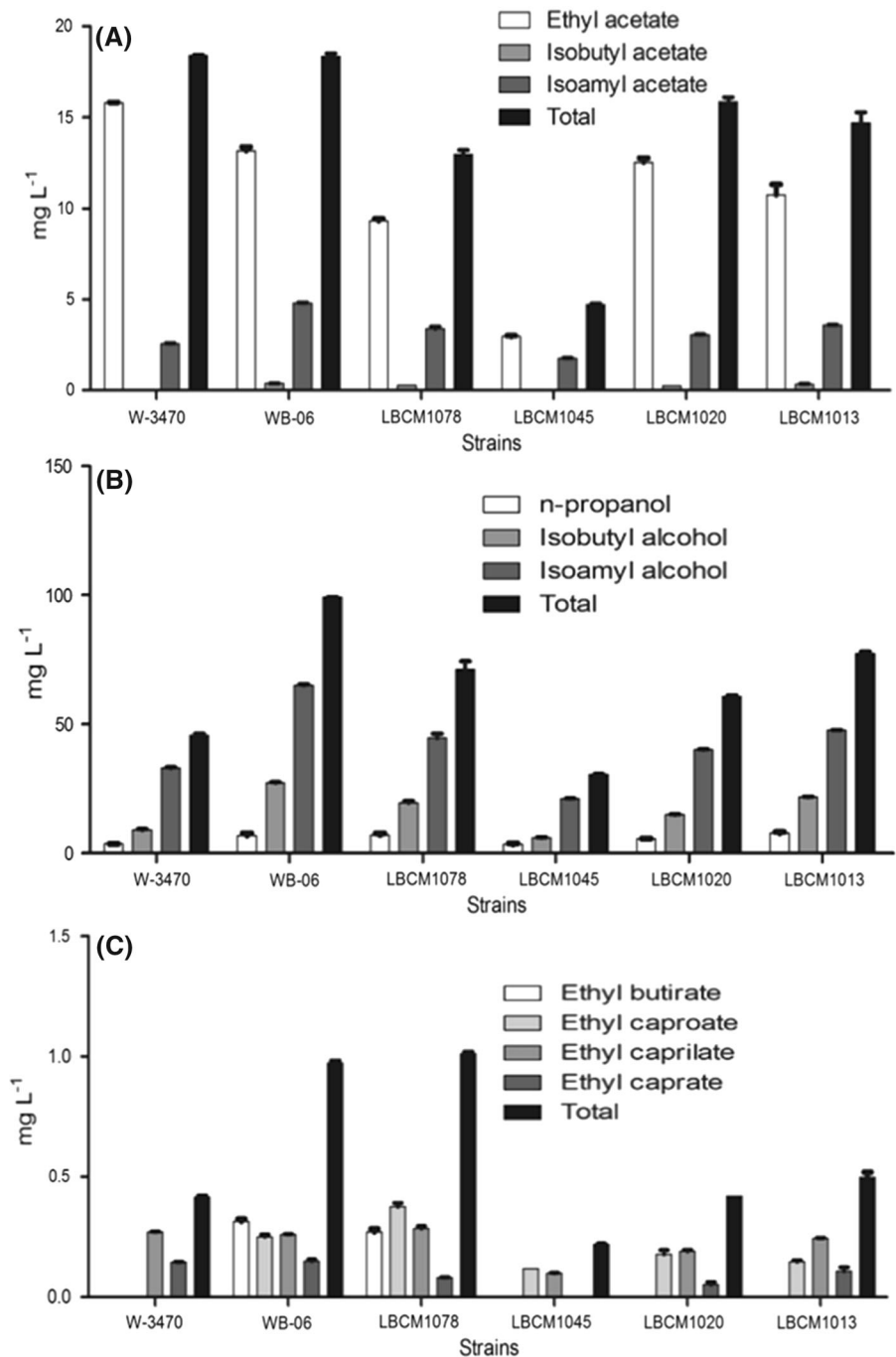
Small-scale beer production

Beer production was performed using the strains LBCM1045 and the commercial brewing *S. pastorianus* W34/70 in order to produce a pilsner style beer, and the strain LBCM1078 and the commercial brewing strain *S. cerevisiae* WB-06 (ale) to produce

Weissbier style beer. The brewing process was measured daily with a final gravity of 4.6 and 3.3 °Plato and percentages of apparent attenuation of 64.4 and 74.6% for LBCM1045 and W34/70, respectively. However, this did not affect the ethanol concentration produced by LBCM1045 and W34/70, presenting ethanol values ranging from 3.8–3.4% v v⁻¹ (Table 5). On the other hand, strains LBCM1078 and WB-06 presented a final gravity of 5.0 and 3.8 °Plato, and percentages of apparent attenuation of 62.1 and 55.3%, respectively. Both strains presented the same ethanol production with values around 4.8% v v⁻¹ of ethanol (Table 5).

Higher alcohols, esters, and carbonyl compound concentrations presented in pilsner style beer produced with strains LBCM1045 and W34/70 did not show differences at statistical levels (Table 5). In both cases, neither isoamyl acetate nor ethyl esters were detected. Weissbiers presented significant difference in relation to *n*-propanol (higher alcohol), ethyl caprylate (ester), and acetaldehyde (carbonyl compound). In the remaining compounds, both strains (LBCM1078 and WB-06) did not present statistical differences in the production of volatile compounds. It was also not possible to detect the presence of isoamyl acetate, ethyl caproate, and ethyl caprylate in any beer

Fig. 2 Flavoring compound production by selected yeast strains isolated from *cachaça* fermentation vats (LBCM1013, LBCM1020, LBCM1045, and LBCM1078) and commercial strains, W-34/70 (lager yeast) and WB-06 (ale yeast). **a** Higher alcohol concentrations (mg L^{-1}). **b** Acetate ester concentrations (mg L^{-1}). **c** Medium-chain fatty acid (MCFA) ester concentrations (mg L^{-1})



sample, but in the beer produced with LBCM1078, ethyl caprylate was detected (0.02 ppm; Table 5).

Among the off-flavor compounds, and in both beer styles, the diacetyl concentration was below the sensorial detection threshold (0.15 ppm; Kobayashi

et al. 2008). Diacetyl is enzymatically reduced to acetoin and finally to 2,3-butanediol inside yeast cells during the beer maturation process (Dequin 2001; Saerens et al. 2010). On the other hand, acetaldehyde (also an off-flavor compound) was detected only

Table 4 Growth rate in maltotriose, transport rate of α -glycosides, and production of 4-vinylguaiaicol of LBCM 45, LBCM78, and the commercial lager strain W34/70

Yeast strain	Specific growth rates (h^{-1}) on 2% maltotriose (w/v)			
	Absence of antimycin A	Presence of antimycin A	α -Glycosides transport rate ($\text{nmol min}^{-1} \text{g of cells}^{-1}$)	Production of 4-vinylguaiaicol ($\text{ppm. g of cells}^{-1}$)
LBCM1045	0.0764 ± 0.005	0.0549 ± 0.0062	676 ± 205	32 ± 4.00
LBCM1078	0.120 ± 0.011	0.0694 ± 0.0068	380 ± 70	38 ± 3.00
W34/70 ^a	0.250 ± 0.008	0.2189 ± 0.0115	480 ± 140	1.68 ± 0.32

^aCommercial brewing strain

Table 5 Physicochemical composition of beer samples produced with different yeast strains

The results are the average of three replicates \pm the standard deviation. Means followed by lower case letters are significantly different from values determined for others strains (Tukey test $p < 0.05$)

ND no detected

^AIsoamyl acetate, ethyl caproate, and ethyl caprate were not detected

Parameter	Weissbier (ale beer)		German pilsner (lager beer)	
	LBCM1078	WB-06	LBCM1045	W-34/70
Higher alcohols (ppm)				
<i>n</i> -Propanol	$4.245 \pm 0.145^{\text{b}}$	$5.176 \pm 0.156^{\text{a}}$	$3.970 \pm 0.008^{\text{b}}$	$4.076 \pm 0.024^{\text{b}}$
Isobutylalcohol	$4.277 \pm 0.173^{\text{ab}}$	$4.425 \pm 0.062^{\text{a}}$	$3.977 \pm 0.016^{\text{c}}$	$4.095 \pm 0.045^{\text{bc}}$
Isoamylalcohol	$11.531 \pm 0.350^{\text{a}}$	$11.628 \pm 0.064^{\text{a}}$	$10.393 \pm 0.107^{\text{b}}$	$10.599 \pm 0.063^{\text{b}}$
Esters (ppm) ^A				
Ethylacetate	$16.770 \pm 3.780^{\text{a}}$	$22.429 \pm 5.622^{\text{a}}$	$14.567 \pm 0.452^{\text{a}}$	$13.778 \pm 0.738^{\text{a}}$
Ethyl caprilate	0.015 ± 0.006	ND	ND	ND
Carbonyl compounds (ppm)				
Acetaldehyde	$1.176 \pm 0.248^{\text{a}}$	$0.806 \pm 0.010^{\text{b}}$	$0.807 \pm 0.005^{\text{b}}$	$0.886 \pm 0.026^{\text{ab}}$
Diacetyl	$0.034 \pm 0.001^{\text{a}}$	$0.033 \pm 0.001^{\text{a}}$	$0.033 \pm 0.001^{\text{a}}$	$0.034 \pm 0.002^{\text{a}}$
Ethanol (% v/v)	$4.80 \pm 0.92^{\text{a}}$	$4.79 \pm 0.88^{\text{a}}$	$3.76 \pm 0.49^{\text{a}}$	$3.41 \pm 0.32^{\text{a}}$
pH	5.90	4.32	4.99	5.20

below 25 ppm (sensory detection threshold). Again, there was no difference in acetaldehyde concentration in the two beer styles. Thus, physicochemical analysis of on- and off-flavor compounds showed the potential use of LBCM1045 and LBCM1078 for beer production (Table 5).

Small-scale *cachaça* production

The results obtained from the analyses of volatile acidity and concentrations of ethanol, higher alcohols, esters, and aldehydes demonstrated that both strains (LBCM1045 and LBCM1078) produced *cachaça* within limits allowed by Brazilian legislation (Brazil 2005; Table 6). The main difference between the strains was the higher production of isoamyl alcohol by LBCM1045 when compared with LBCM1078 (80.9 ± 3.7 and $67.2 \pm 0.9 \text{ mg L}^{-1}$, respectively). On the other hand, the levels of ethyl esters were

comparable in both cases (LBCM1045 with 0.18 ± 0.01 and LBCM1078 with $0.17 \pm 0.01 \text{ mg L}^{-1}$). After distillation, both *cachaça* samples presented alcohol content of 47%.

Selection of *cachaça* yeast strains for bioethanol production

Bioethanol industrial-like fermentations were performed throughout repetitive fermentative cycles interspersed with sulfuric acid treatment at pH 2.0 for 30 min. PE2, an industrial strain, was used as a control. All fermentations had as initial inoculum 162 g of wet yeast mass - about 8% of the bioreactor volume. This mass corresponded approximately to 1.48×10^{10} cells mL^{-1} of PE2 strain and 1.31×10^{10} cells mL^{-1} of LBCM1047 strain. The final cellular concentration after 8 h of fermentation was on average

Table 6 Physico-chemical composition of *cachaça* samples produced by two selected yeast strains (LBCM1045 and LBCM1078) in pilot scale

Yeast strain	Volatile acidity ^a	Acetaldehyde ^b	Ethyl acetate ^b	Methanol ^b	Higher alcohols ^b
LBCM1045	32.00 ± 1.5	19.01 ± 2.52	23.03 ± 0.51	4.02 ± 0.08	243.71 ± 15.41
LBCM1078	13.60 ± 1.41	5.96 ± 1.91	12.54 ± 1.02	2.90 ± 0.20	260.90 ± 34.11
Legal limits ^c	≤ 150	≤ 30	≤ 200	≤ 20	≤ 360

^aAcetic acid (mg)/100 mL must

^bmg/100 mL Anhydrous alcohol

^cAccording to Brazilian legislation

3.84×10^{10} cells mL⁻¹ of PE2 strain and 3.25×10^{10} cells mL⁻¹ of LBCM1047 strain.

The fermentative yield ($Y_{P/S}$) of PE2 varied from 0.41 to 0.49 g g⁻¹, whereas for LBCM1047 strain, it varied from 0.40 to 0.50 g g⁻¹, with an average ethanol production of 66.86 and 69.00 L⁻¹, respectively (Fig. 3). The fermentative yield of PE2 ranged from 80.6 to 95.8%, whereas for LBCM1047 strain, it ranged from 77.4 to 97.9% when compared with the maximum theoretical yield of ethanol, which was 0.51 g for 1 g of consumed carbohydrate.

To measure the efficiency of fermentation, it is useful to calculate the relation between the other organic compounds (e.g., glycerol) and ethanol and to compare their values with those found in the literature (Andrietta et al. 2011). Regarding the presence of

glycerol, fermentations performed with LBCM1047 and PE2 show K_G values of 0.07 and 0.14 g g⁻¹, respectively (Fig. 4a). Considering the presence of organic acids, the ratio of organic acid produced-to-ethanol (K_{AC}) should be the lowest possible. Once again, the values for both yeast strains were similar (Fig. 4b) with K_{AC} values of PE2 ranged from 0.016 to 0.022 g g⁻¹, whereas for LBCM47, it ranged from 0.019 to 0.023 g g⁻¹.

In this work, fermentations were performed for 8 h, which is similar to that found in bioethanol industry (Basso et al. 2011). The volumetric productivity of ethanol ranged between 7.62 and 9.86 g L⁻¹ h⁻¹, whereas no reduction of ethanol production rate was observed during the recycles in both strains (Fig. 5a). In addition to high levels of ethanol production, washing acid resistance is one of the more desirable characteristics in bioethanol yeast producers. PE2 and LBCM1047 presented cellular and bud viability higher than 95% during whole fermentations (data not shown). Regarding the cellular growth rate, both strains showed similar production of biomass per time (Fig. 5b). In turn, the specific ethanol production rate also did not demonstrate significant differences between both strains (Fig. 5c). Another widely used parameter in the alcohol industry is the ratio of ethanol-to-g of cell (K_L) which ranges between 0.04 and 0.05 g g⁻¹ in an optimized industry (Andrietta et al. 2012). In the present work, interestingly, K_L values were up to 400% higher (Fig. 5d).

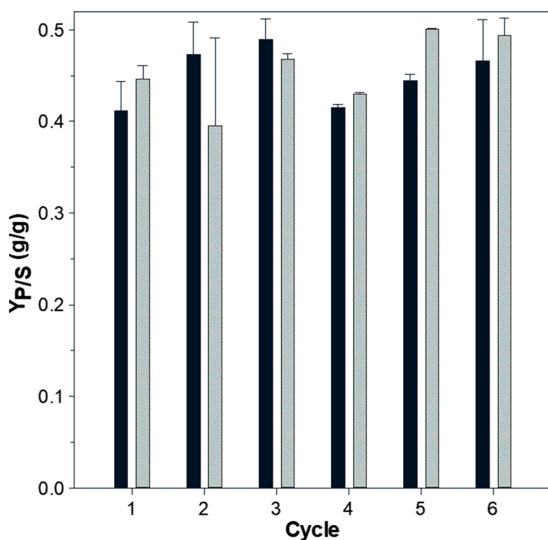


Fig. 3 Ethanol yield ($Y_{P/S}$) of the PE2 (black column), a bioethanol industry yeast strain, and LBCM1047 (gray column), a *cachaça* yeast strain isolated from *cachaça* fermentation vats

Discussion

Considering that yeast strains isolated from *cachaça* fermentation vats are rarely considered as an

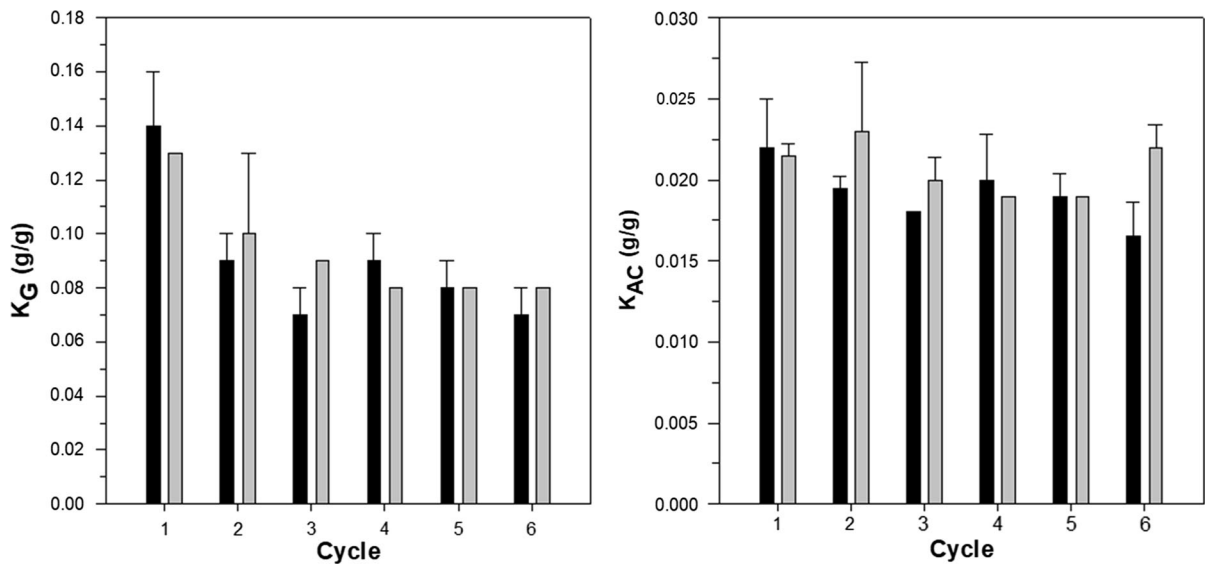
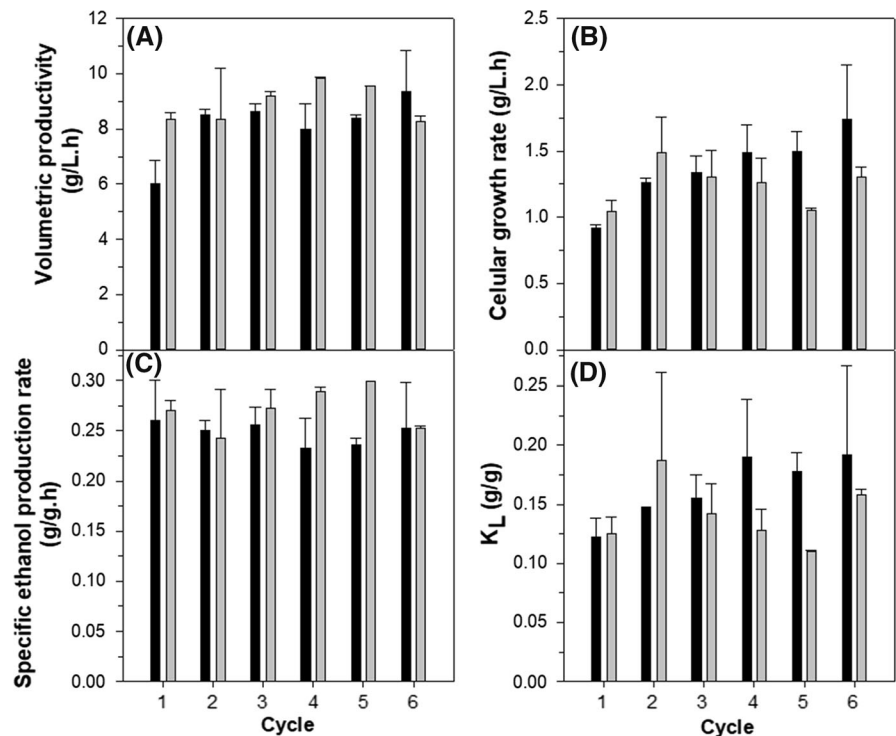


Fig. 4 Production of glycerol, lactic acid, and ethanol by PE2 (black column) and LBCM1047 (gray column) strains. **a** Ratio of production of glycerol-to-ethanol (K_G). **b** Ratio of production of lactic acid-to-ethanol (K_{AC})

Fig. 5 Main fermentative parameters used in bioethanol industry to compare the fermentative capacity of PE2 (black column) and LBCM1047 (gray column) strains. **a** Volumetric productivity [$\text{g} (\text{L h})^{-1}$]. **b** Cellular growth rate [$\text{g} (\text{L h})^{-1}$]. **c** Specific ethanol production rate [$\text{g} (\text{L h})^{-1}$]. **d** Ratio ethanol-to-g of cell (g g^{-1})



alternative source of starters for biotechnological applications, and also taking in account idleness of the infrastructure already existent in *cachaça* distilleries (fermentation vats, storage tanks, bottling machine, etc.), we decided to study the use of *cachaça*

yeast strains for beer and bioethanol production as a broader strategy to optimize their utilization, as well as to offer a possibility to improve the economic profitability of the business.

Thus, the production of beer could be advantageous to the *cachaça* producers since they could produce different beverages during the whole year by using the same yeast, as starter, and using the same facilities. Interestingly, we have already demonstrated that yeast strains locally selected can be used as unique natural factor for obtainment of the protected denomination of origin (PDO; Barbosa et al. 2016).

Therefore, to verify the capacity of *cachaça* yeast strains to produce high-quality beverages, two strains (LBCM1045 and LBCM1078) were used for the production of two different beers (lager and ale) and *cachaça*. Both strains were able to produce beer and *cachaça* with a standard quality. Interestingly, strain LBCM1045 shares the majority of the properties of a commercial lager brewery yeast strain. Considering that lager strains might have resulted from hybridization between an ale *S. cerevisiae* and a *S. eubayanus* strain originally found in Patagonia (Argentina; Libkind et al. 2011), it may be that some hybridization could also have occurred in the case of strain LBCM1045.

Indeed, other cases of hybridization events have been described, involving, for instance, *S. cerevisiae* and *S. kudriavzevii* strains generally present in brewing and wine-making (Querol and Bond 2009). Thus, the coexistence of different yeasts of the genus *Saccharomyces* in wineries and breweries could favor hybridization in such environments by rare mating between diploid strains (Barros-Lopes et al. 2002). In fact, regardless to their origin, hybridization events led to new industrial yeast strains, such as those used in wine and lager beer production, providing new strains with clear advantages over parental ones (González et al. 2007, 2008).

On the other hand, it is known that the capacity of lager strains to grow at low temperatures has been attributed to the cryotolerance of the parental strain *S. bayanus* (or *S. eubayanus*; Libkind et al. 2011). However, the fact that the fermentation process during *cachaça* production rarely falls below 30 °C, it is quite surprising for a strain that presents the capacity to grow at low temperatures (15 °C) to ferment melibiose and to present strong flocculation behavior as observed in the *S. pastorianus* (W34/70), a lager beer strain.

To clarify this apparent contradiction, we have explored the possible hybrid nature of strain LBCM1045 by comparing the sequence of the

mitochondrial gene *COX II* found in the strain LBCM1045 with *S. cerevisiae* S288c and *S. pastorianus* W34/70. Since the results showed a similarity of 99 and 94%, respectively, it is reasonable to speculate that another type of genomic modification has occurred to explain the fermentative behavior of LBCM1045 and/or specific fermentative behavior, such as capacity to ferment at low temperatures, is not necessarily present in a strain because its ancestrally.

In fact, this is still a matter of controversy since it has been demonstrated that other ale-brewing *S. cerevisiae* strains can also tolerate low temperatures (Gallone et al. 2016). Moreover, we have also been able to generate intraspecific hybrid strains (by using only *S. cerevisiae* strains also isolated from *cachaça* distilleries) able to ferment malt extract at 12 °C and produce more ethanol than their corresponding parental strains and comparable to the lager strain *S. pastorianus* W34/70 (Figueiredo et al. 2017).

Interestingly, it has been demonstrated that different types of strains seem to coexist in *cachaça* fermentations with the presence of intraspecific hybrids or mestizo strains (Badotti et al. 2014). Mestizo strains present alleles related to yeast strains found in European wines and similar alleles to those found in strains isolated from traditional fermentations from Latin America, North America, Malaysian, Japan, or West Africa. Therefore, we cannot dismiss the fact that strain LBCM1045 is also a mestizo strain that would present alleles coming from one or more strains and/or that different species had contributed to constitute this new and interesting strain with a lager-like behavior.

Moreover, in spite of the fact that strain LBCM1045 showed good fermentation performance at low temperatures, high flocculation capacity, desirable production of acetate esters (comparable to one commercial lager strain), and its capacity to ferment maltotriose, the higher production of phenolic compounds indicates that additional work must be done to allow its utilization in the production of lager beers. Indeed, we have demonstrated that alternative techniques can be used to create new and interesting strains to be used in beer production (Figueiredo et al. 2017), and this strain can be used for further improvements.

On the other hand, and considering that the Brazilian biofuel industry also uses sugarcane juice to produce ethanol, *cachaça* distilleries could improve their revenues by also producing bioethanol. In fact,

we had already analyzed the potential for ethanol production of the yeast strains isolated from *cachaça* fermentation vats (Conceição et al. 2015). At the laboratory scale, all strains of our collection were screened, aiming to select those with appropriate characteristics for ethanol production such as (i) high ethanol production, (ii) high tolerance to aluminum and zinc ions present in fermentative must used in production of first-generation bioethanol; (iii) low foam production; and (iv) resistance to acid washing. After this screening, we concluded that LBCM1047 showed fermentative yields similar to the yeast most widely commercialized in the Brazilian bioethanol industry, PE2. Also, higher resistance to aluminum ions and pH ranges was observed as compared with others strains. These characteristics in addition to the higher fermentative capacity suggest that this yeast strain has high applicability in the bioethanol industry (Conceição et al. 2015). In spite of the fact that in the fuel ethanol industry flocculation, is not a recommended characteristic for a yeast strain, LBCM1047 was chosen because its flocculative behavior was not strong. Therefore, it was submitted to similar procedures used in the bioethanol industry, such as intercalating fermentation cycles with sulfuric acid washings (pH 2.0) and reusing of biomass.

As is already known, many factors can decrease fermentative capacity during bioethanol production: medium composition, stress conditions, or genetic background of the yeast (Basso et al. 2011). In general, adverse conditions lead to an increase in the production of other compounds such as glycerol and/or organic acids in alcoholic fermentation (Pagliardini et al. 2013). For this reason, ethanol production is not the only parameter that should be analyzed to verify if a strain can produce ethanol in industrial conditions. Ideally, to be used in the bioethanol industry, a yeast strain should present high ethanol yield and low production of other compounds, as well as present high cell viability. Therefore, among the main products frequently analyzed are glycerol (main secondary product of alcoholic fermentation), acids (indicative of contaminations), and biomass production. Concentration of glycerol can bypass up to 10% of carbohydrates present in the fermentative must, with K_G values around of 0.04–0.05 g g⁻¹ (Andrietta et al. 2012); however, in our conditions, the values obtained by both PE2 and LBCM1047 strains are a little higher (0.07–0.14 g g⁻¹). The reduction of K_G values can be

obtained by changing the fermentation conditions from batch to fed-batch system (Alfenore et al. 2002). On the other hand, biomass production, without loss of the ethanol yield, is an interesting factor for industry, since it indicates that the yeast can remain longer in fermentation vats during the full ethanol production cycle, which is approximately 240 days (Andrietta et al. 2011). The high values of K_L presented in this work were probably a consequence of adequate fermentative conditions with temperature control, sterility, and standardization that should favour cellular growth. In the majority of parameters analyzed, LBCM1047 presented a fermentative behavior similar to PE2, highlighted by ethanol production, cellular viability, and low production of acids and glycerol.

In conclusion, we demonstrated that *cachaça* fermentation vats seem to represent a niche with high ecological diversity to select yeast cells that, due to their specific properties, can be used to produce beverages and bioethanol. Considering the economic feasibility, the combination of all these productive chains in a single industry (*cachaça* distilleries) could contribute to improving the financial income of *cachaça* producers, mainly those presenting a small-scale production.

Acknowledgements This work was supported by grants from Coordenação de Aperfeiçoamento de Pessoal de Nível Superior (CAPES/Brazil - Program AUXPE-DINTER 2499/2008); Fundação de Amparo à Pesquisa do Estado de Minas Gerais (FAPEMIG/Brazil - Process APQ-00209-12); and from Conselho Nacional de Desenvolvimento Científico e Tecnológico (CNPq/Brazil - Process 304815/2012-3 - research fellowship to RLB and Process 580185/2008-7). We are grateful to CNPEM and CTBE for helpful assistance with fermentation techniques and chromatographic analysis as well as to multiuser laboratories for mass spectrometry and microscopy: NUPEB, UFOP.

Conflict of interest All co-authors have seen and agreed with the content of the manuscript, and none of the co-authors have any financial interests to disclose.

References

- Alfenore S, Molina-Jouve C, Guillouet S, Uribelarrea J-L, Goma G, Benbadis L (2002) Improving ethanol production and viability of *Saccharomyces cerevisiae* by a vitamin feeding strategy during fed-batch process. *Appl Microbiol Biotechnol* 60:67–72

- Alvarez F, Correa LFdM, Araújo TM, Mota BEF, Conceição LEFR, Castro IM, Brandão RL (2014) Variable flocculation profiles of yeast strains isolated from *cachaça* distilleries. *Int J Food Microbiol* 190:97–104
- Alves SL, Herberts RA, Hollatz C, Trichez D, Miletti LC, De Araujo PS, Stambuk BU (2008) Molecular analysis of maltotriose active transport and fermentation by *Saccharomyces cerevisiae* reveals a determinant role for the AGT1 permease. *Appl Environ Microbiol* 74:1494–1501
- Amorim HV, Lopes ML, de Castro Oliveira JV, Buckeridge MS, Goldman GH (2011) Scientific challenges of bioethanol production in Brazil. *Appl Microbiol Biotechnol* 91:1267–1275
- Andrietta MGS, Stupiello ÉNA, Andrietta SR (2011) Bioethanol-what has Brazil learned about yeasts inhabiting the ethanol production processes from sugar cane? In: Bernardes MAS (ed) *Biofuel production-recent developments and prospects*. INTECH Open Access, pp 67–84
- Andrietta SR, Andrietta MGS, Bicudo MHP (2012) Comparação do rendimento fermentativo utilizando diferentes metodologias de cálculo para a avaliação do desempenho de um processo industrial. *Sociedade dos Técnicos Açucareiros e Alcooleiros do Brasil* 30:41–49
- Badotti F, Vilaça ST, Arias A, Rosa CA, Barrio E (2014) Two interbreeding populations of *Saccharomyces cerevisiae* strains coexist in *cachaça* fermentations from Brazil. *FEMS Yeast Res* 14:289–301
- Barbosa EA et al (2016) Quality improvement and geographical indication of *cachaça* (Brazilian spirit) by using locally selected yeast strains. *J Appl Microbiol* 121:1038–1051
- Barros-Lopes M, Bellon JR, Shirley NJ, Ganter PF (2002) Evidence for multiple interspecific hybridization in *Saccharomyces sensu stricto* species. *FEMS Yeast Res* 1:323–331
- Basso LC, Rocha SN, Basso TO (2011) Ethanol production in Brazil: the industrial process and its impact on yeast fermentation. In: Bernardes MADs (ed) *Biofuel production-recent developments and prospects*. INTECH, Croatia, pp 85–100
- Brányik T, Vicente AA, Dostálek P, Teixeira JA (2008) A review of flavour formation in continuous beer fermentations. *J Inst Brew* 114:3–13
- Brazil (2005) Instrução Normativa n° 13 vol Instrução Normativa n° 13. *Diário Oficial da União, Brasília*
- Bussey H, Umberger HE (1970) Biosynthesis of the branched-chain amino acids in yeast: a leucine-binding component and regulation of leucine uptake. *J Bacteriol* 103:277–285
- Conceição LE et al (2015) Biotechnological potential of yeast isolates from *cachaca*: the Brazilian spirit. *J Ind Microbiol Biotechnol* 42:237–246. <https://doi.org/10.1007/s10295-014-1528-y>
- Dequin S (2001) The potential of genetic engineering for improving brewing, wine-making and baking yeasts. *Appl Microbiol Biotechnol* 56:577–588
- D'Hautcourt O, Smart KA (1999) Measurement of brewing yeast flocculation. *J Am Soc Brew Chem* 57:123–128
- Ekunsumi T, Odunfa S (1990) Ethanol tolerance, sugar tolerance and invertase activities of some yeast strains isolated from steep water of fermenting cassava tubers. *J Appl Bacteriol* 69:672–675
- Faria-Oliveira F, Diniz RH, Godoy-Santos F, Piló FB, Mezadri H, Castro IM, Brandão RL (2015) The role of yeast and lactic acid bacteria in the production of fermented beverages in South America. In: Eissa AHA (ed) *Food production and industry*. Intech, Croatia, pp 107–135
- Figueiredo BIC, Saraiva MAF, Pimenta PPS, Testasica MCS, Afonso LCC, Sampaio GMS, Castro IM, Brandão RL (2017) New lager brewery strains obtained by crossing techniques using *cachaça* (Brazilian spirit) yeast strains. *Appl Environ Microbiol* 83(20):e01582
- Gallone B et al (2016) Domestication and divergence of *Saccharomyces cerevisiae* beer yeasts. *Cell* 166(1397–1410): e1316
- González SS, Gallo L, Climent MD, Barrio E, Querol A (2007) Enological characterization of natural hybrids from *Saccharomyces cerevisiae* and *S. kudriavzevii*. *Int J Food Microbiol* 116:11–18
- González SS, Barrio E, Querol A (2008) Molecular characterization of new natural hybrids of *Saccharomyces cerevisiae* and *S. kudriavzevii* in brewing. *Appl Environ Microbiol* 74:2314–2320
- Haase SB, Reed SI (2002) Improved flow cytometric analysis of the budding yeast cell cycle. *Cell cycle* 1:117–121
- IBGE (2016) Instituto Brasileiro de Geografia e Estatística [Brazilian Institute of Geography and Statistics]. <http://www.ibge.gov.br/>. Accessed 11/10 2016
- Ichikawa E, Hosokawa N, Hata Y, Abe Y, Suginami K, Imayasu S (1991) Breeding of a sake yeast with improved ethyl caproate productivity. *Agric Biol Chem* 55:2153–2154
- Jiranek V, Langridge P, Henschke P (1995) Regulation of hydrogen sulfide liberation in wine-producing *Saccharomyces cerevisiae* strains by assimilable nitrogen. *Appl Environ Microbiol* 61:461–467
- Kobayashi M, Shimizu H, Shioya S (2008) Beer volatile compounds and their application to low-malt beer fermentation. *J Biosci Bioeng* 106:317–323
- Lee S, Robinson F, Wang H Rapid determination of yeast viability. In: *Biotechnology and bioengineering symposium*, Ann Arbor, 1981. vol CONF-810554-. University of Michigan
- Libkind D et al (2011) Microbe domestication and the identification of the wild genetic stock of lager-brewing yeast. *Proc Natl Acad Sci* 108:14539–14544
- Löoke M, Kristjuhan K, Kristjuhan A (2011) Extraction of genomic DNA from yeasts for PCR-based applications. *Biotechniques* 50:325
- Martini C, Margarido LAC, Ceccato-Antonini SR (2010) Microbiological and physicochemical evaluations of juice extracted from different parts of sugar cane stalks from three varieties cultivated under organic management. *Food Sci Technol* 30:808–813
- Nakao Y et al (2009) Genome sequence of the lager brewing yeast, an interspecies hybrid. *DNA Res* 16:115–129
- Oliveira VA et al (2008) Biochemical and molecular characterization of *Saccharomyces cerevisiae* strains obtained from sugar-cane juice fermentations and their impact in *cachaca* production. *Appl Environ Microbiol* 74:693–701. <https://doi.org/10.1128/AEM.01729-07>
- Pagliardini J, Hubmann G, Alfenore S, Nevoigt E, Bideaux C, Guillouet SE (2013) The metabolic costs of improving ethanol yield by reducing glycerol formation capacity

- under anaerobic conditions in *Saccharomyces cerevisiae*. *Microb Cell Fact* 12:29
- Pataro C, Guerra JB, Petrillo-Peixoto ML, Mendonça-Hagler LC, Linardi VR, Rosa CA (2000) Yeast communities and genetic polymorphism of *Saccharomyces cerevisiae* strains associated with artisanal fermentation in Brazil. *J Appl Microbiol* 89:24–31. <https://doi.org/10.1046/j.1365-2672.2000.01092.x>
- Powell CD, Quain DE, Smart KA (2003) The impact of brewing yeast cell age on fermentation performance, attenuation and flocculation. *FEMS Yeast Res* 3:149–157
- Querol A, Bond U (2009) The complex and dynamic genomes of industrial yeasts. *FEMS Microbiol Lett* 293:1–10
- Saerens S, Delvaux F, Verstrepen K, Van Dijck P, Thevelein J, Delvaux F (2008) Parameters affecting ethyl ester production by *Saccharomyces cerevisiae* during fermentation. *Appl Environ Microbiol* 74:454–461
- Saerens SM, Delvaux FR, Verstrepen KJ, Thevelein JM (2010) Production and biological function of volatile esters in *Saccharomyces cerevisiae*. *Microb Biotechnol* 3:165–177
- Satyanarayana T, Umbarger H, Lindegren G (1968) Biosynthesis of branched-chain amino acids in yeast: regulation of leucine biosynthesis in prototrophic and leucine auxotrophic strains. *J Bacteriol* 96:2018–2024
- Schwan RF, Mendonca AT, Silva JJ Jr, Rodrigues V, Wheals AE (2001) Microbiology and physiology of *Cachaca* (Aguardente) fermentations. *Antonie Van Leeuwenhoek* 79:89–96
- Verstrepen K, Derdelinckx G, Verachtert H, Delvaux F (2003) Yeast flocculation: what brewers should know. *Appl Microbiol Biotechnol* 61:197–205
- Vicente MA, Fietto LG, Castro IM, dos Santos AN, Coutrim MX, Brandao RL (2006) Isolation of *Saccharomyces cerevisiae* strains producing higher levels of flavoring compounds for production of “cachaça” the Brazilian sugarcane spirit. *Int J Food Microbiol* 108:51–59. <https://doi.org/10.1016/j.ijfoodmicro.2005.10.018>
- Vidgren V, Multanen J-P, Ruohonen L, Londesborough J (2010) The temperature dependence of maltose transport in ale and lager strains of brewer’s yeast. *FEMS Yeast Res* 10:402–411
- White TJ, Bruns T, Lee S, Taylor T (1990) Amplification and direct sequencing of fungal RNA genes for phylogenetic. In: Inn MA, Gelfrand DH, Sninsky JJ, With, TJ (eds) *PCR protocols: a guide to methods and applications*. Academic Press, New York
- Yu Z, Zhao M, Li H, Zhao H, Zhang Q, Wan C, Li H (2012) A comparative study on physiological activities of lager and ale brewing yeasts under different gravity conditions. *Biotechnol Bioprocess Eng* 17:818–826

RESEARCH ARTICLE

Lpx1p links glucose-induced calcium signaling and plasma membrane H⁺-ATPase activation in *Saccharomyces cerevisiae* cells

Diogo Dias Castanheira, Eduardo Perovano Santana, Fernanda Godoy-Santos, Raphael Hermano Santos Diniz, Fábio Faria-Oliveira, Renata Rebeca Pereira, Maria José Magalhães Trópia, Ieso Miranda Castro and Rogelio Lopes Brandão*

Laboratório de Biologia Celular e Molecular, Núcleo de Pesquisas em Ciências Biológicas, Escola de Farmácia, Universidade Federal de Ouro Preto, Campus do Morro do Cruzeiro, Ouro Preto, MG 35.400-000, Brazil

*Corresponding author: Laboratório de Biologia Celular e Molecular, Núcleo de Pesquisas em Ciências Biológicas/NUPEB, Universidade Federal de Ouro Preto Campus do Morro do Cruzeiro, Ouro Preto, MG 35.400-000, Brazil. Tel/Fax: +55-31-3559-1723; E-mail: rbrand@nupeb.ufop.br

One sentence summary: Relationship between calcium and plasma membrane H⁺-ATPase activation in yeast.

Editor: Terrance Cooper

ABSTRACT

In yeast, as in other eukaryotes, calcium plays an essential role in signaling transduction to regulate different processes. Many pieces of evidence suggest that glucose-induced activation of plasma membrane H⁺-ATPase, essential for yeast physiology, is related to calcium signaling. Until now, no protein that could be regulated by calcium in this context has been identified. Lpx1p, a serine-protease that is also involved in the glucose-induced activation of the plasma membrane H⁺-ATPase, could be a candidate to respond to intracellular calcium signaling involved in this process. In this work, by using different approaches, we obtained many pieces of evidence suggesting that the requirement of calcium signaling for activation of the plasma membrane H⁺-ATPase is due to its requirement for activation of Lpx1p. According to the current model, activation of Lpx1p would cause hydrolysis of an acetylated tubulin that maintains the plasma membrane H⁺-ATPase in an inactive state. Therefore, after its activation, Lpx1p would hydrolyze the acetylated tubulin making the plasma membrane H⁺-ATPase accessible for phosphorylation by at least one protein kinase.

Keywords: calcium signaling; plasma membrane H⁺-ATPase; Lpx1; *Saccharomyces cerevisiae*

INTRODUCTION

Plasma membrane H⁺-ATPase is an essential enzyme for yeast physiology since by pumping protons out of cells it creates the electrochemical potential that allows cells to accumulate nutrients against their concentration gradients and to control intracellular pH (Goffeau and Slayman 1981). This enzyme is regulated both at the transcriptional (Capieaux et al.

1989; Rao, Drummond-Barbosa and Slayman 1993) and at the post-translational (Serrano 1993) levels on glucose addition, this sugar being the most important trigger for its regulation. Originally, it was proposed that H⁺-ATPase post-translational activation would be caused by phosphorylation catalyzed by protein kinases that would have as targets two phosphorylation sites at the plasma membrane H⁺-ATPase C-terminal tail

Received: 8 May 2017; Accepted: 17 November 2017

© FEMS 2017. All rights reserved. For permissions, please e-mail: journals.permissions@oup.com

(Portillo 2000). According to this model, phosphorylation of residue Ser-899 would be responsible for a decrease in K_m for ATP, and phosphorylation of Thr-912 would lead to an increase of V_{max} related to ATP hydrolysis (Portillo, Eraso and Serrano 1991). Later, it was demonstrated that the second phosphorylation site includes another serine residue (Ser-911) that would also be associated with glucose addition (Lecchi et al. 2005, 2007). Moreover, it was confirmed that phosphorylation of both residues (Ser-911 and Thr-912) seems to be connected to the activation process (Mazón, Eraso and Portillo 2015).

Although it has been shown that glucose-induced activation of the plasma membrane H^+ -ATPase is caused by phosphorylation, the search for protein kinases involved in this process led, up to now, to the identification of Ptk2p as a unique protein kinase involved with the phosphorylation of the Ser-899 residue at the C-terminal tail (Goossens et al. 2000; Eraso, Mazón and Portillo 2006). Recently, a wide screening of protein kinases present in yeast cells reconfirmed the essential involvement of Ptk2p in the glucose-induced activation of the plasma membrane H^+ -ATPase. Thus, these data indicate that the current model suggesting the existence of two phosphorylation sites (and another protein kinase indeed involved in this process, besides Ptk2p) seems to be incorrect or, at least, incomplete (Pereira et al. 2015).

Indeed, new elements have been introduced in this scenario confirming the complexity of the mechanism responsible for plasma membrane H^+ -ATPase post-translational activation. Over the years, many results have suggested the existence of a clear relationship between calcium signaling and plasma membrane H^+ -ATPase activation (Cocchetti et al. 1998; Tisi et al. 2002, 2004; Trópia et al. 2006; Pereira et al. 2008; Groppi et al. 2011; Bouillet et al. 2012). *Saccharomyces cerevisiae* as a eukaryotic organism can use calcium-signaling pathways to control different cellular processes (Anraku, Ohya and Iida 1991; Paidhungat and Garrett 1997; Denis and Cyert 2002; Serrano et al. 2002). In the cytosol of yeast cells, the free Ca^{2+} concentration is strictly regulated (Miseta et al. 1999b) by the action of a variety of transporters, channels, pumps and co-transporters (Cyert and Philpott 2013). Ca^{2+} in yeast is retained mainly in the vacuole (Dunn, Gable and Beeler 1994; Miseta et al. 1999a) and the vacuolar pool is maintained mostly by the action of Pmc1p (a Ca^{2+} -ATPase) and Vcx1p (a Ca^{2+}/H^+ exchanger). The release of calcium stored in vacuoles is made through the calcium channel Yvc1p, which has its activity controlled by different cellular stimuli (Cunningham 2011).

Apparently, the connection between calcium signaling and H^+ -ATPase activation starts when glucose-induced phosphatidylinositol-4,5-bisphosphate hydrolysis occurs. Mediated by phospholipase C (encoded by the PLC1 gene), this hydrolysis produces two intracellular messengers: diacylglycerol and inositol 1,4,5-trisphosphate (IP_3) (York et al. 1999; Shears 2000). This Plc1p activation would be initiated in response to a stimulus from protein G (Gpa2p), which in turn would be activated in response to glucose uptake and its phosphorylation by sugar kinases (Bouillet et al. 2012). In turn, the level of IP_3 is regulated by its phosphorylation by Arg82p, an inositol kinase, generating two types of inositol tetrakisphosphate— $I(1,3,4,5)P_4$ and $I(1,4,5,6)P_4$ —and an inositol pentaphosphate, $I(1,3,4,5,6)P_5$ (Saiardi et al. 1999; Odom et al. 2000).

A possible relationship between IP_3 and the vacuolar Ca^{2+} channel, Yvc1p, was demonstrated previously, suggesting that this channel could participate in a mechanism involved in intracellular calcium level control in response to glucose addition. IP_3 would interact directly or indirectly with Yvc1p, regulating the

intensity of calcium signaling in the cytosol (Bouillet et al. 2012). In *arg82Δ* yeast strains, where there is no conversion of IP_3 into IP_4 and/or IP_5 , glucose-induced increase of IP_3 , H^+ -ATPase activation and calcium signaling are more pronounced (Tisi et al. 2004).

At low external calcium concentration, the vacuolar calcium channel Yvc1p's activity seems to become more important for proper glucose-induced calcium signaling and plasma membrane H^+ -ATPase activation. Moreover, there are many pieces of evidence suggesting that the intensity of the intracellular calcium signal, in these conditions, is strongly dependent on the action of Yvc1p (Bouillet et al. 2012) and that there is a connection between the IP_3 signal, Yvc1 activity, calcium signaling and glucose-induced activation of the plasma membrane H^+ -ATPase in yeast cells (Tisi et al. 2004; Trópia et al. 2006). Nevertheless, since no IP_3 receptor homolog has been identified in the *S. cerevisiae* genome (Wera, Bergsma and Thevelein 2001), the existence of such a transduction pathway is still a matter of controversy (Bouillet et al. 2012).

On the other hand, some data suggest the involvement of a multifunctional enzyme in glucose-induced activation of the plasma membrane H^+ -ATPase (Campetelli et al. 2013). By this model, glucose addition would trigger activation of proteolytic activity of Lpx1p, which degrades the tubulin bound to the inactive form of plasma membrane H^+ -ATPase at its C-terminal tail. This degradation releases the C-terminal tail leading to the exposure of sites that are targets of phosphorylation, causing H^+ -ATPase activation (Campetelli et al. 2005, 2013).

Considering these two sets of evidence for H^+ -ATPase activation, calcium involvement and Lpx1p dependence, and the apparent difficulty in finding other protein kinase(s), mainly the calcium-dependent ones, involved in enzyme phosphorylation/activation, we explored a possible relationship between calcium signaling and Lpx1p activation in connection with glucose-induced regulation of the plasma membrane H^+ -ATPase. Here, we demonstrated that calcium signaling is indeed directly related to Lpx1p proteolytic action, and this activation process is clearly related to the plasma membrane H^+ -ATPase.

MATERIAL AND METHODS

Strains and growth conditions

Saccharomyces cerevisiae strains shown in Table 1 were grown in media containing 2% peptone and 1% yeast extract (YP) supplemented with appropriate carbon sources or in SD medium—0.67% yeast nitrogen base without amino acids (Difco, Detroit, MI, USA) supplemented with drop-out amino-acids (leucine, tryptophan, histidine and methionine) and nucleotide (uracil) and 2% glucose. Cells were grown in a rotatory incubator shaker - New Brunswick Model 25 (GMI, Ramsey, MN, USA) at 200 rpm and 30°C until the end of the logarithmic phase ($OD_{600nm} \sim 2.0$). Alternatively, and when requested, yeast cells were grown in induction medium (SD medium supplemented with 8% galactose).

Molecular biology methods and in silico analysis

Yeast cells were transformed by using the lithium acetate protocol (Gietz et al. 1995). A pVTU-apoaequorin plasmid (pVTU-AEQ) was generated by inserting in pVTU XhoI-PstI sites the XhoI-PstI-digested fragment obtained by PCR on pYX212-AEQ (Tisi et al. 2002) using the oligonucleotides 5'-TTTCTCGAGAATCTATACTACAAAAACACATACAGGAA-3' and 5'-TAACTGCAGGCCCTAGGATCCATGGTGAA-3'.

Table 1. *Saccharomyces cerevisiae* strains used in this study.

Strain	Genotype	Source
PJ69-2A	MATa <i>trp1-901 leu2-3, 112 ura3-52 his3-200 gal4Δ gal80Δ</i> <i>LYS2::GAL1-HIS3 GAL2-ADE2 met2::GAL7-lacZ</i>	James Caffrey (Saiardi et al. 2000)
PJ69-4A1	PJ69-2A <i>arg82::KanMX2</i>	James Caffrey (Saiardi et al. 2000)
LBCM 1630	PJ69-2A <i>yvc1::KanMX2</i>	Bouillet et al. (2012)
LBCM 1713	LBCM 1630; <i>lpx1::LEU2</i>	This work
LBCM 1714	PJ69-4A1; <i>lpx1::LEU2</i>	This work
BY4741	MATa <i>his3Δ1 leu2Δ0 lis2Δ0 ura3Δ0</i>	EUROSCARF
BY4741 <i>lpx1Δ</i>	BY4741; <i>lpx1::KanMX4</i>	EUROSCARF
BY4741 <i>ptk2Δ</i>	BY4741; <i>ptk2::KanMX4</i>	EUROSCARF
LBCM 1738	BY4741 <i>lpx1Δ</i> + pYES2/CT-EV	This work
LBCM 1739	BY4741 <i>lpx1Δ</i> + pYES2/CT-LPX1	This work
LBCM 1764	BY4741 <i>lpx1Δ</i> + pYES2/CT-LPX1-MOD	This work

The LPX1 gene was obtained as previously described (Campetelli et al. 2013) and then inserted into the pYES2/CT plasmid (Invitrogen, Carlsbad, CA, USA) allowing inducible expression by galactose of recombinant proteins fused with a 6× His-tag at the C-terminus. For this purpose, plasmid and amplified LPX1 gene were previously digested with KpnI and XbaI enzymes (see Supplementary Material 1) (Fermentas, Waltham, MA, USA). Digested plasmid was treated with shrimp alkaline phosphatase (SAP) (Fermentas) for 1 h at 37°C prior to ligation. The SAP-treated plasmid was used for the T4 ligase reaction (Sigma-Aldrich, St Louis, MO, USA) with LPX1 insert. This ligation reaction was performed at 23°C for 1 h, and *Escherichia coli* strain TOP10 was used for plasmid replication. BY4741 *lpx1Δ* cells were transformed with pYES2/CT + LPX1 (Gietz et al. 1995) and selected in SD medium with 2.5% agar—from here on denominated as pYES2/CT-LPX1. The presence of the gene insertion into the plasmid and correct transformation in bacteria and yeast were confirmed by PCR (forward primer: 5'-AAAGGTACCATGGAACAGAACAGGTCC-3'; reverse primer: 5'-TTTTCTAGATTACAGTTTTGTGTTAGTCG-3'). BY4741 *lpx1Δ* cells were transformed with an empty vector (here denominated as pYES2/CT-EV) as well, to be used as the control treatment.

In order to find regions in Lpx1p protein structure that could interact with Ca²⁺, the WebFEATURE 4.0 server (Liang et al. 2003; Wu, Liang and Altman 2008) was run using a deposited structure (crystal form II; trigonal) of Lpx1p from *S. cerevisiae* (PDB access number: 2y6u) (Thoms et al. 2011) with settings defined to search for all functional sites possibly present in this protein (Supplementary Material 2).

To verify the influence of the C-terminal region of Lpx1p that would interact with Ca²⁺ in Lpx1p activation, this region was removed by treating the LPX1 gene with PvuII enzyme that cuts at 909 bp after the initiation codon. The modified gene was cloned into the pYES2/CT plasmid (see Supplementary Material 3). Digested LPX1 gene and pYES2/CT plasmid were then treated with KpnI. Digested plasmid was used for the T4 ligase reaction (Sigma-Aldrich) with modified LPX1 insert. This ligation reaction was performed at 23°C overnight and *E. coli* strain TOP10 was used for plasmid replication. BY4741 *lpx1Δ* cells were transformed with pYES2/CT + modified LPX1 (Gietz et al. 1995) and selected in SD medium with 2.5% agar—from here on denominated as pYES2/CT-LPX1-MOD. The presence of the gene insertion into the plasmid and correct transformation in bacteria and yeast were confirmed by PCR (forward primer: 5'-AAAGGTACCATGGAACAGAACAGGTCC-

3'; reverse primer: 5'-GCGTGAATGTAAGCGTGAC-3'), by comparing different amplicon sizes between pYES2/CT-LPX1 and pYES2/CT-LPX1-MOD.

Measurement of cytosolic free calcium by bioluminescence assay

By using a standard method, cytosolic free calcium was measured by using the aequorin-based bioluminescence assay (Tisi et al. 2002; Brandão 2014; Tisi, Martegani and Brandão 2015). Yeast strains containing the apoaequorin-expressing plasmid pVTU-AEQ were grown in rich medium (YP with 2% glucose) until they entered the exponential phase. Cells were harvested and washed by filtration with sterile water and resuspended in MES/Tris 0.1 M (pH 6.5). After 90 min of incubation at room temperature, cells were loaded with 50 μM coelenterazine (Sigma-Aldrich, St. Louis, MO, USA) for 20 min. For removal of excess coelenterazine, cells were washed twice by centrifugation (2000 g, 5 min) with MES/Tris 0.1 M pH 6.5. Glucose-induced aequorin luminescence was measured in a Lumat LB 9507 luminometer (Berthold Technologies, Bad Wildbad, Germany) at intervals of 10 s for 1 min before and for at least 10 min after addition of 100 mM glucose (final concentration).

Lpx1p His-tag expression and purification

To obtain cells for Lpx1p His-tag extraction, the *lpx1Δ* mutant transformed with pYES2/CT-LPX1, and pYES2/CT-LPX1-MOD plasmids were grown in SD medium for 24 h. Cells were collected, washed three times by centrifugation (2000 g, 5 min) with sterile water and resuspended in induction medium (SD medium supplemented with 8% galactose). After overnight incubation in a rotatory incubator shaker (New Brunswick Model 25) at 200 rpm and 30°C, cells were harvested by vacuum filtration on glass fiber filters, immediately frozen in liquid nitrogen and stored until use.

Cells were resuspended in lysis buffer (50 mM Na₃PO₄, 300 mM NaCl and 5 mM β-mercaptoethanol), disrupted by vigorous shaking with glass beads (with 90 s intervals on ice for five times) and then centrifuged at 2000 g for 10 min. The resulting supernatant (crude extract) was incubated with HIS-Select nickel affinity gel (Sigma-Aldrich, St. Louis, MO, USA) for 1 h at 4°C with gentle agitation. Unbound proteins were removed by discarding supernatant after centrifugation at 1000 g for 5 min. Proteins bound to resin were eluted with elution buffer (50 mM

Na₃PO₄, 300 mM NaCl, 5 mM β-mercaptoethanol). Induction and protein purification were performed with pYES2/CT-EV strain, to be used as the control treatment. Aliquots (50 μg) of protein fractions were separated by SDS-PAGE using 12% (w/v) polyacrylamide gels. Gels were stained with silver staining and images were captured by Image Scanner software (Thermo Fisher Scientific, Waltham, MA, USA). The molecular masses of the proteins were calculated by interpolating their specific relative migration distances (R_f) in a curve prepared with correspondent values of appropriated molecular mass markers (Supplementary Material 4).

Western blotting assays were performed with eluates obtained from cell extracts of the *lpx1Δ* mutant transformed with pYES2/CT-EV, pYES2/CT-LPX1 and pYES2/CT-LPX1-MOD constructions. Protein content was determined by using the Lowry method (Lowry et al. 1951). Next, the proteins were transferred to nitrocellulose membranes (Thermo Fisher Scientific, Waltham, MA, USA) according to the recommendations of the Bio-Rad Transference Kit (Bio-Rad Laboratories, Hercules, CA, USA). Membranes were blocked for 1 h at room temperature, using PBS containing 0.1% Tween-20 and 5% skimmed milk powder. Furthermore, membranes were incubated with mouse monoclonal primary antibody anti-His (Invitrogen, Carlsbad, CA, USA). Subsequently, membranes were washed and incubated with secondary antibody horseradish peroxidase-goat anti-mouse IgG (H + L) (Invitrogen, Carlsbad, CA, USA). Immunolabeling was visualized using WESTAR Nova 2.0 (Cyanagen, Bologna, Italy) as per the manufacturer's instructions. Images were captured by Image Scanner software (Amersham Biosciences, Bath, UK).

Measurement of proteolytic Lpx1p activity

Calcium dependence of the proteolytic activity of the wild-type and *lpx1Δ* cells was assayed by using azocasein (Thermo Fisher Scientific, Waltham, MA, USA) as substrate (Charney and Tomarelli 1947). Briefly, samples of total membranes containing 50–100 μg protein were added to a reaction mixture (100 mM Tris-HCl, pH 8.0, 0.5% azocasein), with or without the addition of 1 mM calcium, in a final volume of 500 μL. The mixture was kept for 1 h at 40°C, and after this time, the reaction was stopped by adding 250 μL of 10% w/v trichloroacetic acid. The mixture was centrifuged (2000 g, 5 min) to remove coagulated proteins and 500 μL of supernatant was neutralized with 500 μL 5 M KOH, and the absorbance at 428 nm was measured using a BioMate 3 spectrophotometer (Thermo Fisher Scientific, Waltham, MA, USA). A change in absorbance of 0.01 (428 nm) per minute, resulting from azocasein hydrolysis, was defined as one arbitrary unit (AU). The control was obtained by mixing trichloroacetic acid with the azocasein solution prior to the addition of the protein sample (Secades and Guijarro 1999). Protein content was determined by using the Lowry method (Lowry et al. 1951).

An additional Lpx1p activity evaluation was performed with eluates obtained from the Ni-affinity column from *lpx1Δ* mutant transformed with pYES2/CT-LPX1. Samples containing 100 μg protein were dissolved in non-reducing Laemmli buffer (62.5 mM Tris-HCl, pH 6.8, 10% w/v glycerol, 0.001% w/v bromophenol blue) and run at 100 V at 4°C in 8% (w/v) polyacrylamide gel. After electrophoresis, the corresponding Lpx1p bands were excised from the gel and washed three times in 100 mM Tris-HCl buffer, pH 8.0, with gentle agitation, in order to remove excess SDS from the running buffer. Then, they were added to a reaction mixture (100 mM Tris-HCl, pH 8.0, 0.5% azo-

casein), containing 100 μM calcium, in a final volume of 500 μL and the assay was performed as described previously in this work. A negative control was obtained by using the corresponding material from *lpx1Δ* mutant transformed with pYES2/CT-EV.

Measurement of plasma membrane H⁺-ATPase activity

In vivo activation of plasma membrane H⁺-ATPase was detected by using two different standard approaches: indirectly, measuring glucose-induced proton-pumping activity, or directly, in purified plasma membranes by following ATP hydrolysis.

In the first case, around 500 mg (wet weight) of cells grown in YP medium (with 2% glucose) was resuspended in 100 mM Tris-HCl buffer pH 4.5 containing 100 mM KCl and incubated in a vessel in a total volume of 5.0 mL. Changes in pH suspension were recorded before and after addition of 100 mM glucose (final concentration). Calibration pulses of 100 nmol HCl were also added and used as reference in calculations of proton pumping. The maximal rate of proton pumping was calculated from the slope of the line indicating the pH variation in the medium, as described previously, and indicated in mmol H⁺ h⁻¹ g⁻¹ cell (Souza, Tropa and Brandao 2001).

To measure proton-pumping activity from *lpx1Δ* or *yvc1Δ* mutants transformed with pYES2/CT-EV and pYES2/CT-LPX1 vectors, cells grown in SD medium were washed twice by centrifugation (2000 g, 5 min) with 100 mM Tris-HCl buffer pH 4.5 containing 100 mM KCl. After washing, cells were incubated in the same buffer containing 100 mM galactose (final concentration) prior to proceeding with the assay to promote the induction of the LPX1 gene. After incubation with 100 mM galactose for different times (10, 30 or 50 min), cells were washed twice by centrifugation (2000 g, 5 min) with 100 mM Tris-HCl buffer pH 4.5 containing 100 mM KCl, and then used to measure *in vivo* proton-pumping activity as described (Souza, Tropa and Brandao 2001). Cells without incubation with 100 mM galactose were used as controls.

In the second approach, to measure directly the H⁺-ATPase activity, *lpx1Δ* mutant transformed with pYES2/CT-EV and pYES2/CT-LPX1 vectors was collected after overnight incubation in induction medium (SD medium supplemented with 8% galactose) in a rotatory incubator shaker (New Brunswick Model 25) at 200 rpm and 30°C, prior to proceeding with plasma membrane purification. Cells were washed twice by centrifugation (2000 g, 5 min) with 100 mM MES/Tris buffer (pH 6.5), collected on glass fiber filters by vacuum filtration, immediately frozen in liquid nitrogen and stored until use. Cells were disrupted in 100 mM Tris buffer (supplemented with 330 mM sorbitol and 5 mM β-mercaptoethanol), by vigorous shaking with glass beads, with 90 s intervals on ice five times and centrifuged at 2000 g for 10 min. Purified plasma membranes were obtained essentially as described before (dos Passos et al. 1992), with resuspension of plasma membranes in glycerol buffer (20% w/v glycerol, 10 mM Tris, 1 mM β-mercaptoethanol). Protein content was determined by using the Lowry method (Lowry et al. 1951). ATPase activity was determined as described previously (dos Passos et al. 1992).

On the other hand, and to study a direct connection between calcium availability, Lpx1p activity and plasma membrane H⁺-ATPase regulation, we tried to reconstitute *in vitro* the plasma membrane H⁺-ATPase activation. First, to extract plasma membranes, wild-type cells were resuspended in 100 mM MES/Tris buffer (pH 6.5) at a density of 150 mg mL⁻¹ (wet mass) and incubated in a shaking water bath at 30°C. After 4 h, samples (glucose-starved cells) were collected on glass fiber filters

by vacuum filtration and immediately frozen in liquid nitrogen and stored until use. The procedures used to obtain plasma membranes were performed as described previously (dos Passos et al. 1992), without addition of EDTA in lysis and glycerol buffers. Briefly, to obtain a membrane-free extract (MFE), cells were suspended in 100 mM Tris buffer without protease inhibitors (supplemented with 330 mM sorbitol and 5 mM β -mercaptoethanol), disrupted by vigorous shaking with glass beads with 90 s intervals on ice five times, and centrifuged at 2000 *g* for 10 min. The supernatant was then centrifuged at 100 000 *g* for 30 min. After ultracentrifugation, a new supernatant yielded membrane-free extracts (from here on denominated as MFE) from all strains; these as well as HIS-Select nickel affinity gel eluates resulting from the application of crude extract of *lpx1* Δ mutant cells transformed with pYES2/CT-EV, pYES2/CT-LPX1 and pYES2/CT-LPX1-MOD were subsequently submitted to overnight dialysis at 4°C with incubation buffer (50 mM HEPES, 10 mM sodium azide, 5 mM ammonium molybdate). This procedure was necessary in order to remove any interfering compound for *in vitro* H⁺-ATPase activity assay. Protein content was determined by using the Lowry method (Lowry et al. 1951).

In vitro H⁺-ATPase activation was performed by resuspending plasma membrane samples (40 μ g protein) obtained from glucose-starved wild-type cells in an incubation buffer (50 mM HEPES, 10 mM sodium azide, 5 mM ammonium molybdate). Then, 100 μ M Ca²⁺ and/or MFE (50 μ g protein) was added (or not) according to the different tests performed, to a final volume of 250 μ L (more details in Results section). In all samples, 1 mM MgCl₂ (final concentration) was also added. The samples were incubated for 30 min at 30°C in a water bath, for *in vitro* H⁺-ATPase activation. Different calcium concentrations (100 μ M, 1 and 5 mM), different times of incubation (10, 30 and 60 min) and different MFE protein concentrations (50, 100, 200 and 400 μ g) for *in vitro* H⁺-ATPase activation were tested. Sodium orthovanadate of 50 μ M was added as well to verify H⁺-ATPase activity inhibition. MFE and HIS-Select nickel affinity gel eluates were assayed to check for any ATPase activity as control. All results are expressed as percentages relative to their related controls.

To assay H⁺-ATPase activity, the reactions were started with concentrated ATP solution (Sigma-Aldrich) to obtain 2 mM as final concentration. ATPase activity was determined as described previously (dos Passos et al. 1992) and appropriate controls were performed for each assay (see Results section for specific details).

Statistical analysis

The experiments were performed at least three times. Standard deviations were indicated in each figure or table. Statistical analyses were performed by using Student's *t*-test or ANOVA. Differences were considered statistically significant when the *P* value was <0.05.

RESULTS

Lpx1p influences H⁺-ATPase activation, but not intracellular calcium concentration

It was previously suggested that in glucose-induced activation of yeast plasma membrane H⁺-ATPase, calcium signaling is a critical factor (Souza, Tropia and Brandao 2001; Tisi et al. 2004; Trópia et al. 2006; Pereira et al. 2008; Bouillet et al. 2012). However, in the corresponding signal transduction pathway a component that actually would respond to the intracellular calcium signal was

never found. Since the Lpx1p protein also participates in this process (Campetelli et al. 2013), we wondered whether this protease could be a possible candidate that would respond to the calcium signal, thereby explaining its function in plasma membrane H⁺-ATPase glucose-induced activation.

Indeed, as demonstrated in Fig. 1A, plasma membrane H⁺-ATPase glucose-induced activation (measured indirectly by proton-pumping rate) was reduced in strains presenting deletion in the LPX1 gene. Comparable results (i.e. reduced H⁺-ATPase glucose-induced activation) were also observed in *yvc1* Δ strain (absence of Yvc1p reduces glucose-induced calcium signaling by preventing calcium release from the vacuole, which reduces H⁺-ATPase activation). On the other hand, deletion of ARG82 causes a clear stronger glucose-induced activation of the plasma membrane H⁺-ATPase compared with wild-type cells, since these cells present high IP₃ levels in cytoplasm, which enhances calcium release from vacuole leading to an increase in the H⁺-ATPase activity. However, when LPX1 deletion was also included in this *arg82* Δ mutant, H⁺-ATPase activity was reduced as observed in the cell presenting only the *lpx1* Δ mutation. The same standard was also observed in a strain presenting deletions in the YVC1 and LPX1 genes, i.e. H⁺-ATPase activity showed comparable low levels to *yvc1* Δ cells. The same was observed in the double mutant *yvc1* Δ *lpx1* Δ (Fig. 1A).

In the same set of strains and in similar conditions, the influence of LPX1 deletion in calcium signaling was assessed (Fig. 1B). Initially, it was observed that the strain with single LPX1 deletion showed calcium signaling comparable to wild-type cells. When LPX1 was deleted in combination with ARG82, there was a stronger intracellular calcium signal, as observed in *arg82* Δ mutant cells. Calcium signaling was reduced in *yvc1* Δ cells and in the double mutant *yvc1* Δ *lpx1* Δ strain. Therefore, the results shown in Fig. 1 suggest that Lpx1p is not necessary for generation of calcium signal on glucose treatment; however, it is required for calcium-mediated activation of the H⁺-ATPase. Thus, Lpx1p should work downstream of IP₃ and calcium signaling and, consequently, can form a link between the calcium signal and the H⁺-ATPase function.

Moreover, this hypothesis was also reinforced by the fact that a database search, using Lpx1p crystal structure, indicated the presence of a potential region for calcium interaction with a high-confidence prediction (95% precision performance) located at its C-terminus (Supplementary Material 2), suggesting that this domain would be an EF-hand calcium-binding domain.

Overexpression of LPX1 in an *lpx1* Δ mutant restores normal proton-pumping rate and increases H⁺-ATPase activity

An *lpx1* Δ mutant yeast strain expressing the LPX1 gene fused with a His-tag at the 3'-extremity in a galactose-inducible vector (pYES2/CT-LPX1) was generated to verify the potential connection between calcium signaling and Lpx1p activation. As control, the *lpx1* Δ yeast strain was transformed with the corresponding empty vector (pYES2/CT-EV). In order to check the suitability of these constructions, transformant yeasts were submitted to galactose induction for different incubation times (10, 30 and 50 min for pYES2/CT-LPX1 and 50 min for pYES2/CT-EV). After induction, glucose-induced extracellular acidification was performed. As shown in Fig. 2A, cells expressing the LPX1 gene presented an increase in proton-pumping rates after galactose induction (*P* < 0.05), when compared with non-induced cells. After 10, 30 and 50 min, proton-pumping rate was increased

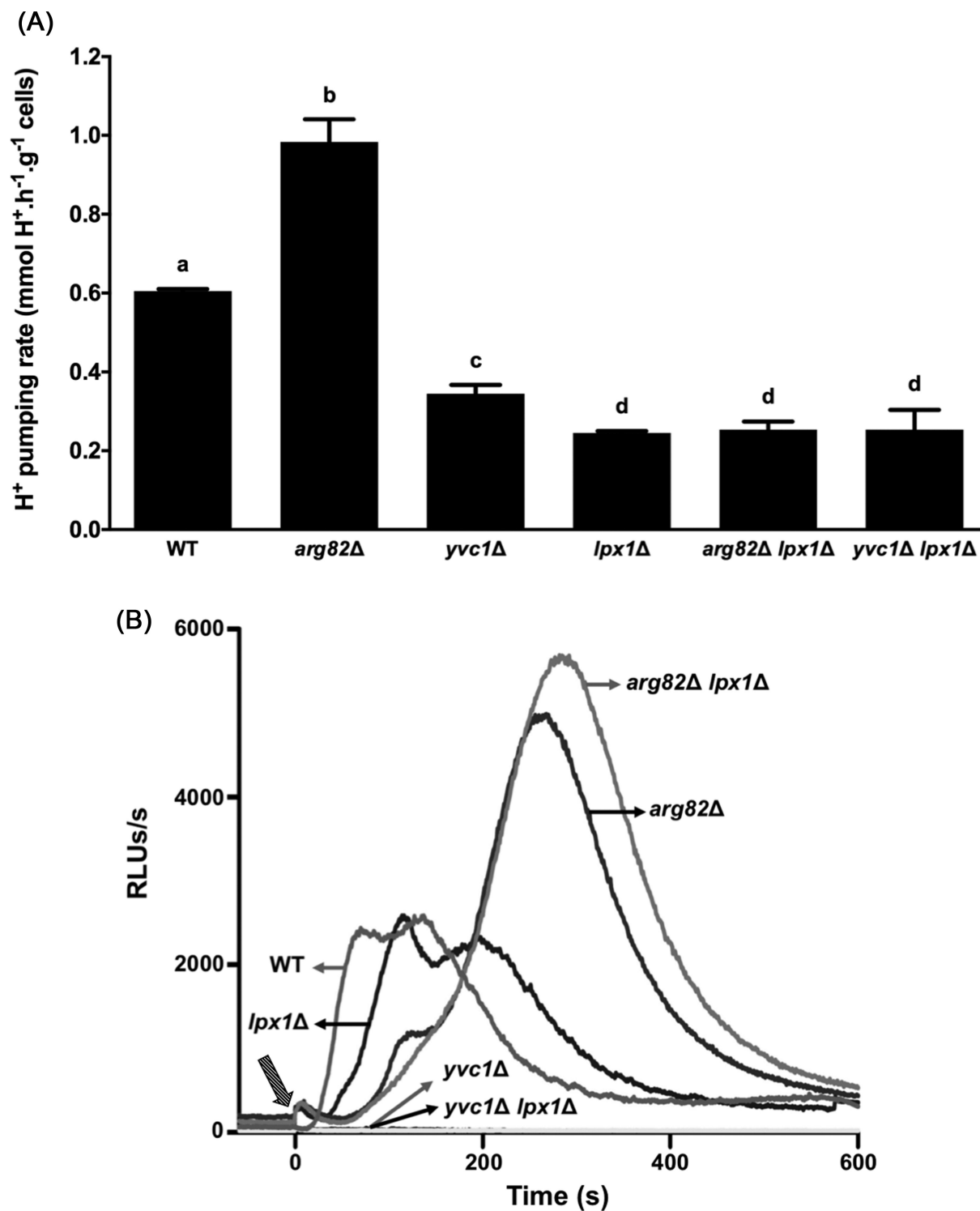


Figure 1. Effects of different gene deletions on H⁺-ATPase proton-pumping activity and intracellular calcium signaling in *S. cerevisiae* cells (genetic background PJ69-2A). (A) Proton-pumping activity was measured with around 500 mg of cells, after addition of 100 mM glucose (final concentration). (B) Cytosolic free calcium was measured by using a standard aequorin-based bioluminescence assay after addition of 100 mM glucose (final concentration), indicated by a striped arrow at '0' s, in yeast strains containing apoaequorin-expressing plasmid pVTU-AEQ and loaded with 50 μM coelenterazine. Different letters indicate that mean values are statistically different ($P < 0.05$). RLUs/s: relative luminescence units per second.

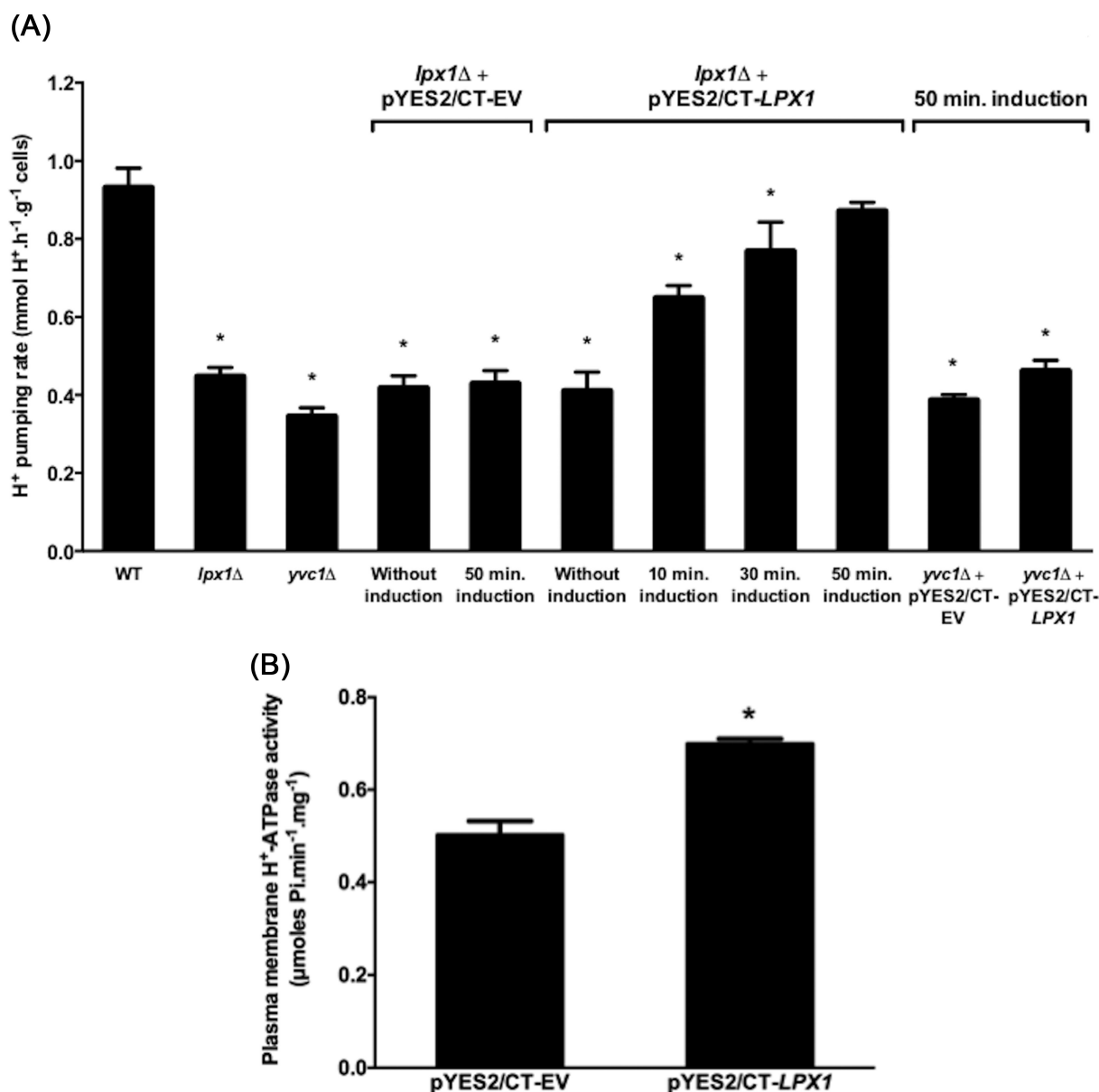


Figure 2. Plasma membrane proton-pumping rate and ATPase activity in *lpx1*Δ mutant transformed with pYES2/CT-EV and pYES2/CT-LPX1 vectors after induction by galactose in different times. Wild-type strain (BY4741) and the corresponding *lpx1*Δ and *yvc1*Δ mutants were used as controls. (A) Proton-pumping rate was measured with around 500 mg of cells after induction for different times with 100 mM galactose. Cells without incubation with 100 mM galactose were used as controls. (B) To measure ATPase activity from purified plasma membrane H⁺-ATPase, cells were collected after overnight induction with galactose, and membranes were obtained as described previously with a standard method. Different letters and asterisk indicate that mean values are statistically different ($P < 0.05$).

to 58.0%, 87.3% and 112.4%, respectively, compared with cells without galactose induction. Proton-pumping activity after 50 min induction in pYES2/CT-LPX1 cells was comparable to the wild-type strain ($P > 0.05$). Cells transformed with the empty plasmid did not exhibit any increase in proton-pumping rate after 50 min galactose induction, showing the same rate as found in the *lpx1*Δ strain ($P > 0.05$). Interestingly, when the *yvc1*Δ mutant was also transformed with such constructions and exposed to galactose, there was no increase in the H⁺-pumping rate even after 50 min, with the activity remaining comparable to that registered for the *yvc1*Δ mutant (Fig. 2A). These results suggest that the activity of the calcium channel Yvc1 is not controlled by Lpx1p.

In addition, to check the role of Lpx1p in H⁺-ATPase activation, ATPase activity was measured in purified plasma membranes of the *lpx1*Δ yeast strains transformed with pYES2/CT empty vector (pYES2/CT-EV) and the one containing the LPX1 gene (pYES2/CT-LPX1). After overnight galactose induction, plasma membranes from strain pYES2/CT-LPX1 showed higher activity ($P < 0.05$) than purified plasma membranes from the control strain, pYES2/CT-EV (Fig. 2B).

Proteolytic activity of Lpx1

Initially, crude extracts of *lpx1*Δ strains transformed with pYES2/CT-EV (empty vector, used as control), pYES2/CT-LPX1

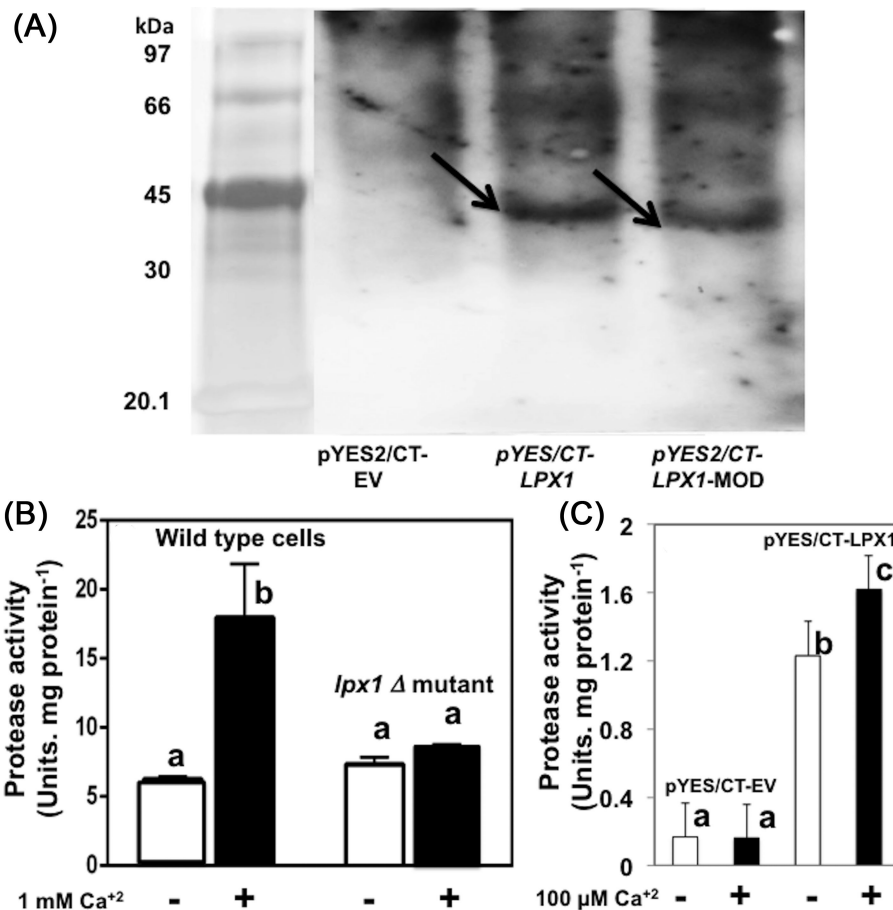


Figure 3. Lpx1p His-Tag expression and proteolytic activity. Cells were incubated overnight in induction medium, collected and disrupted in lysis buffer. Resulting supernatant (crude extract) was incubated with HIS-Select nickel affinity gel (Sigma-Aldrich). Unbound proteins were removed by centrifugation. Column-bound proteins were recovered with elution buffer. (A) Western blotting assay using anti-His antibodies in samples of nickel-column eluates obtained from *lpx1*Δ strain transformed with the empty vector pYES2/CT-EV and vectors carrying pYES2/CT-LPX1 or pYES2/CT-LPX1-MOD. Arrows indicate specific bands. (B) Proteolytic activity of total membranes from wild-type and *lpx1*Δ mutant was assessed by using azocasein as substrate. A protein fraction was added to a reaction mixture (100 mM Tris-HCl, pH 8.0, 0.5% azocasein) with or without addition of calcium. One enzymatic activity unit was defined as a change in absorbance of 0.01 (428 nm) per minute in these conditions. (C) Lpx1p activity was evaluated in excised protein bands obtained from SDS-PAGE gels after electrophoresis of eluates of the *lpx1*Δ mutant transformed from pYES2/CT-EV and pYES2/CT-LPX1 vectors. Samples (100 μg of protein) were dissolved in non-reducing Laemmli buffer and run in non-reducing conditions at 4°C. Lpx1p bands (indicated by arrows in A) and the corresponding region obtained from the control system (indicated by a circle in A) were excised from gel and added to a reaction mixture (100 mM Tris-HCl, pH 8.0, 0.5% azocasein), with or without addition of calcium. One enzymatic activity unit was defined as a change in absorbance of 0.01 (428 nm) per minute in these conditions. In all cases, results are expressed as specific activity (as mg protein⁻¹). Different letters and asterisk indicate that mean values are statistically different ($P < 0.05$).

(vector containing LPX1 whole gene) and pYES2/CT-LPX1-MOD (vector containing a modified LPX1 gene, where the binding calcium domain was removed) were prepared and applied to a nickel column, to perform Lpx1p (or Lpx1p-MOD) His-tag purification. In order to confirm the presence of His-tagged Lpx1 proteins, a western blotting assay was performed (Fig. 3A) with eluates obtained from *lpx1*Δ cells transformed with pYES2/CT-EV, pYES2/CT-LPX1 and pYES2/CT-LPX1-MOD (without calcium-binding domain). The results demonstrated that the eluates from the nickel column recovered from *lpx1*Δ cells presented specific bands only in extracts obtained from *lpx1*Δ cells transformed with pYES2/CT-LPX1 and pYES2/CT-LPX1-MOD. Furthermore, no band was detected in the extract obtained from the strain transformed with the empty vector. Additionally, reduction in molecular mass of the Lpx1p from 49 to 41 kDa was confirmed in a western blotting experiment that used extracts obtained from *lpx1*Δ cells transformed from pYES2/CT-LPX1

and pYES2/CT-LPX1-MOD, respectively. These results were supported by differences in their specific relative migration distances (R_f) (Supplementary Material 4).

The proteolytic activity of Lpx1 and its Ca²⁺ dependence was demonstrated by two different approaches: first, we isolate total membranes from wild-type and *lpx1*Δ cells and the activity was tested using a non-specific substrate (azocasein). As demonstrated in Fig. 3B, the presence of 1 mM calcium increases the proteolytic specific activity (AU/mg protein⁻¹) in samples from wild-type cells; on the other hand, this effect was not observed in membrane samples obtained from the *lpx1*Δ mutant cells.

Another experiment was performed to confirm the proteolytic activity of Lpx1. The corresponding protein bands obtained from PAGE gels of eluate from the *lpx1*Δ mutant transformed with pYES2/CT-LPX1 vector showed proteolytic activity clearly affected by the presence of 100 μM calcium. Excised gel fractions obtained from the strain transformed with an empty

vector showed no proteolytic activity, even in the presence of calcium (Fig. 3C).

In vitro plasma membrane H⁺-ATPase activation

In order to confirm the connection between calcium signaling, Lpx1p activity and H⁺-ATPase activation, an *in vitro* system to reconstitute H⁺-ATPase was used. Initially, purified plasma membranes and dialyzed MFE obtained from glucose-starved wild-type cells were prepared. In these conditions, plasma membrane H⁺-ATPase is in a non-activated state (probably with acetylated tubulins bounded to the H⁺-ATPase C-terminal tail as described by Campetelli *et al.* (2013)). MFE provides the *in vitro* system with all elements required for H⁺-ATPase activation, including Ptk2p (required for H⁺-ATPase phosphorylation) and Lpx1p (necessary for acetylated tubulin proteolysis).

To achieve the most suitable conditions for this *in vitro* activation assay, different calcium concentrations (100 μ M, 1 and 5 mM), different times of incubation (10, 30 and 60 min) and different MFE protein concentrations (50, 100, 200 and 400 μ g) for *in vitro* H⁺-ATPase activation were tested to define the most suitable conditions (data not shown). Thus, adequate conditions for the assay were as follows: 30 min of incubation with 50 μ g of protein from MFE and with the addition of 100 μ M calcium.

When purified plasma membranes obtained from the wild-type glucose-starved cells were incubated only with (i) dialyzed MFE from the same strain or (ii) only calcium, there was no H⁺-ATPase activation in comparison with the activity detected when only purified plasma membrane from wild-type glucose-starved cells was used (Fig. 4A). However, when purified plasma membranes were combined with both MFE and calcium, H⁺-ATPase activation was observed (47.5% increase in activity, $P < 0.05$). Additionally, activity was strongly reduced (77.4% reduced, $P < 0.05$) when 50 μ M sodium orthovanadate, a specific plasma membrane H⁺-ATPase inhibitor, was added. This seems to confirm that ATP hydrolytic activity measure in this assay was due to plasma membrane H⁺-ATPase (Fig. 4A).

All *in vitro* plasma membrane H⁺-ATPase activity rates measured in these assays ranged between 0.10 and 0.28 μ mol P_i min⁻¹ mg⁻¹ protein. There was no ATPase activity detected when the assay was performed with only MFE or eluates from all strains used in *in vitro* activation (data not shown).

Then, to confirm the connection between calcium signaling, Lpx1p activity and Ptk2p (a protein kinase) in the context of the phosphorylation/activation of H⁺-ATPase, this *in vitro* H⁺-ATPase activation was tested using purified membranes obtained from wild-type cells and different MFEs prepared from *ptk2Δ* and *lpx1Δ* mutant strains. As can be seen in Fig. 4B, the addition of MFE obtained from *lpx1Δ* alone or in combination with 100 μ M calcium does not result in any increase of the H⁺-ATPase activity ($P > 0.05$). When using MFE from *ptk2Δ* mutants, a slight increase (11.8%, $P < 0.05$) was verified on addition of 100 μ M calcium.

Moreover, there was no increase in H⁺-ATPase activity when the Ni-column eluate obtained from the *lpx1Δ* strain transformed with an empty vector (pYES2/CT-EV, used as control) was assessed, even with calcium addition combined with MFE from *lpx1Δ* or *ptk2Δ* strains (data not shown). Also, there was no increase ($P > 0.05$) in H⁺-ATPase activity when Ni-column eluate obtained from the *lpx1Δ* strain transformed with pYES2/CT-LPX1 vector was associated with MFE prepared from the *ptk2Δ* mutant, with or without 100 μ M calcium addition (Fig. 4C, first two columns at left side). At the same time, when the Ni-column elu-

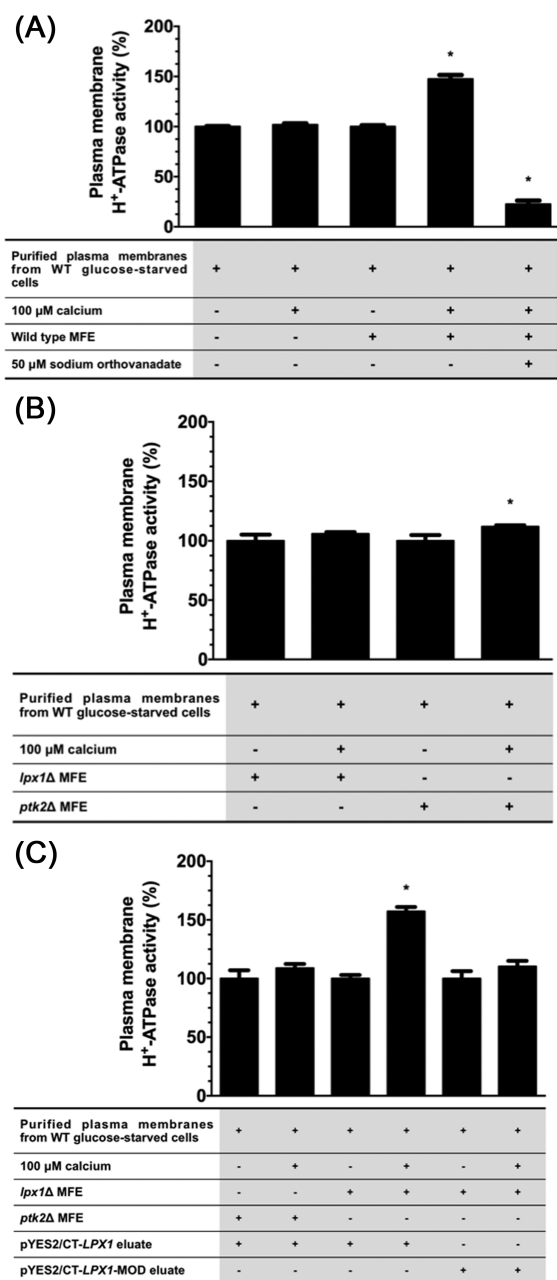


Figure 4. H⁺-ATPase *in vitro* activation assay. (A) Effect of calcium, membrane-free extract (MFE) and sodium orthovanadate addition in H⁺-ATPase *in vitro* activation assay. A method to evaluate *in vitro* H⁺-ATPase activation was established in this work. Purified plasma membranes and dialyzed MFE from BY4741 cells were used. Plasma membranes from glucose-starved wild-type cells were added to incubation buffer. Calcium and/or MFE was added accordingly to the different assays performed. To verify H⁺-ATPase activity inhibition, 50 μ M of sodium orthovanadate (specific H⁺-ATPase inhibitor) was added. (B) Effect of Lpx1p and Ptk2p on H⁺-ATPase *in vitro* activation. Plasma membranes from glucose-starved wild-type cells were added to incubation buffer. MFE from *lpx1Δ* strain (lacking Lpx1p) and calcium were added according to the different assays performed. (C) Plasma membranes from glucose-starved wild-type cells were added to incubation buffer with MFE from *lpx1Δ* or *ptk2Δ* strains. Eluates resulting from the application of cell extracts of *lpx1Δ* mutant (transformed with pYES2/CT-LPX1 or pYES2/CT-LPX1-MOD vectors) to a Ni-affinity column, with or without calcium addition, were used to evaluate the H⁺-ATPase *in vitro* activation. All results are expressed as a percentage relative to wild-type control assay with plasma membranes only. Asterisks indicate that mean values are statistically different from those seen in each relative control used ($P < 0.05$).

ates obtained from the *lpx1Δ* strain transformed pYES2/CT-LPX1 vector was added to the incubation system, in association with MFE from *lpx1Δ* strain, a clear increase (57.3%; $P < 0.05$) in H^+ -ATPase activity was only observed when 100 μ M calcium was present (central two columns in Fig 4C). On the other hand, with Ni-column eluates obtained from the *lpx1Δ* strain transformed with pYES2/CT-LPX1-MOD vector, any increase of the H^+ -ATPase activity was observed in association with MFE from *lpx1Δ* even in the presence of 100 μ M calcium (Fig. 4C, two last columns at right side).

DISCUSSION

In the past 20 years, a large amount of evidence has suggested that glucose-induced activation of plasma membrane H^+ -ATPase is clearly dependent on calcium metabolism (dos Passos et al. 1992; Brandão et al. 1994; Coccetti et al. 1998; Souza, Tropic and Brandao 2001; Trópia et al. 2006; Pereira et al. 2008; Bouillet et al. 2012). Nevertheless, until now, a Ca^{2+} -dependent protein kinase that could be involved in H^+ -ATPase activation through phosphorylation has never been identified. In fact, it was demonstrated that protein kinase Ptk2p would be the enzyme responsible for glucose-induced phosphorylation of residue Ser-899, located at the H^+ -ATPase C-terminal tail, leading to a K_m reduction of the ATPase (Goossens et al. 2000; Pereira et al. 2015), but this kinase does not seem to belong to any calcium responsive class of protein kinases. Moreover, neither a second protein kinase (which would be responsible for the phosphorylation of Ser-911/Thr-912 residues) nor any other Ca^{2+} -dependent protein has ever been described as being involved in this activation process. Therefore, to overcome this apparent contradiction, it seems necessary to us to develop different strategies to demonstrate how glucose-induced calcium signaling would be connected to the plasma membrane H^+ -ATPase activation process.

Interestingly, it was already proposed that a serine protease is related to H^+ -ATPase activation. These pieces of evidence suggest that activation of the H^+ -ATPase would require a glucose-induced hydrolysis of an acetylated tubulin to liberate its C-terminal tail, making it available for phosphorylation and activation (Campetelli et al. 2013). This proteolytic action is exerted by a serine protease encoded by the LPX1 gene (Campetelli et al. 2005, 2013), and, as a new component of this elaborated pathway, it could be investigated as a possible candidate that would respond to the calcium signal, thereby explaining its function in the glucose-induced activation of plasma membrane H^+ -ATPase.

We also found that Lpx1p presents a potential region for calcium interaction (an EF-hand, calcium-binding domain), apparently located at its C-terminus, when a search with WebFEATURE was made. WebFEATURE allows scanning for different functional sites in proteins using predicted 3D molecular structure (Liang et al. 2003; Wu, Liang and Altman 2008). The EF-hand motif is the most common calcium-binding motif found in proteins. In a large number of proteins, this motif does indeed bind calcium (or, in some cases, magnesium) and these proteins exert diverse functions such as calcium buffering in cytosol, signal transduction between cellular compartments and muscle contraction (Lewit-Bentley and Réty 2000). Thus, this predicted that an EF-hand calcium-binding domain in the structure of Lpx1p could be responsible for calcium interaction and possibly regulate its activity. Additionally, Thoms et al. (2011) found, also in a

search for functional sites in the Lpx1p structure, that the cap domain of this protein shows similarity to calmodulin, a well-known intracellular protein target of Ca^{2+} in eukaryotes. According to these authors, this cap covers the Lpx1p active site, and its N-terminal loop shows characteristics indicating high flexibility, which could suggest that this loop might act as a lid that can regulate access to the active site (Thoms et al. 2011). Curiously, it seems that Lpx1p also exhibits acyl hydrolase and phospholipase A activities and can be found in peroxisomes (Thoms et al. 2008); it also shows an ambiguous distribution (Huh et al. 2003).

Therefore, Lpx1p can be considered a good candidate to form a link between calcium signaling and glucose-induced plasma membrane H^+ -ATPase activation. This possibility was initially investigated by using strains with single or combined deletions in different genes: ARG82, YVC1 and LPX1. Cells with deletion in ARG82 (which encodes an inositol kinase responsible for the phosphorylation of IP₃) have an increase in both glucose-induced calcium signaling and H^+ -ATPase activation (Tisi et al. 2004; Trópia et al. 2006; Pereira et al. 2008). This increase suggests that H^+ -ATPase activation is dependent on calcium signaling. As demonstrated here, deletion of LPX1 alone or in combination with ARG82 led to a reduction in the glucose-induced activation of the plasma membrane H^+ -ATPase. Nevertheless, in the *lpx1Δ* mutant the calcium signaling was comparable to wild-type cells. Additionally, in the double mutant *arg82Δ lpx1Δ*, glucose-induced calcium signaling was also higher, as in the single mutant *arg82Δ*, suggesting that Lpx1p is not directly involved in calcium signaling. These results were also confirmed when calcium signaling and proton-pumping activity were measured in *yvc1Δ* and *yvc1Δ lpx1Δ* strains.

An alternative explanation for these results would be the existence of a signal transduction pathway, in which a glucose-induced calcium signal would be responsible for protease Lpx1p activation. According to a model suggested before (Campetelli et al. 2013), this protease hydrolyzes an acetylated tubulin bound to the H^+ -ATPase C-terminal tail, making this region accessible to protein kinases. Indeed, here we demonstrated that the *lpx1Δ* strain expressing the LPX1 gene inserted in a galactose-inducible vector (pYES2/CT-LPX1) showed progressive increase in the *in vivo* H^+ -ATPase activity, confirming that Lpx1p is indeed essential to H^+ -ATPase activation. The results of a similar experiment done with the *yvc1Δ* mutant transformed with the same vector also suggest that the calcium channel Yvc1 is not controlled by Lpx1p.

These results, combined with proteolytic activity assays, indicate that Lpx1p proteolytic activity could be the target of calcium signaling, making the C-terminal tail of the H^+ -ATPase accessible to phosphorylation performed by at least one protein kinase (Ptk2p).

To verify the direct connection between calcium signaling, Lpx1p activity and H^+ -ATPase activation, it was necessary to establish an *in vitro* system by which it would be possible to reconstitute the plasma membrane H^+ -ATPase activation. Thus, when purified plasma membrane (isolated from wild-type cells) was incubated with MFE from *lpx1Δ* or *ptk2Δ* strains, in the presence of 100 μ M calcium, H^+ -ATPase activation was absent or had a slight increase, respectively. This suggests once again that these two proteins (Lpx1 and Ptk2) are necessary to trigger a proper activation. Moreover, calcium and Lpx1p addition (obtained from the eluate of a Ni-affinity column of a cell extract of the *lpx1Δ* mutant transformed with a pYES2/CT-LPX1 vector), combined with MFE from *lpx1Δ* cells (which gives other

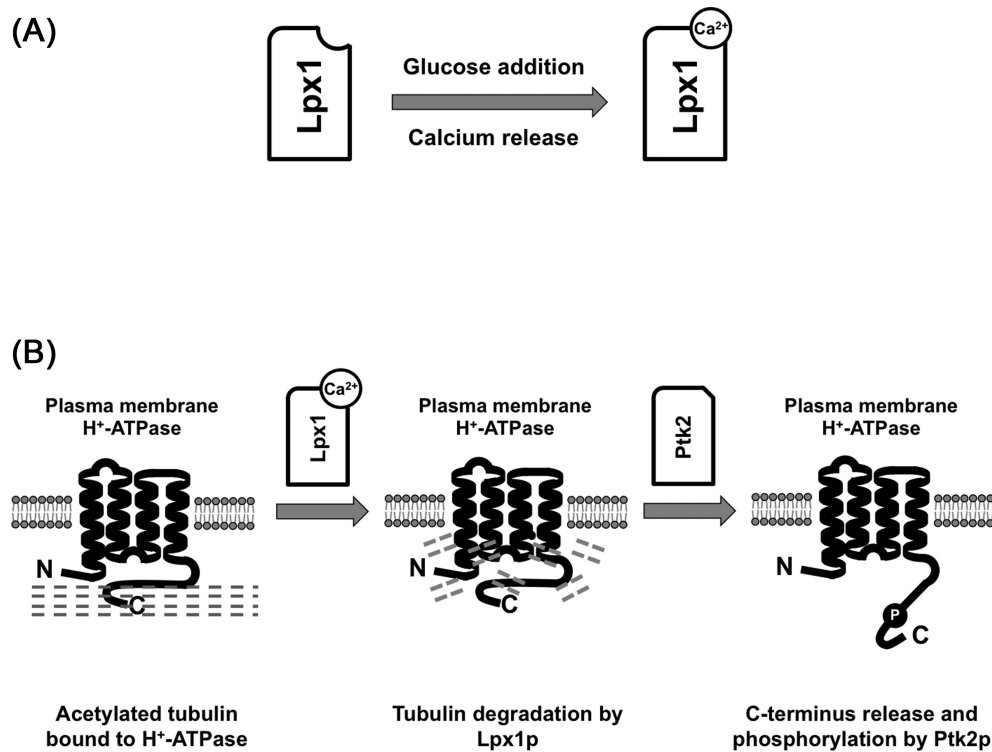


Figure 5. Lpx1p calcium binding and H⁺-ATPase activation. (A) Proposed mechanism by which Lpx1p is possibly regulated by calcium availability. In the presence of glucose, calcium is released into cytoplasm and binds to Lpx1p. (B) After calcium binding, Lpx1p is able to degrade acetylated tubulin bound to plasma membrane H⁺-ATPase releasing its C-terminal tail. This would make the H⁺-ATPase C-terminus phosphorylation sites accessible to at least one protein kinase (Ptk2p) making possible the enzyme activation.

components necessary for activation, but not Lpx1p), resulted in an increase of H⁺-ATPase activity only when 100 μ M calcium is also present. However, in similar conditions when the MFE from *ptk2 Δ* strain was used, no increase in H⁺-ATPase activity was observed, even in the presence of 100 μ M calcium. These results reinforce the importance of Ptk2p in the activation process of H⁺-ATPase. Finally, when modified Lpx1p protein (without the C-terminal tail portion that potentially interacts with Ca²⁺) was used in combination with MFE from *lpx1 Δ* cells and calcium, no increase in the H⁺-ATPase activity was observed.

Altogether, these approaches suggest that most probably glucose-induced calcium signaling is connected to plasma membrane H⁺-ATPase activation through a calcium-induced activation of the serine protease Lpx1p. Thus, with the results presented here, the following mechanism can be proposed: on glucose addition, Ca²⁺ binds to Lpx1p, leading to its activation making possible the degradation of the acetylated tubulin bound to the plasma membrane H⁺-ATPase. Therefore, the H⁺-ATPase C-terminal tail would be accessible to phosphorylation performed by at least one protein kinase (Ptk2p) leading to the activation of the plasma membrane H⁺-ATPase (Fig. 5).

Therefore, taking together the data from our previous work (dos Passos et al. 1992; Brandão et al. 1994; Coccetti et al. 1998; Souza, Tropic and Brandao 2001; Trópia et al. 2006; Pereira et al. 2008; Groppi et al. 2011; Bouillet et al. 2012) and the new results shown in this work, we suggest the existence of a signal transduction pathway with two branches, by which glucose addition controls calcium availability in the cytosol with a direct consequence for plasma membrane H⁺-ATPase activa-

tion (Fig. 6). In the first branch, glucose uptake and its subsequent phosphorylation generate a signal (probably sugar phosphates) that would stimulate G protein Gpa2p to interact with and/or activate phospholipase C (Plc1p). Then, Plc1p would hydrolyze phosphatidylinositol-4,5-bisphosphate, generating diacylglycerol and IP₃. IP₃ would interact, directly or indirectly, with Yvc1p regulating the intensity of calcium signaling in the cytosol (Bouillet et al. 2012). In the second branch, devoted to the control of Pmc1p Ca²⁺-ATPase activity, the glucose sensor Snf3p (Özcan and Johnston 1999) could also detect sugar phosphates (Dlugai et al. 2001), and in some way transduce this signal leading to an increase in Pmc1p activity (Souza, Tropic and Brandao 2001; Trópia et al. 2006; Pereira et al. 2008). The balance between these two branches would be responsible for the transient nature of calcium signaling. This calcium signaling seems to be responsible for activation of Lpx1p, which hydrolyzes an acetylated tubulin bound to plasma membrane H⁺-ATPase, allowing thus the H⁺-ATPase C-terminal tail to be released, enabling phosphorylation of C-terminal sites of the H⁺-ATPase and in this way its activation.

Beyond representing a clear advance in our understanding of how glucose-induced calcium signaling and plasma membrane H⁺-ATPase activation would be connected, these findings can help in the elaboration of new strategies to find out the identity of all protein kinases that are involved in plasma membrane H⁺-ATPase phosphorylation. Perhaps, the fact that a proteolytic degradation of acetylated tubulin precludes and/or occurs in parallel with phosphorylation could help in conceiving new approaches to identify those protein kinases in addition to Ptk2p.

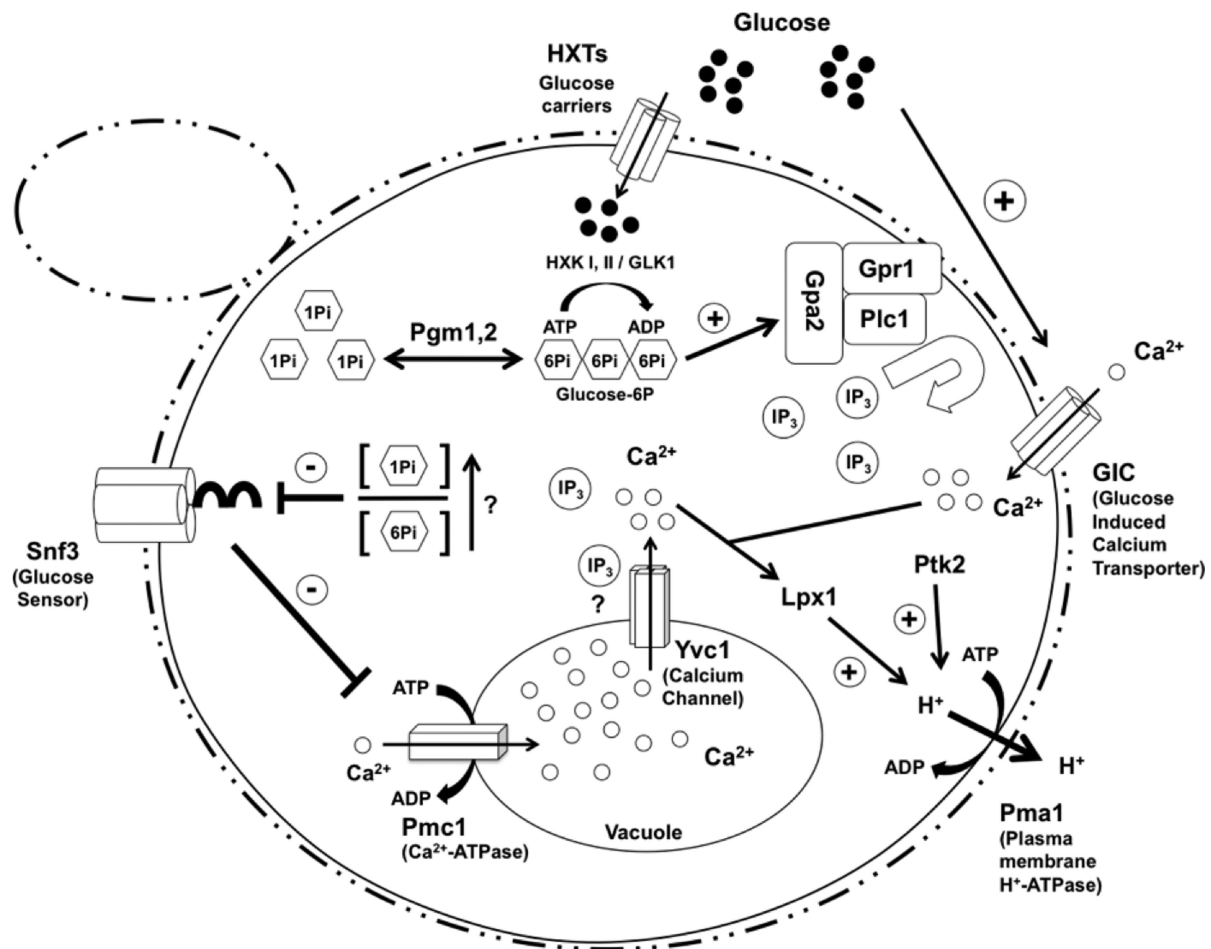


Figure 6. Working model: glucose-induced activation of plasma membrane H^+ -ATPase in yeast cells. A signal transduction pathway with two branches, resulting in intracellular calcium-signal generation, is triggered by internalization followed by phosphorylation of glucose, which generates a signal (maybe relative amounts of glucose-6-P and/or glucose-1-P) that would stimulate the complex constituted of the G protein, Gpa2p, and phospholipase C eliciting the activation of the phospholipase C. Then, phosphatidylinositol-4,5-bisphosphate hydrolysis would generate diacylglycerol and IP_3 . In the first branch, IP_3 would act directly or indirectly on the vacuolar calcium channel Yvc1p leading to an increase in the intracellular calcium signal. Besides that, in a second branch, the C-terminal tail of the glucose sensor Snf3p controlling the activity of the vacuolar Ca^{2+} -ATPase, Pmc1p, would detect the signal. The final intensity of the calcium signal would be the result of the partial contribution of each branch of this system. This calcium signaling seems to be responsible for activation of Lpx1p, which hydrolyzes an acetylated tubulin bound to plasma membrane H^+ -ATPase, allowing thus the H^+ -ATPase C-terminal tail to be released, enabling phosphorylation of C-terminal sites of the H^+ -ATPase and in this way its activation.

SUPPLEMENTARY DATA

Supplementary data are available at [FEMSYR](https://www.femsyr.com) online.

ACKNOWLEDGEMENTS

We are also grateful to Dr James Caffrey from National Institute of Environmental Health Sciences, USA, for the strains used in this work and to Marco Vanoni (Università di Milano-Bicocca, Milan, Italy) for pVTU-AEQ and pYX212-AEQ plasmids.

FUNDING

This work was partially financed by grants from Universidade Federal de Ouro Preto, from Fundação de Amparo a Pesquisa do Estado de Minas Gerais (FAPEMIG), Process CBB 824/06; from Conselho Nacional de Desenvolvimento-CNPq, Process 304815/2012-3 (research fellowship to RLB), Process 475672/08-5 (research grant) and CAPES, Process 2041/2012 (PhD fellowship to FFO), Process PNPD/2013 (research fellowships to RHSD), Pro-

cess PNPD 2755/2011 (research fellowships to FGS), Process BEX 11122/13-7 (PhD Sandwich fellowship to DDC).

Conflict of Interest. None declared.

REFERENCES

- Anraku Y, Ohya Y, Iida H. Cell cycle control by calcium and calmodulin in *Saccharomyces cerevisiae*. *Biochim Biophys Acta* 1991;1093:169-77.
- Bouillet LE, Cardoso AS, Perovano E *et al*. The involvement of calcium carriers and of the vacuole in the glucose-induced calcium signaling and activation of the plasma membrane H^+ -ATPase in *Saccharomyces cerevisiae* cells. *Cell Calcium* 2012;51:72-81.
- Brandão RL, de Magalhães-Rocha NM, Alijo R *et al*. Possible involvement of a phosphatidylinositol-type signaling pathway in glucose-induced activation of plasma membrane H^+ -ATPase and cellular proton extrusion in the

- yeast *Saccharomyces cerevisiae*. *Biochim Biophys Acta* 1994;**1223**:117–24.
- Brandão RL. The relationship between glucose-induced calcium signaling and activation of the plasma membrane H⁺-ATPase in *Saccharomyces cerevisiae* cells. In: Nakamura S (ed.). *Handbook of H⁺-ATPases*. Singapore: Pan Stanford Publishing Pte Ltd, 2014, 431–48.
- Campetelli AN, Monesterolo NE, Previtali G et al. Activation of H⁺-ATPase by glucose in *Saccharomyces cerevisiae* involves a membrane serine protease. *Biochim Biophys Acta* 2013;**1830**:3593–603.
- Campetelli AN, Previtali G, Arce CA et al. Activation of the plasma membrane H⁺-ATPase of *Saccharomyces cerevisiae* by glucose is mediated by dissociation of the H⁺-ATPase-acetylated tubulin complex. *FEBS J* 2005;**272**:5742–52.
- Capieaux E, Vignais ML, Sentenac A et al. The yeast H⁺-ATPase gene is controlled by the promoter binding factor TUF. *J Biol Chem* 1989;**264**:7437–46.
- Charney J, Tomarelli RM. A colorimetric method for the determination of the proteolytic activity of duodenal juice. *J Biol Chem* 1947;**171**:501–5.
- Cocchetti P, Tisi R, Martegani E et al. The PLC1 encoded phospholipase C in the yeast *Saccharomyces cerevisiae* is essential for glucose-induced phosphatidylinositol turnover and activation of plasma membrane H⁺-ATPase. *Biochim Biophys Acta* 1998;**1405**:147–54.
- Cunningham KW. Acidic calcium stores of *Saccharomyces cerevisiae*. *Cell Calcium* 2011;**50**:129–38.
- Cyert MS, Philpott CC. Regulation of cation balance in *Saccharomyces cerevisiae*. *Genetics* 2013;**193**:677–713.
- Denis V, Cyert MS. Internal Ca²⁺ release in yeast is triggered by hypertonic shock and mediated by a TRP channel homologue. *J Cell Biol* 2002;**156**:29–34.
- Đlugai S, Hippler S, Wiczorke R et al. Glucose-dependent and -independent signalling functions of the yeast glucose sensor Snf3. *FEBS Lett* 2001;**505**:389–92.
- dos Passos JB, Vanhalewyn M, Brandao RL et al. Glucose-induced activation of plasma membrane H⁺-ATPase in mutants of the yeast *Saccharomyces cerevisiae* affected in cAMP metabolism, cAMP-dependent protein phosphorylation and the initiation of glycolysis. *Biochim Biophys Acta* 1992;**1136**:57–67.
- Dunn T, Gable K, Beeler T. Regulation of cellular Ca²⁺ by yeast vacuoles. *J Biol Chem* 1994;**269**:7273–8.
- Eraso P, Mazón MJ, Portillo F. Yeast protein kinase Ptk2 localizes at the plasma membrane and phosphorylates *in vitro* the C-terminal peptide of the H⁺-ATPase. *Biochim Biophys Acta* 2006;**1758**:164–70.
- Gietz RD, Schiestl RH, Willems AR et al. Studies on the transformation of intact yeast cells by the LiAc/SS-DNA/PEG procedure. *Yeast* 1995;**11**:355–60.
- Goffeau A, Slayman CW. The proton-translocating ATPase of the fungal plasma membrane. *Biochim Biophys Acta* 1981;**639**:197–223.
- Goossens A, de La Fuente N, Forment J et al. Regulation of yeast H⁺-ATPase by protein kinases belonging to a family dedicated to activation of plasma membrane transporters. *Mol Cell Biol* 2000;**20**:7654–61.
- Gropi S, Belotti F, Brandão RL et al. Glucose-induced calcium influx in budding yeast involves a novel calcium transport system and can activate calcineurin. *Cell Calcium* 2011;**49**:376–86.
- Huh W-K, Falvo JV, Gerke LC et al. Global analysis of protein localization in budding yeast. *Nature* 2003;**425**:686–91.
- Lecchi S, Allen KE, Pardo JP et al. Conformational changes of yeast plasma membrane H⁺-ATPase during activation by glucose: role of threonine-912 in the carboxy-terminal tail. *Biochemistry* 2005;**44**:16624–32.
- Lecchi S, Nelson CJ, Allen KE et al. Tandem phosphorylation of Ser-911 and Thr-912 at the C terminus of yeast plasma membrane H⁺-ATPase leads to glucose-dependent activation. *J Biol Chem* 2007;**282**:35471–81.
- Lewit-Bentley A, Réty S. EF-hand calcium-binding proteins. *Curr Opin Struct Biol* 2000;**10**:637–43.
- Liang MP, Banatao DR, Klein TE et al. WebFEATURE: an interactive web tool for identifying and visualizing functional sites on macromolecular structures. *Nucleic Acids Res* 2003;**31**:3324–7.
- Lowry OH, Rosebrough NJ, Farr AL et al. Protein measurement with the Folin phenol reagent. *J Biol Chem* 1951;**193**:265–75.
- Mazón MJ, Eraso P, Portillo F. Specific phosphoantibodies reveal two phosphorylation sites in yeast Pma1 in response to glucose. *FEMS Yeast Res* 2015;**15**:fov030.
- Miseta A, Fu L, Kellermayer R et al. The Golgi apparatus plays a significant role in the maintenance of Ca²⁺ homeostasis in the *ups33Δ* vacuolar biogenesis mutant of *Saccharomyces cerevisiae*. *J Biol Chem* 1999a;**274**:5939–47.
- Miseta A, Kellermayer R, Aiello DP et al. The vacuolar Ca²⁺/H⁺ exchanger Vcx1p/Hum1p tightly controls cytosolic Ca²⁺ levels in *S. cerevisiae*. *FEBS Lett* 1999b;**451**:132–6.
- Odom AR, Stahlberg A, Wentte SR et al. A role for nuclear inositol 1,4,5-trisphosphate kinase in transcriptional control. *Science* 2000;**287**:2026–9.
- Özcan S, Johnston M. Function and regulation of yeast hexose transporters. *Microbiol Mol Biol R* 1999;**63**:554–69.
- Paidhungat M, Garrett S. A homolog of mammalian, voltage-gated calcium channels mediates yeast pheromone-stimulated Ca²⁺ uptake and exacerbates the *cdc1* (Ts) growth defect. *Mol Cell Biol* 1997;**17**:6339–47.
- Pereira MB, Tisi R, Fietto LG et al. Carbonyl cyanide m-chlorophenylhydrazone induced calcium signaling and activation of plasma membrane H⁺-ATPase in the yeast *Saccharomyces cerevisiae*. *FEMS Yeast Res* 2008;**8**:622–30.
- Pereira RR, Castanheira D, Teixeira JA et al. Detailed search for protein kinase(s) involved in plasma membrane H⁺-ATPase activity regulation of yeast cells. *FEMS Yeast Res* 2015;**15**:fov003.
- Portillo F. Regulation of plasma membrane H⁺-ATPase in fungi and plants. *Biochim Biophys Acta* 2000;**1469**:31–42.
- Portillo F, Eraso P, Serrano R. Analysis of the regulatory domain of yeast plasma membrane H⁺-ATPase by directed mutagenesis and intragenic suppression. *FEBS Lett* 1991;**287**:71–4.
- Rao R, Drummond-Barbosa D, Slayman CW. Transcriptional regulation by glucose of the yeast PMA1 gene encoding the plasma membrane H⁺-ATPase. *Yeast* 1993;**9**:1075–84.
- Saiardi A, Caffrey JJ, Snyder SH et al. Inositol polyphosphate multikinase (*ArgR/III*) determines nuclear mRNA export in *Saccharomyces cerevisiae*. *FEBS Lett* 2000;**468**:28–32.
- Saiardi A, Erdjument-Bromage H, Snowman AM et al. Synthesis of diphosphoinositol pentakisphosphate by a newly identified family of higher inositol polyphosphate kinases. *Curr Biol* 1999;**9**:1323–6.
- Secades P, Guijarro JA. Purification and characterization of an extracellular protease from the fish pathogen *Yersinia ruckeri* and effect of culture conditions on production. *Appl Environ Microb* 1999;**65**:3969–75.

- Serrano R. Structure, function and regulation of plasma membrane H⁺-ATPase. *FEBS Lett* 1993;**325**:108–11.
- Serrano R, Ruiz A, Bernal D et al. The transcriptional response to alkaline pH in *Saccharomyces cerevisiae*: evidence for calcium-mediated signalling. *Mol Microbiol* 2002;**46**:1319–33.
- Shears SB. Transcriptional regulation: a new dominion for inositol phosphate signaling? *Bioessays* 2000;**22**:786–9.
- Souza M, Tropicia M, Brandao R. New aspects of the glucose activation of the H⁺-ATPase in the yeast *Saccharomyces cerevisiae*. *Microbiology* 2001;**147**:2849–55.
- Thoms S, Debelyy MO, Nau K et al. Lpx1p is a peroxisomal lipase required for normal peroxisome morphology. *FEBS J* 2008;**275**:504–14.
- Thoms S, Hofhuis J, Thöing C et al. The unusual extended C-terminal helix of the peroxisomal α/β -hydrolase Lpx1 is involved in dimer contacts but dispensable for dimerization. *J Struct Biol* 2011;**175**:362–71.
- Tisi R, Baldassa S, Belotti F et al. Phospholipase C is required for glucose-induced calcium influx in budding yeast. *FEBS Lett* 2002;**520**:133–8.
- Tisi R, Belotti F, Wera S et al. Evidence for inositol triphosphate as a second messenger for glucose-induced calcium signalling in budding yeast. *Curr Genet* 2004;**45**:83–9.
- Tisi R, Martegani E, Brandão RL. Monitoring yeast intracellular Ca²⁺ levels using an in vivo bioluminescence assay. *Cold Spring Harb Protoc* 2015;**2015**:210–3.
- Trópia M, Cardoso A, Tisi R et al. Calcium signaling and sugar-induced activation of plasma membrane H⁺-ATPase in *Saccharomyces cerevisiae* cells. *Biochem Biophys Res Commun* 2006;**343**:1234–43.
- Wera S, Bergsma JCT, Thevelein JM. Phosphoinositides in yeast: genetically tractable signalling. *FEMS Yeast Res* 2001;**1**:9–13.
- Wu S, Liang MP, Altman RB. The SeqFEATURE library of 3D functional site models: comparison to existing methods and applications to protein function annotation. *Genome Biol* 2008;**9**:R8.
- York JD, Odom AR, Murphy R et al. A phospholipase C-dependent inositol polyphosphate kinase pathway required for efficient messenger RNA export. *Science* 1999;**285**:96–100.

RESEARCH PAPER

Screening of Yeasts Isolated from Brazilian Environments for the 2-Phenylethanol (2-PE) Production

Lorena Azevedo de Lima, Raphael Hermano Santos Diniz, Marisa Vieira de Queiroz, Luciano Gomes Fietto, and Wendel Batista da Silveira

Received: 5 April 2018 / Revised: 23 May 2018 / Accepted: 8 June 2018
© The Korean Society for Biotechnology and Bioengineering and Springer 2018

Abstract Phenylethanol alcohol, or 2-phenylethanol (2-PE) production by yeasts has been considered a promising alternative to its chemical synthesis. In order to evaluate the potential of yeast strains isolated from different Brazilian environments, we evaluated the 2-PE production of 267 strains. Among them, the *Kluyveromyces marxianus* CCT 7735 yeast stood out as being the best 2-PE producer. The *K. marxianus* CCT 7735 growth was impaired by 2-PE; nevertheless, this effect is less pronounced than the inhibition reported for certain *Saccharomyces cerevisiae* strains. The maximum 2-PE titer obtained under optimized conditions was 3.44 g/L, 28% higher than the titer achieved under unoptimized conditions. The optimized conditions were: 30°C, and glucose and L-phe concentrations of 3.0 and 4.0 g/L, respectively. Moreover, the specific production rate of 2-PE increased twofold compared to the unoptimized conditions.

Keywords: aromatic compound, L-phenylalanine, optimization, *Kluyveromyces marxianus*

Lorena Azevedo de Lima, Marisa Vieira de Queiroz, Wendel Batista da Silveira*
Departamento de Microbiologia, Instituto de Biotecnologia Aplicada à Agropecuária-BIOAGRO, Universidade Federal de Viçosa, Av. PH Rolfs s/n, Campus universitário, Viçosa - MG, Brazil
Tel: +55-31-38992956; Fax: +55-31-38992573
E-mail: wendel.silveira@ufv.br

Luciano Gomes Fietto
Departamento de Bioquímica e Biologia Molecular, Universidade Federal de Viçosa, Av. PH Rolfs s/n, Campus universitário, Viçosa - MG, Brazil

Raphael Hermano Santos Diniz
Instituto Federal de Educação, Ciência e Tecnologia de Minas Gerais - Campus Ouro Preto, Ouro Preto - MG, Brazil

1. Introduction

2-phenylethanol is a higher aromatic alcohol characterized by its rose-like aroma and colorless aspect with worldwide market production of 2-PE estimated at approximately 10,000 tons in 2010 [1]. It is one of the most important ingredients in perfume compositions [2]. In the beverage industry, it influences the aroma of wines and beers and has great application in the formulation of other products such as detergents and pharmaceutical compounds. In addition, several studies have shown its antimicrobial effect on phytopathogenic microorganisms [3,4]. Since the extraction process from flowers is economically costly, most 2-PE used in industry is obtained from chemical synthesis. However, it is not an environment-friendly process because the chemical synthesis of 2-PE uses benzene and ethylene, potentially toxic compounds [5]. Thus, there is great interest in biotechnological processes as an alternative for 2-PE production. This aromatic alcohol is produced by yeasts from either L-phenylalanine (L-phe) via the Erlich pathway or by *de novo* synthesis from sugars [6]. Nevertheless, the biotechnological production of 2-PE titer is low compared to chemical synthesis. Over the last few years, many studies have reported the potential of yeasts for 2-PE production from L-phe as the precursor. Up to now, most of the studies on 2-PE production have been conducted on the yeast *Saccharomyces cerevisiae*. Curiously, there is little exploration of the productive potential of non-*Saccharomyces* yeasts; it is well documented that non-conventional yeasts are able to grow in a greater diversity of carbon sources, temperatures and capable of producing different compounds than *S. cerevisiae*. It is estimated that Brazil hosts approximately 20% of the microbial world's

diversity [7]; however, it is still largely unknown or has not been fully explored, opening perspectives for yeast selection with suitable features for the production of aroma compounds. In this context, we evaluated the potential of yeasts previously isolated from dairy industries, and the soil from two National Parks and the Amazonian rubber tree. In this study, we selected the *K. marxianus* CCT 7735 strain as being the best producer of 2-PE. Indeed, *K. marxianus* strains are considered suitable for aromatic compound production. It is noteworthy that this yeast is capable of assimilating a variety of substrates, displays a high growth rate and has Generally Recognized as Safe (GRAS) status [8-10].

2. Material and Methods

2.1. Yeast strains and medium

The yeasts used in this work belong to the culture collection of both the Microbial Physiology and Molecular Genetic of Fungi laboratories of the Department of Microbiology, at the Federal University of Viçosa (UFV). These yeasts were isolated from Brazilian dairy industry, Serra dos Orgãos National Park (22°54' S and 42°09' W), and native Amazonian rubber trees (*Hevea brasiliensis*). Yeast cells were maintained in YP medium containing per liter: glucose 20 g, peptone 20 g, yeast extract 10 g, with the addition of 40% glycerol (v/v) at -80°C. At the screening stage, yeast cells were cultured on synthetic defined medium (SD), which consisted of (g/L): L-phenylalanine - L-phe (Sigma Chemical Co., MO, USA) 8.0, glucose 20.0, Yeast Nitrogen Base - YNB - without amino acids and ammonium sulfate (Sigma Chemical Co., MO, USA) 6.7, pH 5.0. The YNB medium was sterilized by autoclaving at 121°C for 15 min, while phenylalanine was sterile-filtered on membrane (0.22 µm, Merck Millipore Co., Germany).

2.2. Screening of 2-PE producer yeasts

In order to obtain yeasts with the potential to produce 2-PE from L-phe, a primary screening was performed in which the yeast strains were grown on SD and 2-PE production was evaluated. These cells grown in SD and that produced 2-PE, were submitted to a secondary screening to evaluate the 2-PE production via the *de novo* pathway. For this phase, an SD medium, previously described, was used except that the yeast extract, 10.0 g/L, was utilized as the nitrogen source instead of L-phe. At both screening stages, batch cultures were carried out in 125 mL Erlenmeyer flasks containing 25 mL of medium, at 30°C, with a stirring rate of 200 rpm for 48 h. The inoculums were adjusted to an initial optical density at 600 nm (OD_{600nm}) of 0.2.

2.3. Inhibitory effect of 2-PE on cell growth

The selected strain - *Kluyveromyces marxianus* CCT 7735, previously designated as UFV-3, was grown on SD medium supplemented by 2-PE concentrations ranging from 0.5 to 3.0 g/L. The inhibitory effect was expressed as the ratio of the specific growth rate in medium with 2-PE (μ_{2PE}) to the specific growth rate in the medium without 2-PE (μ).

2.4. Optimization of the 2-PE production

Optimization of the 2-PE production by *K. marxianus* CCT 7735 was achieved in three steps evaluating the effects of the both L-phe and glucose concentrations and temperature. The pre-inoculum obtained in SD medium was harvested and used as inoculum for the growth in medium containing L-phe concentrations ranging from 1.0 to 14.0 g/L for 72 h. The effect of the glucose concentration was evaluated ranging in concentration from 5 to 100 g/L. Subsequently, the temperature effect was evaluated ranging from 25 to 37°C. Batch cultures were carried out in 125 mL Erlenmeyer flasks containing 25 mL of medium with a stirring rate of 200 rpm for 72 h.

2.5. Determination of dry weight and specific growth rate

The dry weight of biomass was determined in samples of 10 mL by centrifugation at 10,000×g for 5 min at 4°C. The wet pellets were washed twice, dried for 24 h at 105°C and then weighed [11]. A linear regression of the plot of the absorbance 600 nm (A_{600}) versus dry weight allowed for calculating the dry mass (gdw) from the absorbance. The specific growth rate (/h) was determined by the angular coefficient from exponential regression of the plot of gdw (g/L) versus time (h) at the exponential growth phase.

2.6. Analytical procedures

The supernatant was passed through a 0.13 mm syringe filter (0.45 µm, Merck Milipore Co., GER) prior to injection into the HPLC (CTO-20A, Shimadzu, Japan). Five microliters of sample were injected and passed through a RP-C18 column (Kinetex C18 250×4.6 mm, 5 µm, Phenomenex, California, USA), and the compounds 2-PE and L-phe were detected by a UV-Visible Detector (SPD-10A, Shimadzu, Japan) at 258 nm. 35% sterile water and 65% (v/v) methanol were pumped isocratically through a Shimadzu LC-20A pump at 0.5 mL/min. The column was kept at room temperature. Ethanol and sugars were analyzed by the HPLC by injecting 10 µL into an ion exchange column (Aminex HPX-87H 300×7.8 mm, 9 µm, Bio-Rad, Munich, Germany) with 5 mmol H₂SO₄ as eluent at 0.6 mL/min, at 60°C with detection by refraction index (RID-20A, Shimadzu, Japan). Quantification of all substances

was performed by calibration and verification with external standards.

2.7. Determination of fermentative parameters

The 2-PE yield (Y_p g/g) was determined by angular coefficient from a linear regression of the plot cell dry weight (gdw) (g/L) versus 2-PE concentration (g/L). Cell biomass yield ($Y_{x/s}$ g/g) was determined by angular coefficient from a linear regression of the plot gdw versus L-phe and sugar concentrations (g/L). Specific 2-PE production rate (q_p , g/g/h) and specific sugar consumption rate (q_s , g/g/h) were determined multiplying the respective yields by the specific growth rate (/h). All linear regression was carried out at the exponential growth phase. Volumetric productivity (Q_p , g/L) was calculated by the equation:

$$Q_p = \frac{P_f - P_i}{h}$$

In which P_f = the final concentration of product, P_i , the initial concentration of product and h , the fermentation periods.

2.8. Statistical analysis

Statistical analyses were carried out using the R 3.0.2 software package (www.r-project.org). A completely randomized design (CRD) was adopted and all experiments were conducted in duplicates. The significance level used in the statistical tests was $p = 0.05$.

3. Results and Discussion

3.1. Yeast screening for 2-PE production

Initially, 267 yeast strains were analyzed to verify their ability to produce 2-PE from L-phe at 30°C. Among them, thirty six strains were capable of producing 2-PE, but twenty strains produced concentrations exceeding 1.5 g/L. It is noteworthy that a number of yeasts, even under unoptimized conditions, produced 2-PE concentrations above 2.0 g/L (data not shown), which are superior to titers obtained by other yeasts such as *Pichia fermentans* L-5, *K. marxianus* CBS600, *S. cerevisiae* Ye9-612, *Yarrowia lipolytica* NCYC3825, *Candida glycerinogenes* WL201-5 and *S. cerevisiae* W303-1A [12-16]. These results show that there is a great number of yeasts in several ecological niches with biotechnological potential not yet explored. During the second stage of the screening, we evaluated the ability of the yeasts selected (20 strains) to produce 2-PE in synthetic medium without L-phe, i.e. via the *de novo* pathway. Fifteen yeasts were capable of producing 2-PE via the *de novo* pathway. It is important to point out that *K. marxianus* CCT 7735 produced 174 mg/L of 2-PE (Fig. S1), this titer being superior to the maximum concentration obtained by

an engineered *S. cerevisiae* (96 mg/L) via *de novo* [17] and presented the highest 2-PE yield per cell mass (17.0 mg/g, Fig. S2) compared to the other yeasts analyzed by Shen *et al.* [17]. Therefore, taking into account that *K. marxianus* CCT 7735 yeast also stands out as a promising 2-PE producer via the *de novo* pathway, it was selected for further studies. In addition, the genome of this strain had been recently sequenced, which is important in the establishment of further metabolic engineering approaches [18]. Indeed, *K. marxianus* strains have been highlighted as promising 2-PE producers [19-22,9].

3.2. Inhibitory effect of 2-PE on *K. marxianus* CCT 7735 growth

Taking into account that product inhibition is undesirable in the production of metabolites of industrial interest, we evaluated the effect of 2-PE on *K. marxianus* CCT 7735 growth (Fig. 1). The inhibitory effect was more pronounced with the increase of 2-PE concentration and at 2.5 g/L growth was inhibited by 64%. In a similar 2-PE concentration (2.4 g/L), the *S. cerevisiae* R-UV3 strain was inhibited by 76% [11]. The growth rate in the presence of 2.5 and 3.0 g/L 2-PE declined from 0.31 /h (absence of 2-PE) to 0.1 /h and to 0.07 /h, respectively. Studies reported that at 2.0 g/L, 2-PE completely inhibited the growth of *S. cerevisiae* W303-1A and *S. cerevisiae* Giv 2009 [23,16]. The 2-PE targets in yeasts are not well known; however, DNA synthesis seems to be one of them, at least in *Schizosaccharomyces pombe* [24]. Nevertheless, these authors did not find out the primary effect of 2-PE. Improvement in tolerance to high 2-PE concentrations in *K. marxianus* CCT 7735 can be addressed in future studies to make it more suitable to bioprocesses.

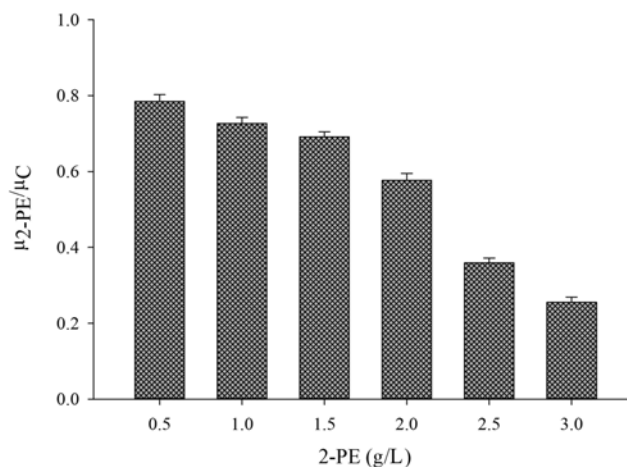


Fig. 1. Effect of 2-PE concentration on growth of *K. marxianus* CCT 7735. μ_{2-PE} —growth specific to addition of 2-PE in the medium, μ_C —growth specific without 2-PE in the medium.

Table 1. 2-PE production in synthetic medium containing L-phe concentrations ranged from 1.0 to 14.0 g/L, as the sole nitrogen source

Initial L-phe (g/L)	Relative consumption (%)	2-PE (g/L)
14.0	13.94	2.56*
12.0	16.07	2.54*
10.0	20.64	2.52*
8.0	25.77	2.50*
6.0	35.44	2.48*
4.0	62.79	2.47*
2.0	93.17	2.00
1.0	96.44	1.20

Metabolites were measured after 72 h of growth at 30°C in defined medium and are expressed in g/L.

*Values that are not significantly ($\alpha=0.05$) different according to the Tukey test.

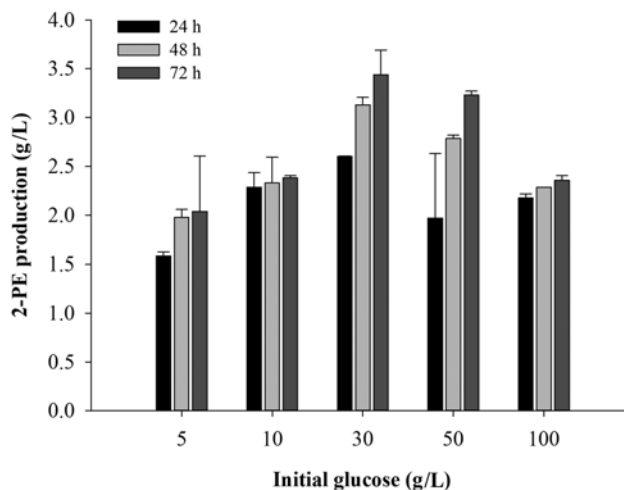
3.3. Influence of L-phe concentration on 2-PE production by *K. marxianus* CCT 7735

A number of studies have shown that 2-PE production can be improved by adding L-phe as the sole nitrogen source; however, we observed that this amino acid (8.0 g/L) is not completely consumed after 48 h at the screening stage. Based on this, we evaluated the influence of the L-phe concentration on the 2-PE production by *K. marxianus* CCT 7735. The L-phe was not totally consumed in the concentrations evaluated. Additionally, its consumption decreased at higher L-phe concentrations (Table 1). Moreover, we observed that L-phe concentrations above 4.0 g/L did not lead to the increase of the 2-PE titer. Consistent with our results, Fabre *et al.* [25] also verified that the increase of the L-phe concentration from 2.0 to 5.0 g/L did not improve the production of 2-PE by *K. marxianus* DSM 5422. According to these results, Stark *et al.* [23] reported that L-phe did not achieve total conversion into 2-PE by *S. cerevisiae* Ye9-612. It is important to point out that the 2-PE titer (2.47 g/L) obtained in our study at 4.0 g/L of L-phe was higher than that reported with *S. cerevisiae* Ye9-612 E (0.85 g/L) [14].

The volumetric productivity achieved at 4.0 g/L of PE was 121 mg/L/h (Table 4), which was close to that obtained by *S. cerevisiae* R-UV3 during batch cultivation in a bioreactor [11]. However, these authors used 10.0 g/L of L-phe. In our study, the specific production rate was two-fold higher than that obtained by *K. marxianus* CBS 600, which was cultured at a high L-phe concentration (10.0 g/L) [8]. It should be noted that the final L-phe concentration remaining in the medium containing 4.0 g/L of L-phe was 1.45 g/L (37.21%).

3.4. Effect of glucose concentration on 2-PE production

We observed that the glucose was completely consumed

**Fig. 2.** Effect of glucose concentration on 2-PE production by *K. marxianus* CCT 7735. Cells were grown at 30°C in minimal supplemented medium.

after 12 h (Fig. S3). On the other hand, L-phe was not efficiently consumed, impairing 2-PE production. Based on these results, we hypothesize that L-phe consumption after 12 h was impaired by the consumption of the energy source. To address this question, we evaluated the effect of glucose concentration on the 2-PE production (Fig. 2). Interestingly, we observed that the 2-PE production and productivity increased with an increase in the glucose concentration up to 30.0 g/L, reaching the values of 3.40 g/L and 47.8 mg/L/h, respectively (Table 2). Furthermore, we verified that the residual concentration of L-phe decreases at 50.0 g/L of glucose. Taking into account that the glucose was not, in fact, completely consumed after 12 h of growth (data not shown), the higher L-phe consumption was due to the presence of the remaining carbon source. Therefore, it seems reasonable to consider that L-phe consumption relies on either ATP or electrochemical gradient generated from glucose catabolism. On the other hand, there was a decline in 2-PE production from medium containing glucose 100.0 g/L. This result seems to be

Table 2. Effect of glucose concentration on 2-PE production

Initial glucose (g/L)	2-PE (g/L)	Q _{2-PE} (mg/L/h)	Residual L-phe (g/L)
5.0	2.04 ± 0.57	28.08 ± 0.57	1.95 ± 0.45
10.0	2.38 ± 0.02	33.50 ± 0.02	1.82 ± 0.02
30.0	3.40 ± 0.25*	47.80 ± 0.25*	0.99 ± 0.04
50.0	3.23 ± 0.04*	45.00 ± 0.04*	0.69 ± 0.07
100.0	2.36 ± 0.05	33.21 ± 0.05	1.93 ± 0.06

Metabolites were measured after 72 h of growth at 30°C in defined medium with L-phe 4.0 g/L. Data represent the average ±SD of duplicate cultivations.

*Values that are not significantly ($\alpha=0.05$) different according to the Tukey test.

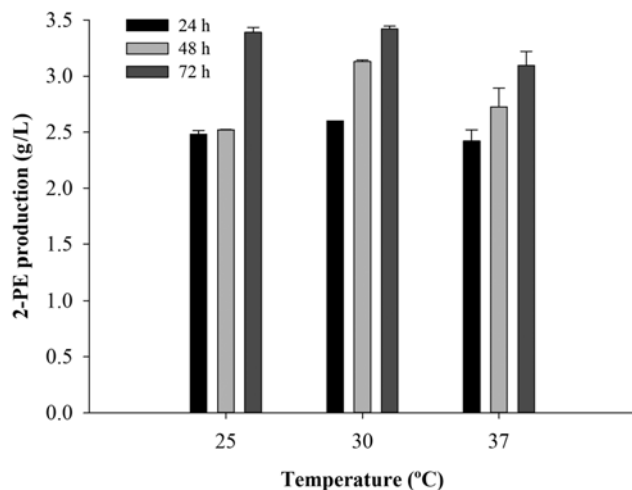


Fig. 3. Effect of temperature on 2-PE production by *K. marxianus* CCT 7735. Cells were grown in minimal medium at temperature ranged from 25 to 37°C.

related to the increase of ethanol concentration in medium containing high glucose concentration (Fig. S4); in fact, ethanol negatively affects the plasma membrane and consequently the nutrient uptake. It is noteworthy that *K. marxianus*, in contrast to *S. cerevisiae*, is not tolerant to ethanol [26]. From a production point of view, it is important to point out that the highest titer (3.40 g/L, Fig. 3) obtained at glucose 30 g/L was higher than those obtained under unoptimized conditions.

3.5. The effect of temperature on 2-PE production

The effect of temperature was evaluated in a culture medium containing 30.0 g/L of glucose. The temperature ranged from 25 to 37°C (Fig. 3). The highest 2-PE titers were obtained at both 25°C and 30°C; there was no statistical difference between them and volumetric productivity was 52.08 mg/L/h and 65.21 mg/L/h, respectively (Table 3). Although *K. marxianus* CCT 7735 is a thermotolerant yeast, 2-PE production was lower at 37°C. In contrast, previous studies have shown that ethanol production was higher at temperatures around 37°C [27,28]. Therefore,

Table 3. Temperature effect on 2-PE production

Temperature (°C)	2-PE _{72h} (g/L)	Q _{2-PE} _{48h} (mg/L/h)	Residual L-phe (g/L)
25	3.30 ± 0.04*	52.08 ± 0.000	0.69 ± 0.04
30	3.44 ± 0.25*	65.21 ± 0.001	1.00* ± 0.10
37	3.09 ± 0.13	43.00 ± 0.004	1.14* ± 0.15

Metabolites were measured after 48 h and 72 h of growth in defined medium with L-phe 4.0 g/L and glucose 30.0 g/L. Data represent the average ±SD of duplicate cultivations.

*Values that are not significantly ($\alpha=0.05$) different according to the Tukey test.

Table 4. Fermentative parameters of the 2-PE production by *K. marxianus* CCT7735 under both unoptimized and optimized conditions in the exponential phase

	Unoptimized medium	Optimized medium
2-PE (g/L)*	2.47	3.44
Y _{2-PE/L-phe} (g/g)	0.68	0.80
Y _{2-PE/glu} (g/g)	0.067	0.075
q _{2-PE} (mg gcd/w/h)	85	160
q _{L-phe} (mg gcd/w/h)	230	300
q _{glu} (g gcd/w/h)	2.3	1.38
Q _{2-PE} (mg/L/h)	112	121

*Metabolites measured at 72h - maximum concentration

Y_{2-PE/L-phe} yield of 2-PE based on L-phe consumed

Y_{2-PE/glu} yield of 2-PE based on Glucose consumed

q_{2-PE} specific productivity

q_{L-phe} specific productivity of L-phe consumption

q_{glu} specific productivity of Glucose consumption

Q_{2-PE} volumetric productivity

elevated temperatures seem to favor the ethanol production in *K. marxianus*. Furthermore, the volumetric productivity achieved at 30°C was superior to that obtained by a *S. cerevisiae* hybridized strain (54 mg/L/h) [29], highlighting the potential of *K. marxianus* CCT 7735 for 2-PE production.

Consistent with previous studies carried out with other *K. marxianus* strains, we observe that the 2-PE production is growth-associated (Fig. 4). We verified that the yeast was in a stationary phase after 24 h of growth and glucose was totally consumed. In spite of glucose depletion, L-phe was only slightly consumed after 24 h of growth, which in turn led to the increase of the 2-PE concentration. It should be noted that this increase occurred during the same period in which the ethanol produced was consumed. These results indicate that ethanol metabolism provided energy for both L-phe consumption and 2-PE production.

In agreement with our results Fabre *et al.* [25] observed the L-phe consumption and 2-PE production from medium containing ethanol as a carbon source. It has been assumed that the amino acid transporters (AAT) are H⁺-symporters [30]. Taken together, our results show that the L-phe consumption in *K. marxianus* relies on the energy source consumption, which leads to the H⁺ gradient formation. Indeed, L-phe uptake was higher in the presence of glucose, which is consistent with the fact that this sugar releases more energy than ethanol. Importantly, we observe that under optimized conditions, that is, L-phe and glucose concentrations of 4.0 g/L and 30 g/L, respectively, and temperature of 30°C, the specific production rate of 2-PE increased two-fold compared to the unoptimized condition. In addition, the yields of 2-PE and volumetric production also

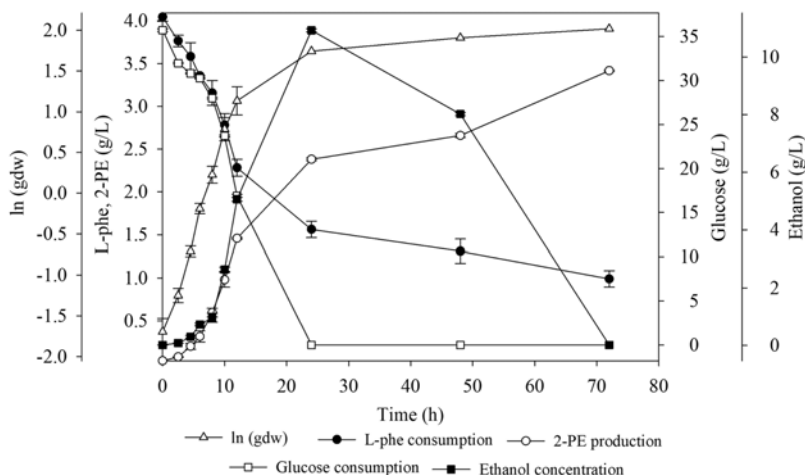


Fig. 4. Growth and 2-PE production of *K. marxianus* CCT 7735. *K. marxianus* CCT 7735 was grown on minimal medium with glucose 30 g/L and L-phe 4.0 g/L at 30°C. Growth rate was determined from the exponential phase in the growth curve.

increased (Table 4). Furthermore, the specific consumption rate of L-phe was superior under optimized conditions, which is consistent with the higher specific production rate of 2-PE.

4. Conclusion

Twenty yeast strains were capable of producing the highest 2-PE concentrations in medium containing L-phe as the nitrogen source. Among them, fifteen also stood out in 2-PE production in the absence of L-phe via *de novo* synthesis. *K. marxianus* CCT 7735 was found to be the best producer of 2-PE in this study. The optimization strategy allowed us to improve the 2-PE titer and the specific production rate by *K. marxianus* CCT 7735. The optimal conditions evaluated in this study were: glucose and L-phe concentrations of 30 g/L and 4.0 g/L, respectively. Despite 2-PE production being higher at 30°C, *K. marxianus* CCT 7735 was also able to produce high 2-PE concentration at 37°C. *K. marxianus* CCT 7735 growth was negatively affected by 2-PE. Nevertheless, this effect is less pronounced than the inhibition reported for a number of *Saccharomyces cerevisiae* strains in the literature.

Acknowledgments

The authors thank the Universidade Federal de Viçosa, National Council for Scientific and Technological Development (CNPq), Coordination for the Improvement of Higher Education Personnel (CAPES), Fundação de Amparo à Pesquisa de Minas Gerais (FAPEMIG) for their financial support for the research and the scholarship.

Electronic Supplementary Material (ESM) The online version of this article (doi: 10.1007/s12257-018-0119-6) contains supplementary material, which is available to authorized users.

References

- Hua, D. and P. Xu (2011) Recent advances in biotechnological production of 2-phenylethanol. *Biotechnology Advance.* 29: 654-660.
- Gupta, C., D. Prakash, and A. S. Gupta (2015) Biotechnological approach to microbial based perfumes and flavours. *J. Microbiol. Exp.* 2: 34.
- Mo, E. K. and C. K. Sung (2007) Phenylethyl alcohol (PEA) application slows fungal growth and maintains aroma in strawberry. *Postharvest Biol. Technol.* 45: 234-239.
- Liu, P., Y. Cheng, M. Yang, Y. Liu, K. Chen, C. Long, and X. Deng (2014) Mechanisms of action for 2-phenylethanol isolated from *Kloeckera apiculata* in control of *Penicillium molds* of citrus fruits. *BMC Microbiol.* 14: 242.
- Bauer, K., H. Surburg, and J. Panten (2001) *Common fragrance and flavor materials: preparation, properties and uses*, 4th ed., pp. 28, Wiley-VCH, Weinheim, Germany.
- Etschmann, M. M. W., W. Bluemke, D. Sell, and J. Schrader (2002) Biotechnological production of 2-phenylethanol. *Appl. Biotechnol.* 59: 1-8.
- Pylro, V. S., et al. (2014) Brazilian microbiome project: revealing the unexplored microbial diversity-challenges and prospects. *Microb. Ecol.* 67: 237-241.
- Etschmann, M. M. W., D. Sell, and J. Schrader (2005) Production of 2-phenylethanol and 2-phenylethylacetate from L-phenylalanine by coupling whole-cell biocatalysis with organophilic pervaporation. *Biotechnol. Bioeng.* 92: 624-634.
- Morrissey, J. P., M. M. W. Etschmann, J. Schrader and G. M. Billerbeck (2015) Cell factory applications of the yeast *Kluyveromyces marxianus* for the biotechnological production of natural flavour and fragrance molecules. *Yeast* 32: 3-16.
- Löser, C., T. Urit, and T. Bley (2014) Perspectives for the biotechnological production of ethyl acetate by yeasts. *Appl. Microbiol. Biotechnol.* 98: 5397-5415.

11. Wang, H., Q. Dong, A. Guan, C. Meng, X. Shi, and Y. Guo (2011) Synergistic inhibition effect of 2-phenylethanol and ethanol on bioproduction of natural 2-phenylethanol by *Saccharomyces cerevisiae* and process enhancement. *J. Biosci. Bioeng.* 112: 26-31.
12. Huang, C. J., S. L. Lee, and C. C. Chou (2000) Production and molar yield of 2-Phenylethanol by *Pichia fermentans* L-5 as affected by some medium components. *J. Biosci. Bioeng.* 90: 142-147.
13. Etschmann, M. M. W., D. Sell, and J. Schrader (2003) Screening of yeasts for the production of the aroma compound 2-phenylethanol *microbiology* in a molasses-based medium. *Biotechnol. Lett.* 25: 531-536.
14. Eshkol, N., M. Sendovski, M. Bahalul, T. Katz-Ezov, Y. Kashi, and A. Fishman (2009) Production of 2-phenylethanol from L-phenylalanine by a stress tolerant *Saccharomyces cerevisiae* strain. *J. Appl. Microbiol.* 106: 534-542.
15. Celińska, E., P. Kubiak, and W. Białas (2013) *Yarrowia lipolytica*: the novel and promising 2-phenylethanol producer. *J. Ind. Microbiol. Biotechnol.* 40: 389-92.
16. Lu, X., Y. Wang, H. Zong, H. Ji, B. Zhuge, and Z. Dong (2016) Bioconversion of L-phenylalanine to 2-phenylethanol by the novel stress-tolerant yeast *Candida glycerinogenes* WL2002-5. *Bioeng.* 0: 1-6.
17. Shen, L., Y. Nishimura, F. Matsuda, J. Ishii, and A. Kondo (2016) Overexpressing enzymes of the Ehrlich pathway and deleting genes of the competing pathway in *Saccharomyces cerevisiae* for increasing 2-phenylethanol production from glucose. *J. Biosci. Bioeng.* 122: 34-39.
18. Silveira, W. B., et al. (2014) Genomic sequence of the yeast *Kluyveromyces marxianus* CCT 7735 (UFV-3), a highly lactose-fermenting yeast isolated from the Brazilian dairy industry. *Genome Announc.* 2: 1-2.
19. Etschmann, M. M. W. and J. Schrader (2006) An aqueous–organic two-phase bioprocess for efficient production of the natural aroma chemicals 2-phenylethanol and 2-phenylethylacetate with yeast. *Appl. Microbiol. Biotechnol.* 71: 440-443.
20. Gao, F. and A. J. Daugulis (2009) Bioproduction of the aroma compound 2-phenylethanol in a solid–liquid two-phase partitioning bioreactor system by *Kluyveromyces marxianus*. *Biotechnol. Bioeng.* 104: 332-338 .
21. Gethins, L., O. Guner, A. Demirkol, M. C. Rea, C. Stanton, R. P. Ross, Y. Yuceer, and J. P. Morrissey (2014) Influence of carbon and nitrogen source on production of volatile fragrance and flavour metabolites by the yeast *Kluyveromyces marxianus*. *Yeast*
22. Kim, T., S. Lee, and M. Oh (2014) Biosynthesis of 2-phenylethanol from glucose with genetically engineered *Kluyveromyces marxianus*. *Enzyme and Microb. Technol.* 61: 44-47.
23. Stark, D., D. Zala, T. Münch, B. Sonnleitner, I. W. Marison, and U. von Stockar (2003) Inhibition aspects of the bioconversion of L-phenylalanine to 2-phenylethanol by *Saccharomyces cerevisiae*. *Enzyme Microb. Technol.* 32: 212-223.
24. Bostock, C. J. (1970) The effect of 2-phenyl ethanol on the DNA synthesis cycle of *Schizosaccharomyces Pombe*. *J. Cell Sci.* 7: 523-530.
25. Fabre, C. E., P. J. Blanc, and G. Goma (1998) 2-Phenylethyl alcohol: an aroma profile. *Perfum. Flavor.* 23: 43-45.
26. Diniz, R. H. S., et al. (2017). Transcriptome analysis of the thermotolerant yeast *Kluyveromyces marxianus* CCT 7735 under ethanol stress. *Appl. Microbiol. Biotechnol.* 101: 6969-6980.
27. Diniz, R. H. S., M. Q. R. B. Rodrigues, L. G. Fietto, and F. M. L. Passos nad W. B. Silveira (2014) Optimizing and validating the production of ethanol from cheese whey permeate by *Kluyveromyces marxianus* UFV-3. *Biocatal. Agric. Biotechnol.* 3: 111-117.
28. Ferreira, P. G., et al. (2015). Optimizing ethanol production by thermotolerant *Kluyveromyces marxianus* CCT7735 in a mixture of sugarcane bagasse and ricotta whey. *Food Sci. Biotechnol.* 24: 1421-1427.
29. Mierzejewska, J., A. Tymoszevska, K. Chreptowicz, and K. Krol (2017) Mating of 2 laboratory *Saccharomyces cerevisiae* strains resulted in enhanced production of 2-phenylethanol by biotransformation of L-Phenylalanine. *J. Mol. Microbiol. Biotechnol.* 27: 81-90.
30. André, B. (1995) An overview of membrane transport proteins in *Saccharomyces cerevisiae*. *Yeast* 11: 1575-1611.